POLITECNICO DI TORINO

Master's Degree in Environmental and Land Engineering

Master Thesis

CONFLICT IN UKRAINE: ASSESSING PHENOLOGICAL CHANGES IN GRAIN PRODUCTION AREAS OF UKRAINE DURING THE RUSSO-UKRAINIAN CONFLICT USING NDVI TIME SERIES DERIVED FROM SENTINEL-2 DATA

Supervisors

Prof. Piero Boccardo

Prof. Paolo Dabove

Candidate

Laura Mena Sanchez

March 2024

Abstract

This study employs Sentinel-2 Level 2A satellite images, categorized as Analysis Ready Data (ARD), to investigate the impact of the Russia-Ukraine conflict on agriculture. The focus is on phenological changes in three designated zones. The eligibility criteria for the designated zones are determined by their proximity to the frontline, the significance of their agricultural sector, and the degree of direct impact experienced. These impacts encompass various factors such as city occupations, illegal annexation of territories, displacement of civilians, bombings, and international condemnations linked to these events. The processing flow involves the development of a QGIS model for automated operations, including NDVI calculation, image cropping, and statistical value computation. The widely used Normalized Difference Vegetation Index (NDVI) is calculated using the Raster calculator algorithm. Clipping operations are performed to focus on relevant areas, and statistical indicators are computed within each parcel using the Zonal statistics algorithm. Excel operations are then utilized for constructing NDVI time series, allowing for visual comparisons of crop behavior and subsequent clustering based on phenological patterns. The results reveal a general decrease in NDVI values across all zones after the conflict onset, indicating potential disruptions in vegetation development cycles. While the study provides valuable insights, future research should expand to a national level and incorporate higher-resolution satellite data and field verifications for enhanced robustness.

Table of Contents

Table of Figures

Acknowledgements

¿A dónde quieres que regrese tu alma?

En primer lugar, me agradezco a mí por haber hecho todo lo posible para llegar hasta aquí, aun cuando tantas veces temiste, te cuestionaste y dudaste, a mí por sacar ánimos y fuerzas cuando no las sentía para igual avanzar. Gracias a la Laura de hace unos 6 años que se metió esto en la cabeza, no alcanzaras a imaginas todo lo que has crecido, conocido y aprendido gracias a esa decisión. En segundo lugar, a mi familia, por ponerle plumas a mis alas, por creer en mí de una manera en la que ni yo misma lo logro hay veces, por guiarme, ser aliento y luz cuando me sentía perdida, por nunca juzgarme y siempre dejarme ser. A mis amigos gracias por compartir sus seres conmigo, por sostenerme tantas veces, escucharme, darme aliento y sobre todo fe. Agradezco infinitamente a la vida por haber puesto siempre a las personas correctas a lo largo de mi vida. Por último, agradezco a mi amada alma mater, ese universo que trajo nuevas esperanzas y nuevos rumbos a mi vida; gracias por mostrarme nuevos posibles, por forjar mis conocimientos y mis causas; y gracias a todos los docentes por compartir su conocimiento y ser parte de este logro en mi vida.

1. Introduction

1.1. Objectives of the investigation work

Armed conflicts pose a significant threat to a nation's food security, encompassing risks in trade, pricing dynamics, logistical operations, and agricultural production, among other factors. The ongoing conflict between Russia and Ukraine assumes a global dimension, amplifying concerns for global food security. These nations stand as pivotal contributors to the global agricultural market, serving not only as major exporters of agricultural commodities but also as primary suppliers of food products and fertilizers worldwide.

In 2021 alone, both Russia and Ukraine prominently featured among the top three global exporters of key commodities such as wheat, barley, maize, rapeseed and rapeseed oil, sunflower seed, and sunflower oil. The repercussions of the conflict extend beyond national borders, impacting the intricate web of international food trade and supply chains.

The agricultural production of both countries, serving as a pivotal sector in their respective economies, positions them as key suppliers in global grain markets. Additionally, they play a crucial role as the primary source of grain imports for countries falling within the Least Developed Country (LDC) and Low-Income Food-Deficit Country (LIFDC) groups. For instance, in 2021, Eritrea sourced 100% of its wheat imports from Ukraine (47%) and Russia (53%) (Fao & Stepanov, 2022).

This conflict holds implications for various nations, potentially leading to escalated prices or shortages of products on store shelves. The consequences may vary, triggering a food crisis in some regions while impacting the economic landscape for others.

In the face of such circumstances, the need to monitor critical factors like agricultural yield, cultivated areas, and effective harvest zones becomes crucial, accompanied by the necessity to estimate the consequential impacts on global supply. However, due to security conditions associated with the ongoing conflict, certain on-site studies or data collection initiatives cannot be effectively executed.

In this challenging context, agricultural remote sensing emerges as an indispensable ally in addressing these limitations. By leveraging cutting-edge technologies, remote sensing facilitates a rapid and comprehensive assessment of the aforementioned factors. This is particularly advantageous in regions that may be remote or inaccessible due to conflict-related issues, where traditional field studies are impeded (Fao & Stepanov, 2022; Ma et al., 2022; Matuszak, 2021; Meijl et al., 2022; Skakun et al., 2019).

Satellite imagery from advanced constellations, such as Sentinel-2, provides wide-swath, high-resolution, multi-spectral imaging data that empowers the calculation of indices like the Normalized Difference Vegetation Index (NDVI). This index finds various applications, including the estimation of vegetation productivity, the extraction of vegetation phenology (Li et al., 2022; Perry et al., 2022), detection of changes in vegetation, and mapping land cover and its changes (Chen et al., 2021). The vegetation phenology particularly allows a comprehensive understanding of the temporal patterns and life cycle events of vegetation, which is significant for monitoring changes in ecological systems, agricultural practices, and vegetation.

In this study, will be establish a comprehensive database using optical satellite images from the Sentinel-2 constellation to undertake a spatiotemporal assessment to explore the potential impacts that the ongoing military conflict between Ukraine and Russia may have had on agricultural activities in Ukraine. Specifically, our aim is to evaluate whether there has been a discernible change in the phenology of crops during the years 2022-2023, which coincide with the current years of conflict, in comparison to the phenology observed in the years

2019, 2020, and 2021, covering the months from April to October, encompassing the period for winter crop harvesting and the sowing and crop harvesting of summer crops.

To ascertain if these changes can be linked to the present conflict, a comparative analysis will be conducted across three distinct zones in Ukraine, applying the following criteria:

Zone A encompasses a region situated far from the active war front, with no significant recorded instances of combat or attacks by Russian military forces. It remains firmly under the control of the Ukrainian government.

In Zone B, the territory is currently occupied by Russian forces, and they maintain control. This zone has experienced a considerable number of combats and/or attacks by Russian military forces.

Zone C represents an area that was under Russian occupation but has been successfully liberated by the Ukrainian government. This zone also witnessed a significant number of combats and/or attacks by Russian military forces during the conflict.

The analysis will encompass the following considerations:

-Temporal Shifts in Crop Phenology: Examining alterations in the timing of key agricultural events, such as planting, flowering, and harvesting, to discern any anomalous patterns indicative of conflict-related disruptions.

-Land Use Dynamics: Investigating changes in crop types, to identify potential adaptations or constraints imposed by the conflict.

-Remote Sensing Data: Leveraging advanced technologies, such as remote sensing data from sources like Sentinel-2, to provide a comprehensive spatiotemporal perspective. This will enable a more detailed and accurate assessment of agricultural landscapes, considering factors like vegetation indices and land cover changes.

By systematically applying these criteria across the designated zones, this study aims to provide an analysis of the impact of the military conflict on agricultural management practices in Ukraine. The differentiated assessment across zones will facilitate an understanding of the varying degrees of influence that conflict dynamics may exert on agricultural systems and contribute valuable insights to the broader discourse on the resilience and adaptability of agricultural practices in conflict-affected regions.

1.2. Structure of the work

The work will be structured as follows: Chapter 2: Provides a socio-political context on the current conflict and highlights why it is crucial to consider the risks it poses to global food security.

Chapter 3: Offers a comprehensive overview of the geography, climate, and soils in Ukraine. Additionally, describes the three designated study zones where the comparative analysis will take place and the main agricultural products in each of them.

Chapter 4: is dedicated to explaining the fundamental concepts of remote sensing utilized in this study. It also offers a detailed description of the software applications and the additional information used to confront the analysis.

Chapter 5: presents the proposed methodology.

Chapter 6: highlights the main findings and implications of the study.

Chapter 7: is dedicated to the conclusions.

2. Literature Review

2.1. Socio political context

The Russian invasions into Ukraine in the southeastern part had their most recent episode in 2014. It was then that the current President of Russia, Vladimir Putin, ordered his troops to invade the Crimean Peninsula, taking advantage of the political conflict in Ukraine at that time. Through a vote declared illegal by the Ukrainian people and international organizations, Russia annexed Crimea, claiming to do so to defend its interests and Russian-speaking citizens in the region. Since then, the border regions of Donetsk and Luhansk have become war zones, marked by uprisings of pro-Russian rebels, leading to an ongoing civil war.

This tension between the two countries persisted over the years, and between January and April 2021, Russia began moving military troops to Ukraine. This act culminated in the Russian invasion that started on February 24, 2022. President Putin initiated a "special military operation" in Ukraine, ordering troops to mobilize towards various points on the border and launching airstrikes on cities, airports, and communication routes in Ukraine. In response, the current President of Ukraine, Volodymyr Zelensky, declared martial law in the country, severed diplomatic ties with Russia, and urged his troops to inflict the maximum possible casualties on the invading Russian forces. Next, the main events at the national and local levels will be listed in chronological order: the onset of the war, city occupations, illegal annexation of territories, displacement of civilians, bombings, and international condemnations related to these events:

National level:

24 February 2022: In an early morning address on Russian state television, President Putin announces Russian forces will carry out “a special military operation” in Ukraine. Ukraine’s President Zelenskyy introduces martial law

and closes Ukraine's airspace (*Ukraine Conflict: Russian Forces Attack from Three Sides*, 2022)

28 February 2022: Russian forces launch rocket attacks that kill "dozens" of civilians in Ukraine's second city, Kharkiv, and begin a renewed assault on the capital Kyiv.

2 March 2022: Russian forces in Ukraine move to tighten their siege of key cities, including the capital, Kyiv, and the southern port of Mariupol.

9 August 2022: The United Nations refugee agency, the UNHCR, reveals more than 10.5 million people have crossed the border from Ukraine since Russia's invasion began on 24 February.

16 September 2022: The UN food chief says the world is facing "a global emergency of unprecedented magnitude," with up to 345 million people at risk of starvation and 70 million pushed closer to starvation by the war in Ukraine.

30 September 2022: President Putin signs "accession treaties" formalizing Russia's illegal annexation of four occupied regions in Ukraine. Russia later vetoes a Western bid at the UN Security Council to condemn its annexations of Ukrainian territory. Specifically, the regions of Luhansk, Donetsk, Kherson, and Zaporizhzhia.

5 October 2022: President Putin signs the laws to formally absorb four Ukrainian regions into Russia (Walker, 2023)

October 8, 2022: Crimea bridge attack: In another major blow to Moscow, the only bridge connecting Russia with the Crimean Peninsula was severely damaged by an explosion. The Kerch Strait road-and-rail bridge is both strategically important and hugely symbolic. It was opened by Putin in 2018, four years after Russia illegally annexed Crimea from Ukraine (*Russia-Ukraine War Explosion on 12-Mile Crimea Bridge Kills 3*, 2022)

October 10, 2022: Kyiv blackout: A new phase of the war began when Russia launched the first of several waves of missile strikes on Ukraine's critical energy infrastructure. Using missiles, artillery shells and Iranian-made drones, Moscow began targeting Ukrainian power facilities, leaving large

areas of the country without power and water (*On Day Two of Massive Air Strikes, Russia Targeted Ukraine's Power Infrastructure Ukrainian Regions Report How Much Damage They Took Today*, 2022)

24 February 2023: First anniversary of Russia's invasion into Ukraine.

17 March 2023: The International Criminal Court issues an arrest warrant for President Vladimir Putin. (*ICC Judges Issue Arrest Warrant for Vladimir Putin over Alleged War Crimes*, 2023)

25 May 2023: Alexander Lukashenko, the Belarusian president, confirms that the relocation of some tactical nuclear weapons from Russia to Belarus has started. This is the Kremlin's first deployment of such bombs outside of Russia since the 1991 fall of the Soviet Union.

12 September 2023: G7 foreign ministers condemn the staging of what they call "sham elections" by Russia in occupied Ukrainian territories.

10 October 2023: Russia is defeated in its attempt to regain a seat in the UN's top human rights body, which voted last year to suspend Moscow after its invasion of Ukraine.(Walker, 2023)

Zone A:

4 June 2023: During the early hours of the morning Ukrainian officials reported that air defense systems had repelled a missile attack on Kyiv. However, two missiles struck an airfield near Kropyvnytskyi (*Russian Air Strikes Repelled over Kyiv, but Hit Regional Airfield*, 2023)

Zone B:

24 February 2022: A second wave of Russian missile bombings targeted the cities of Kyiv, Odesa, Kharkiv, and Lviv. Heavy ground fighting was reported in the Donetsk and Luhansk oblasts (*Ukraine Hit by Second Wave of Missile Strikes – Official*, 2022)

2 March 2022: Vadym Boichenko, the mayor of Mariupol, reported that residential areas were being "relentlessly" shelled by the Russian military,

with "scores of" casualties among civilians (*Ukraine Live Updates: Russia Attacks Key Ukraine Cities as Invasion Intensifies*, 2022)

9 March 2022: Mariupol maternity hospital attack: A maternity hospital in the southeastern city of Mariupol was hit by a Russian missile. The attack came despite Russia agreeing to a 12-hour pause in hostilities to allow refugees to evacuate (Walker, 2023)

14 March 2022: Civilians were able to evacuate Mariupol for the first time (*Russian Air Strikes Repelled over Kyiv, but Hit Regional Airfield*, 2023)

16 March 2022: The regional drama theater in Mariupol, sheltering around 1,000 civilians, was bombed later that day (*Ukrainian Officials Accuse Russia of Shelling Civilians Fleeing Mariupol*, 2022)

19 March 2022: Russian forces bombed an art school in Mariupol where 400 people were taking shelter (*Ukraine Accuses Russia of Bombing Mariupol School Sheltering 400*, 2022)

27 March 2022: Russian military continued missile strikes across Ukraine including the cities of Lutsk, Kharkiv, Zhytomyr and Rivne, while Mariupol was again subjected to sustained shelling.(*"It's 2 p.m. in Kyiv. Here's What You Need to Know,"* 2022)

17 May 2022: Ukrainian forces surrendered to Russian and DPR (Donetsk People Republic) troops and were evacuated from the Azovstal plant, marking the end of the Siege of Mariupol (*Longest Battle Ends as Ukrainian Troops Evacuated from Mariupol Steel Mill*, 2022)

21 September 2022: A record 215 Ukrainian soldiers, including fighters who led the defense of the Azovstal steelworks in Mariupol, were released in a prisoner exchange with Russia after mediation by Turkish President Recep Tayyip Erdoğan (*Ukraine Announces Exchange Of 215 Prisoners Of War*, 2022)

16 July 2023: Explosions were reported in cities across Russian-occupied Ukraine, including in Luhansk, Berdiansk and Mariupol (*Loud Explosions Heard in Occupied Luhansk, Berdiansk, Mariupol*, 2023)

13 August 2023: In occupied Mariupol, Ukrainian partisans reportedly set fire to a Russian military base near the Azovstal complex, resulting in the loss of at least ten Russian soldiers, three trucks, and five cars. (*Official: Partisans Set Russian Base on Fire in Mariupol*, 2023)

Zone C:

24 February 2022: Later that day, Russian troops entered the city of Kherson and took control of the North Crimean Canal, which allowed them to resume water supply to the peninsula. (*Russian Troops Enter Ukraine's Kherson Oblast: Defense Ministry*, 2022)

1 March 2022: In southern Ukraine, the city of Kherson was reportedly under attack by Russian forces.(*Ukraine Conflict: Russia Bombs Kharkiv's Freedom Square and Opera House*, 2022)

2 March 2022: Russian troops captured the city of Kherson, beginning a military occupation of the city and oblast. down six Bayraktar TB2 drones in the previous 24 hours. (*What Happened on Day 7 of Russia's Invasion of Ukraine*, 2022)

11 June 2022: President Zelenskyy said that Ukraine had launched airstrikes in Russian-occupied Kherson (*Zelenskyy Says New Air Raids Launched in Russian-Held Kherson*, 2022)

13 August 2022: Ukraine claimed to have destroyed the last bridge to the Kakhovka Hydroelectric Power Plant, the last bridge for Russian forces to transit in or out of Kherson (*Ukrainian Forces Destroy Last Remaining Bridge Used by Russian Military in Kherson Region*, 2022)

29 September 2022: Putin signed decrees recognizing the sovereignty and independence of Kherson and Zaporizhzhia Oblasts (*Putin Signs Decrees Recognizing So-Called Independence of Kherson, Zaporizhzhia Regions*, 2022)

November 12, 2022: After eight months of brutal Russian occupation, the southern city of Kherson was liberated on November 12, prompting scenes

of celebration by residents. (*Kherson Ours': Ukraine Celebrates after Russian Retreat*, 2022)

15 December 2022: The Kherson military administration stated that the city was hit 86 times with "artillery, MLRS, tanks, mortars and UAVs," in the past 24 hours.(*Ukraine Launches 'Most Massive Strike' on Occupied Donetsk Region since 2014, Russia-Installed Mayor Says*, 2022)

24 December 2022: Russian forces shelled Kherson leaving 10 dead and 55 injured according to Ukrainian officials. (*At Least 10 Killed in Kherson Shelling, Fueling Anger Over Christmas Strikes*, 2022)

3 May 2023: Twenty-four civilians were killed in Kherson city due to Russian shelling.(*Russia-Ukraine Updates: Russia Opens Probe into Kremlin Attack*, 2023)

25 June 2023: Shelling and air strikes by Russian forces were reported in Kherson, Sumy and Chernihiv oblasts.(*Military: Russian Forces Shell Bordering Chernihiv, Sumy Oblasts*, 2023)

15 October 2023: Two airstrikes on infrastructure facilities in Kherson resulted in electricity and water outages in the city. (*Military: Russian Forces Shell Bordering Chernihiv, Sumy Oblasts*, 2023)

2.2. Global food supply implications

Ukraine has consistently held a notable position as one of the leading global exporters of cereals, oilseeds, vegetables, and agricultural commodities for several consecutive years (Fao & Stepanov, 2022). The exportation of food products serves as the primary source of hard currency inflows into the country. However, the recent invasion has set off significant repercussions within Ukraine's agricultural sector, giving rise to a multifaceted crisis. This crisis not only entails shortages of crucial resources like fertilizers, seeds, and fuel but also casts a shadow over the livelihoods of 25% of the rural population, impacting their agricultural production (FAO, 2022).

The regions directly impacted by the conflict, particularly those on the frontline experience the full impact of these consequences, and the repercussions extend further to the central oblasts. For many rural households, the primary source of income is derived from the production or sale of agricultural products, encompassing both crops and livestock. The repercussions of the conflict extend beyond individual households to agribusiness entities like UkrLand Farming and HarvEast, both reporting losses of control over substantial land holdings (Mousseau & Devillers, 2023). The Nasa Earth Observatory's estimate that 22% of Ukraine's farmland is now under the control of Russian army forces further accentuates the severity of the situation, particularly in regions responsible for 28% of winter crop production (Dryancour, 2023).

Zooming out to a national level, Ukrainian farmers are facing challenges related to access to fuel and electricity due to the constant attacks on energy infrastructure and storage facilities. The blockading of Black Sea ports, crucial for grain exports, coupled with limited transportation alternatives like rail, river, or road transport, has resulted in a breakdown of supply chains. In stark contrast to the pre-war scenario, where Ukraine exported 5-6 million tons of grains per month, March 2022 witnessed a drastic drop to around 0.2 million tons, compelling the country to store harvested grains. This logistical disruption and bottlenecks have consequently triggered an upsurge in food prices and global shortages (Movchan, 2022).

On a global scale, the principal importers of Ukraine's agri-food products are Asia, Africa, and Europe, encompassing countries that often fall into the categories of Least Developed Countries or Low-Income Food-Deficit Countries. Adding another layer to this complex situation is the fact that many of these countries import not only from Ukraine but also from Russia, which has been subjected to penalties regarding the transportation and pricing of products thereby increasing vulnerability (Fao & Stepanov, 2022).

Countries displaying heightened vulnerability in their domestic markets include Lebanon, Tunisia, Sri Lanka, the Netherlands, Lithuania, Kenya, and Poland.

This poses a substantial challenge for lower-middle-income countries, as the escalating prices of imports further strain their financial capacity. The interconnectedness of these issues paints a somber picture of the profound impact of the conflict, both at a national and global level. (Movchan, 2022)

.

3. Characterization of the study sites

The spatiotemporal analysis of NDVI profiles was applied to three distinct zones in Ukraine, situated at diverse geographical locations relative to the war front line, to ascertain if these changes can be linked to the current conflict. The following provides a concise yet comprehensive description of the country and each area of interest, encompassing factors such as climate, soil, and agricultural activities.

3.1. Geography, Climate and Soils

3.1.1. Geography

Ukraine is located in Eastern Europe and is the second-largest European Country. It shares borders at north with Belarus, in the west with Hungary, Poland and Slovakia, in the south-west with Moldova and Romania, and with Russia in the west. The total area of the country encompasses some 603,500 thousand square kilometers, which translates into roughly 5.7% of the total land mass of Europe or 0.44 percent of the globe. The 96% of its total area is land and the remaining 4% is water. The geographic features across its regions exhibit considerable diversity, encompassing highlands and lowlands alike, mostly fertile steppes and plateaus. The mountains can be found in the western part of the country with the Carpathian Mountains, with Hoverla standing as the highest peak at 2,061 meters (Central Intelligence Agency., 2023).

The extensive hydrology network is an important aspect of the country's geography and infrastructure. It is composed by several major rivers as the Dnieper (Dnipro), the Dniester (Dnister), Pripyat, the Southern Bug (Pivdennyi Buh), Desna and the Donets, being the Dnieper River the longest one, it flows from north to south and empties into the Black Sea *Figure 3.1.* Ukraine also has numerous lakes and reservoirs, most of them smaller than 10 km^2. Many reservoirs are created for water supply, irrigation, and hydroelectric power generation(Matuszak, 2021). But even with the abundance in water sources, the south and southeast parts of the country

face a water deficit for agriculture, due to the typical high temperatures, dry climate and more recent, the droughts caused by climate change.(JRC MARS Bulletin-Global Outlook Crop Monitoring European Neighbourhood Ukraine, 2022).

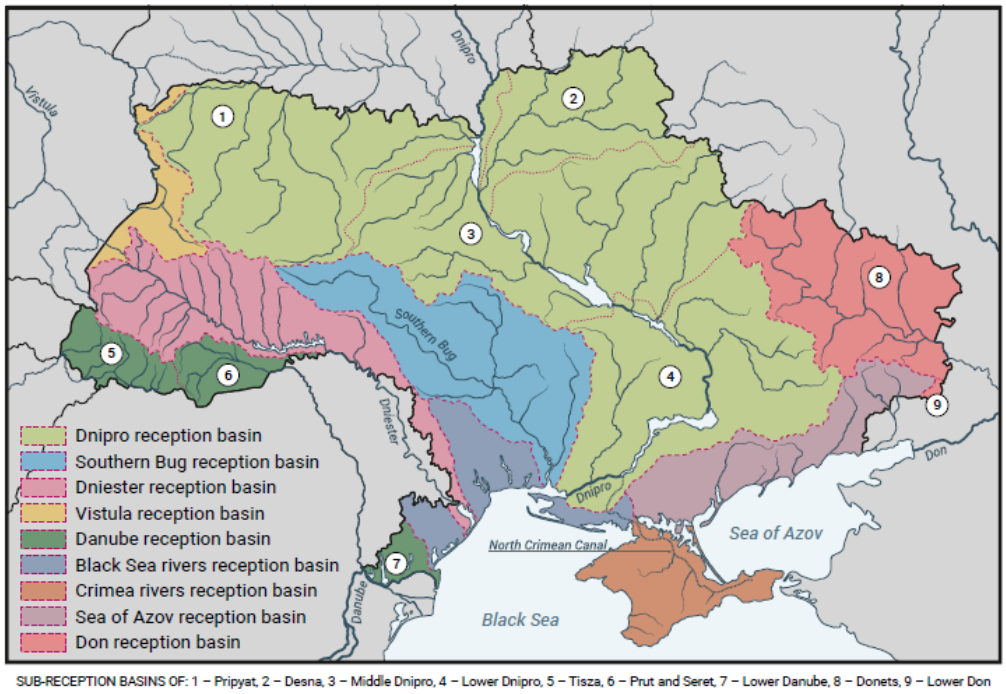

Figure 3.1 River Network of Ukraine (Matuszak, 2021)

3.1.2. Climatic conditions

The climatic characteristics across Ukraine exhibit notable regional variations. The western and northern oblasts fall within the moderate continental climate zone, characterized by hot summers and cold winters. Moving towards the eastern and central oblasts, the climate shifts to a continental zone marked by hot summers, lower humidity levels, and year-round precipitation. The southern oblasts experience a temperate maritime climate, featuring warm summers and milder winters compared to other regions. A limited coastal stretch along the southern coast of Crimea falls

within the subtropical Mediterranean zone, diversifying the country meteorological profile(Morton et al., 2005a).

Winter months in Ukraine typically experience average temperatures ranging from -5°C to -10°C. As Spring arrives, temperatures see a rise, fluctuating between 5°C and 15°C. Moving into Summer, the average temperatures span from 20°C to 25°C, occasionally surpassing 30°C, particularly in the southern and central regions (*World Data Ukraine*, n.d.). Early Autumn maintains a relatively mild climate, with temperatures ranging between 10°C and 15°C before gradually descending as the season progresses.

The annual temperature averages in Ukraine exhibits regional variability. In the northern regions, the average annual temperatures typically range from 6°C to 8°C, while in the southern regions, temperatures tend to be higher, ranging from 11°C to 13°C. This temperature gradient corresponds to a similar geographical pattern in the distribution of solar irradiation. The northwest experiences fewer sunlight hours per year, with totals below 1600, while the Black Sea coasts enjoy more abundant sunlight, exceeding 2200 hours annually.

The average amount of precipitation varies according to the season and the regions. The maximum precipitations take place in the summer months and for the northern and western oblast it is 550mm while in the south it is 440mm per year (Matuszak, 2021).

All the climatic conditions mentioned above, determined the vegetation zones in which Ukraine is divided. The oblasts in the moderate continental climate zone are dominate by mixed forests and wooded steppe. The continental zone by the steppe.

3.1.3. Soils

Ukraine soils is one of the most high-quality fertile soils in the world. The country accounts for one-third of the global black soil (or chernozem) area; These soils encompass 41% of the country's total land area, and roughly half

of its agricultural land is underlain by them. These soils feature a humus content layer with depths ranging from 40 cm to 1 meter. The other type of soils that cover the territory from the most fertile one's to the least are: Kastanozem 14% of the territory, featuring a humus content of 3-4% and a soil layer thickness of roughly 0.5 m; Alluvial soils 4.5%. Cambisols make up about 19% of the nation's territory, with a humus content ranging from 1% to 2.5%. Podzolic soils, constituting roughly 6% of the land, primarily consist of sandy and infertile soils. The remaining 7% of the country's area comprises various other soil types *Figure 3.2* and *Figure 3.3*. (Agricultural Sector of Ukraine Securing the Global Food Supply, 2018).

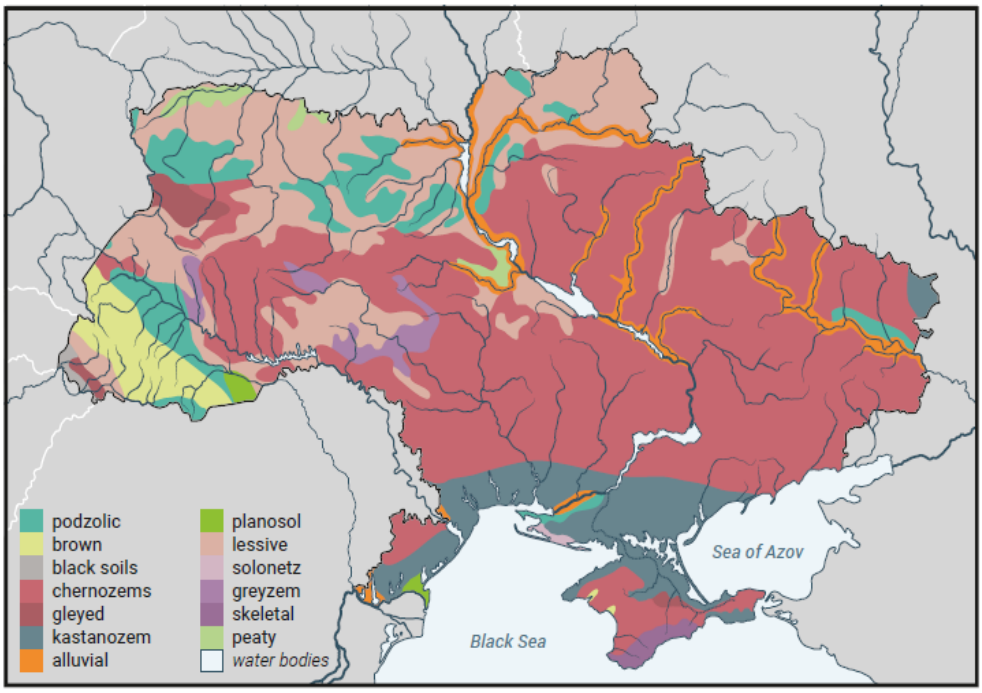

Figure 3.2 Soils of Ukraine (Matuszak, 2021)

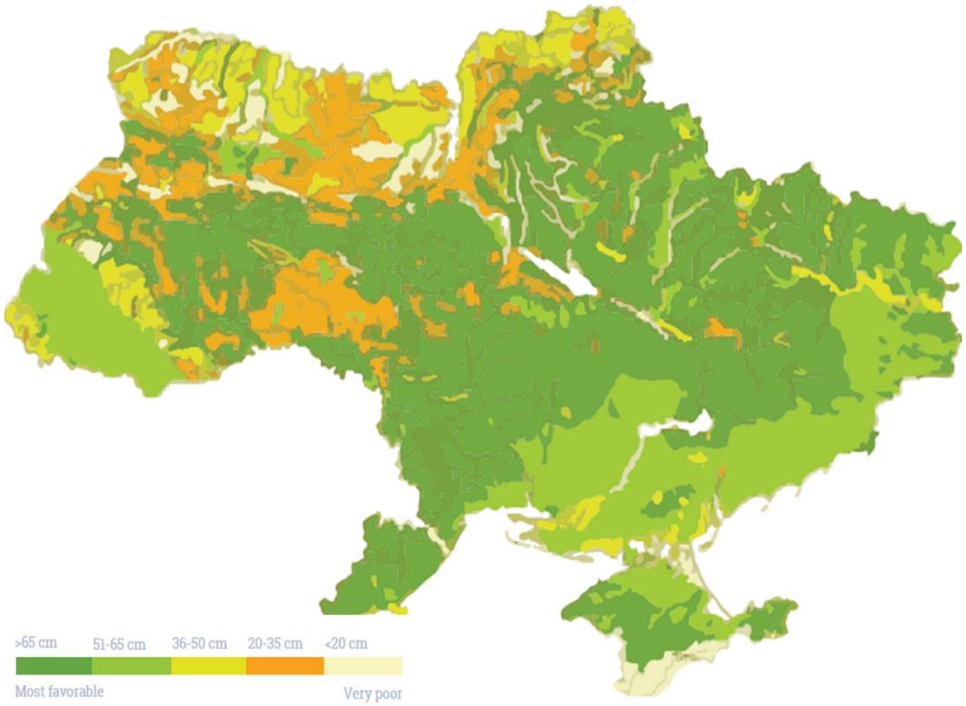

Figure 3.3 Depth of humus layer in Ukraine Soils (Agricultural Sector of Ukraine Securing the Global Food Supply, 2018)

As the climatic conditions, the distribution of soils in Ukraine exhibits distinct patterns across its geographical regions *Figure 3.2.* In the northern part of the country, a more heterogeneous distribution is observed, characterized by a prevalence of lessive soils. Moving towards the central region, there is a notable abundance of black soils. Conversely, in the southern regions along the coastlines of the Black Sea and the Sea of Azov, a dominance of kastanozem soils is identified.

3.1.3.1. Soils degradation

One of the critical challenges confronting the country's agricultural production is the degradation of its soils. In a 2014 investigation conducted by the FAO, it was estimated that 40% of the country exhibited varying levels of erosion across its territory, while another 40% was at risk of experiencing erosion caused by water and wind (Fao, 2014). This situation has been exacerbated by climate change and the rise in extreme events, such as droughts, that it entails. Additionally, contributing

factors include deforestation, intensive agricultural practices, and insufficient soil management methods(Land Degradation Neutrality Target Setting Programme (LDN TSP), 2018). According to various criteria, the average percentage of humus content has experienced a decline of 0.2% between 1990 and 2015(Matuszak, 2021), furthermore an important amount of nutrients like, nitrogen, phosphorus, and potassium, are removed from the land each year.

A portion of land degradation in Ukraine can be attributed to the ongoing military conflict. Specifically, regions like Donetsk and Luhansk are disproportionately affected, given their prolonged period of contention. It is estimated that a total area of 7 thousand square kilometers is contaminated with explosive ordnance (Land Degradation Neutrality Target Setting Programme (LDN TSP), 2018). Beyond the immediate risks posed by these conflicts, which often unfold in areas housing chemical, energy, and metallurgical facilities, among others, there is a pressing concern for the environmental consequences and the potential long-term impact on soil quality.

The country has intensified its efforts to enhance climate resilience and soil fertility, placing significant emphasis on soil conservation to minimize degradation. Measures such as conservation agricultural practices and reforestation have been actively implemented to safeguard and enhance the health of the soil.

3.2. Agriculture

The favorable climatic conditions and the abundance of fertile soils aforementioned have positioned Ukraine as one of the leading global producers and exporters of agricultural products, earning it the esteemed title of the “Breadbasket of Europe”. The most cultivated lands are those situated in Chernozem belt, that is from the central part of the country to the eastern border. Additionally, the advantage of having 95% of its territory as flatlands has proven beneficial for agricultural activities. (Morton et al., 2005). The country

boasts 42.2 million hectares of agricultural land, with 76% dedicated to arable land, 13% to pastures, 6% to grasslands, and 2% to perennial plantings(Agricultural Sector of Ukraine Securing the Global Food Supply, 2018).

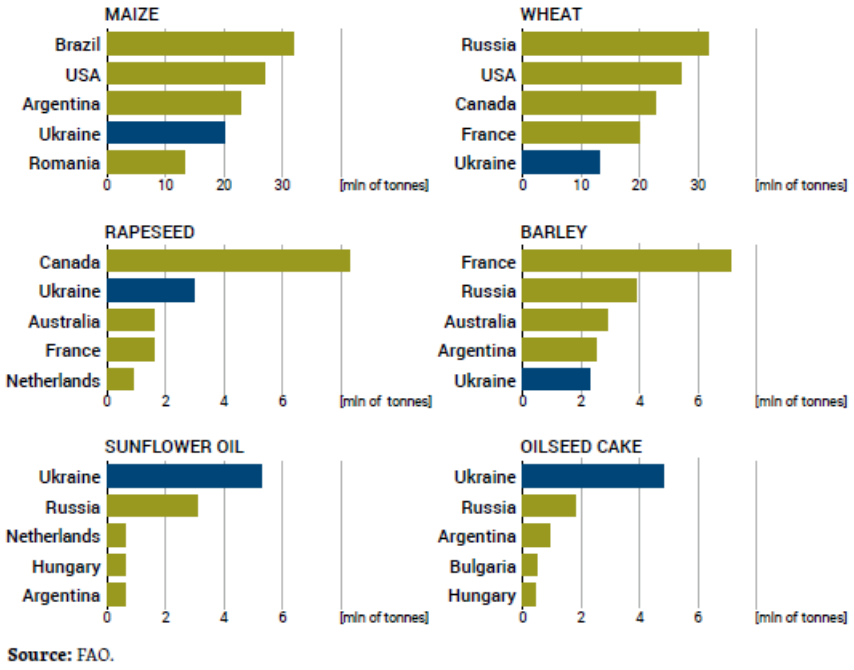

Figure 3.4 Largest exporters of selected agricultural products in 2019 (Matuszak, 2021)

Only in 2019, 46.4% of the total country's area was cultivated. The products that position Ukraine among the top global exporters include cereals, oilseeds, and vegetable oils. As illustrated in *Figure 3.4*, for the year 2019, Ukraine secured the first position as the global exporter of oilseed cake and sunflower oil, the second position for rapeseed, the fourth for maize, and the fifth for wheat and barley. This data highlights Ukraine's significant contribution to the international market in key agricultural commodities.

The primary agricultural activities are categorized as follows: Cereals, with predominant cultivation of maize, wheat, and barley; Industrial crops, including oil crops and sugar beets such as sunflower, rapeseed, and soybean;

Vegetables and tubers, encompassing tomatoes, cabbage, cucumbers, onions, carrots, beets, pumpkins, squash, and watermelons; and Plants for animal fodder such as alfalfa, clover and various grasses. (Matuszak, 2021)

3.3. Sites Description

The phenological analysis of the main crops was applied to three study areas impacted at varying levels by the conflict, each of them characterized by distinct soil compositions, crop diversity, and fields geometries. The location of the three study sites is shown in *Figure* 3.5. The objective is to ascertain whether there has been a significant change in the phenology of crops and whether such changes can be linked to the ongoing conflict. The main characteristics of the three study areas were summarized in Table 1.

Study site	Zone A	Zone B	Zone C
Oblast	Kirovohrad	Donetsk	Kherson
Closest major city	Kropyvnytskyi	Mariupol	Kherson
Extent (pixels)	450779	496780	736358
Extent (ha)	4699,945	5149,458	4058,273
Number of parcels	37	38	53
Number of sentinel-2 scenes	120	77	75

Table 1

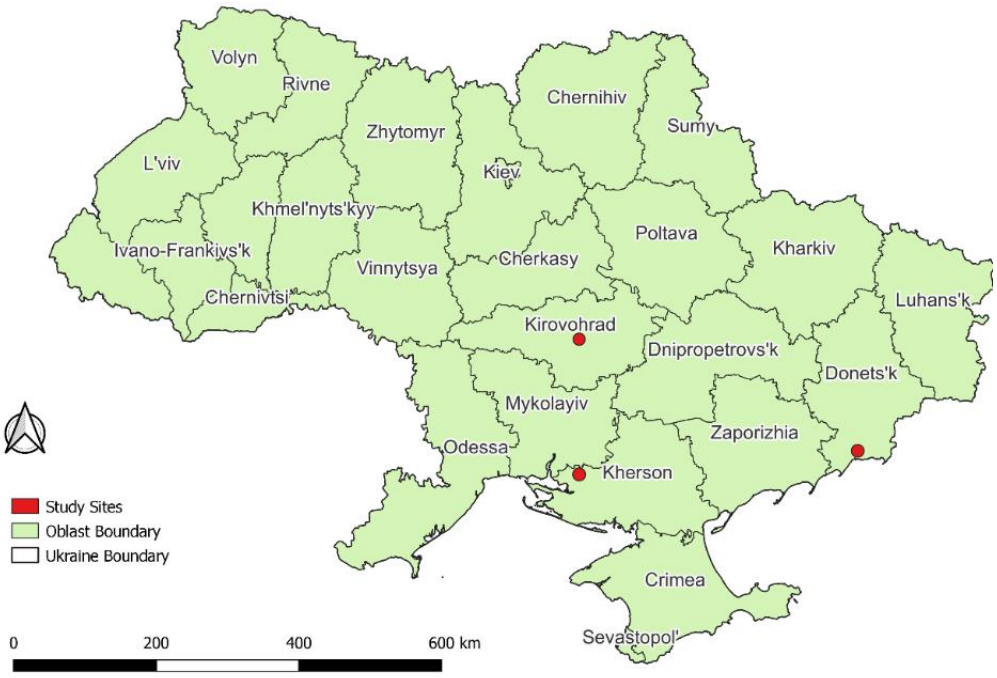

Figure 3.5 Location of the three study sites overlaid on the boundaries of administrative units

3.3.1. Zone A

Premise: this zone corresponds to a territory situated away from or distant to the war front, where a significant number of combats and/or attacks by Russian military forces have not been recorded, and it remains under the control of the Ukrainian government.

The area of interest is situated in the southeastern vicinity of Kropyvnytskyi city, a central Ukrainian city serving as the administrative center of Kirovohrad Oblast. Agricultural activities are a significant component of its economy. In the year 2019, this oblast exhibited the highest percentage of land allocated to agricultural activities, with 69.3% of the total oblast area under cultivation, being sunflower the dominant crop in terms of acreage. The primary crops cultivated in Kirovohrad Oblast include sunflower, corn,

wheat, sugar beet, soybean, rapeseed, and barley. It is characterized by cold and snowy winters and hot summers, the temperatures in summer months range from 20 °C to 30 °C.

The study site is precisely located with geographical coordinates in Degrees, Minutes, and Seconds (DMS) as follows: 48°27'24.4476"N, 32°13'6.9744"E at the northwest and 48°24'3.0492"N, 32°19'14.4912"E at the southeast, referencing the EPSG: 4326-WGS 84 coordinate system. The total area covered by the study spans 4699,945 hectares (Table 1), and a total of 37 parcels were delineated *Figure* 3.6.

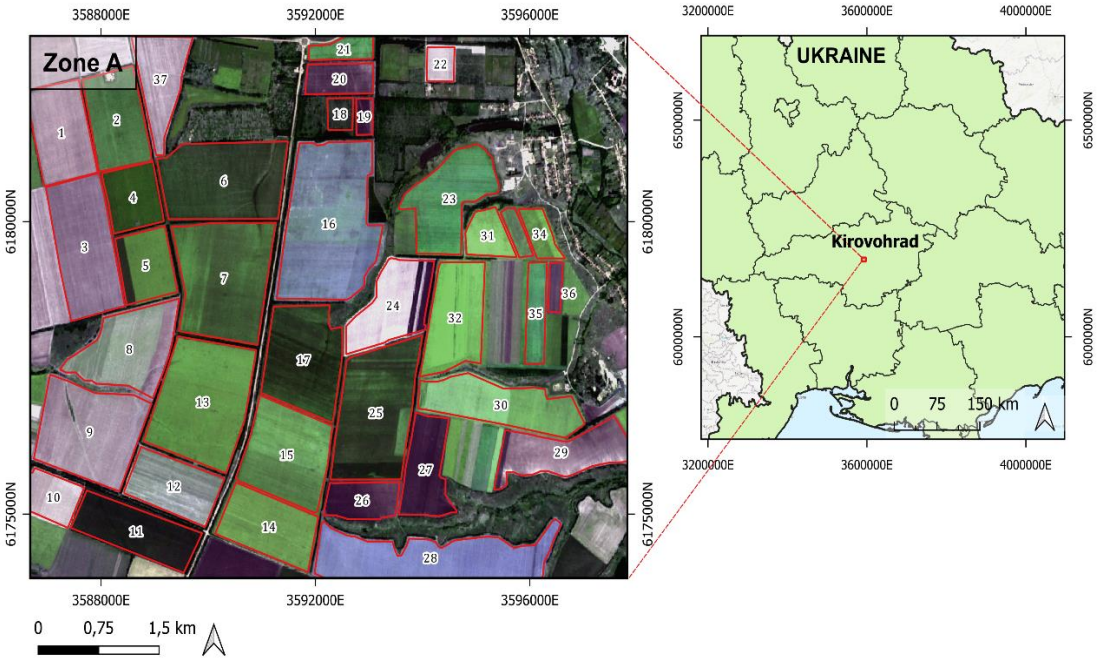

Figure 3.6 Zone A Kirovohrad oblast, Ukraine

The depiction of Sentinel-2 satellite images utilized for this zone, covering the period from March to September 2019-2023, is illustrated in *Figure* 3.7. These images were sourced exclusively from the European Space Agency (ESA) Copernicus Open Access Hub. Rigorous criteria were applied to ensure minimal cloud coverage, with certain months lacking scenes due to the requirement of less than 10% cloud coverage. Specifically, the analysis focused on the utilization of visible bands 4 and the near-infrared band (band

8). In 2019, there were a total of 27 available images, with a minimum of 2 images utilized each month. In 2020, 30 images were collected, excluding May, which lacked a cloud-free image. In 2021, 20 images were gathered, ensuring at least one image per month. For 2022, 23 images were acquired, and September did not have a cloud-free image. Lastly, in 2023, a total of 24 images were obtained, ensuring at least one image for every month. It's noteworthy that this zone had the highest number of available images.

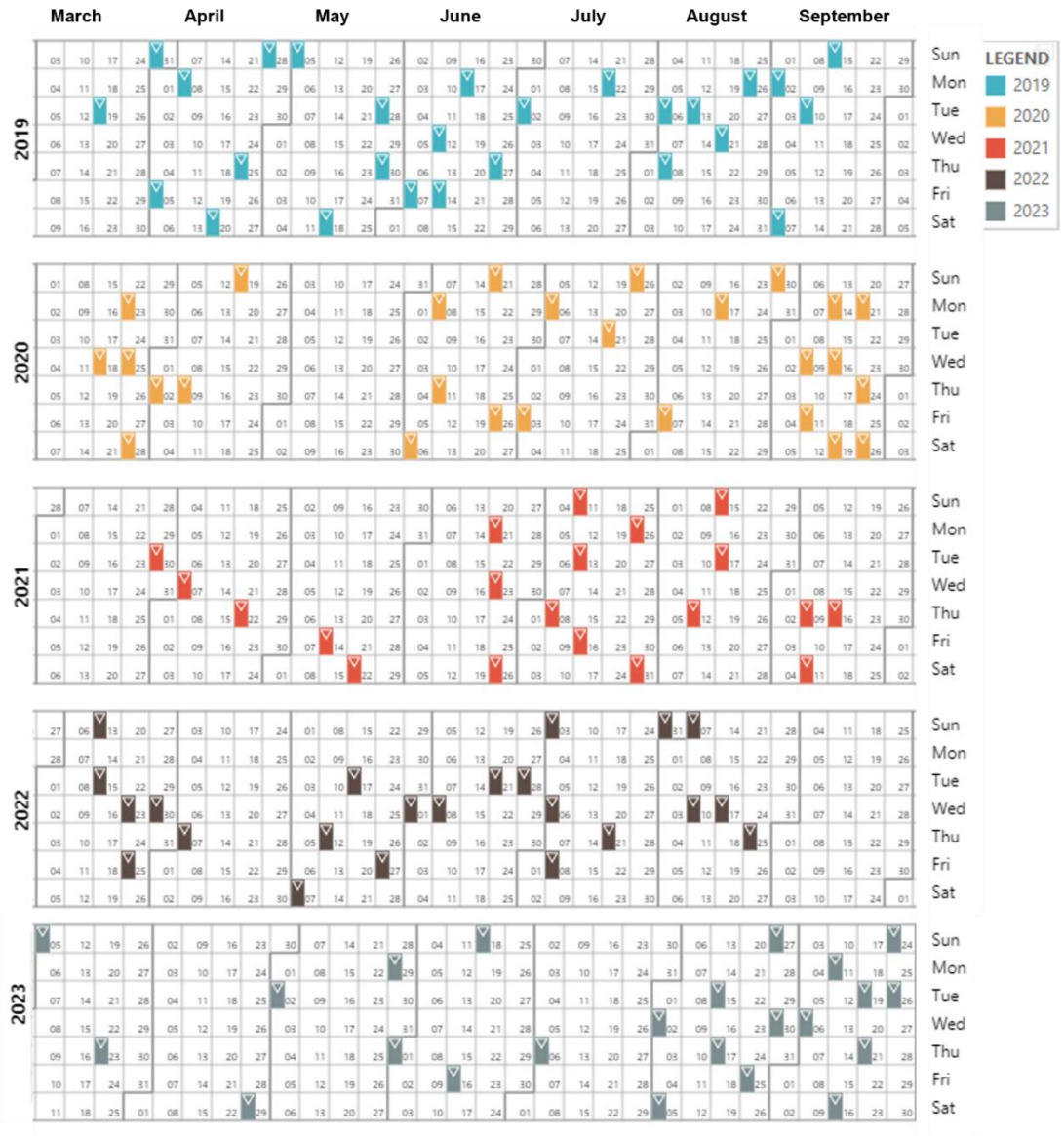

Figure 3.7 Acquisition dates of sentinel-2 images Zone A

3.3.2. Zone B

Premise: This zone corresponds to a territory captured by Russian forces and still under their control.

The area of interest is situated in the northeastern proximity of Mariupol city, the second largest city in the Donetsk oblast of Ukraine. Mariupol is situated on the northern coast of the Sea of Azov. Agricultural activities play a pivotal role in the region, with over half of the land cultivated in 2019. The primary crops cultivated in Donetsk oblast include wheat, sunflower, barley, corn, sugar beet, and rapeseed. The region experiences a humid continental climate, characterized by warm summers and cold winters, with temperatures ranging from 20 °C to 30 °C.

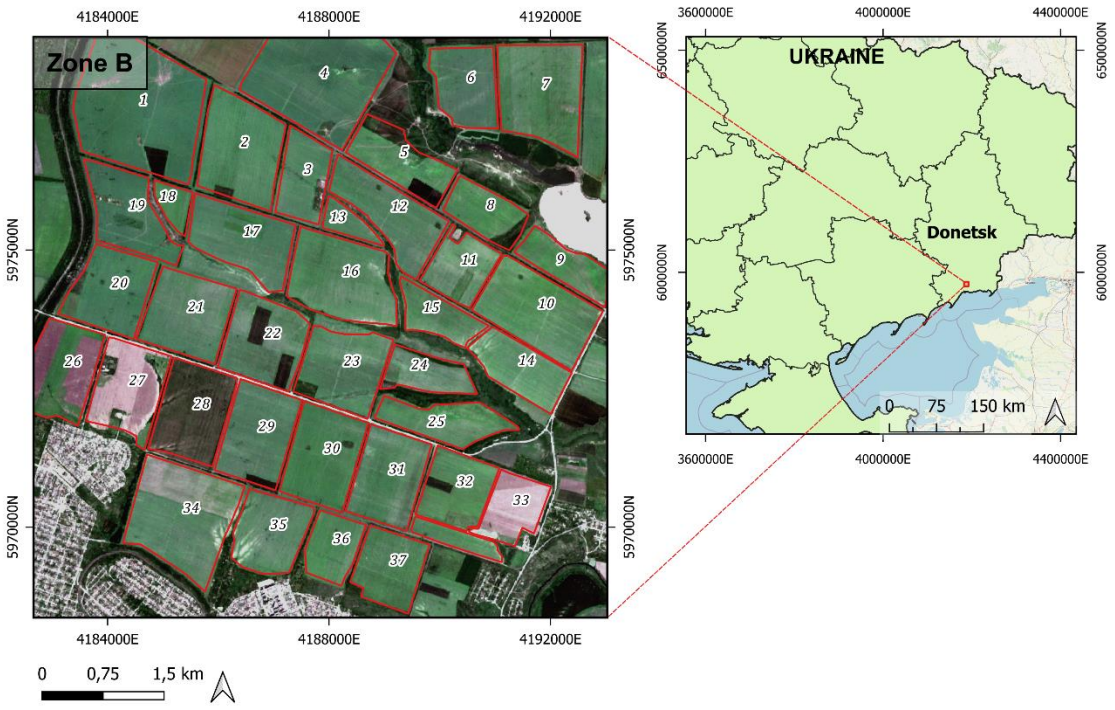

Figure 3.8 Zone B Donetsk oblast, Ukraine

The study site is precisely located with geographical coordinates in Degrees, Minutes, and Seconds (DMS) as follows: 47°13'32.5272"N, 37°34'24.0276"E

at the northwest and 47°9'37.0764"N, 37°40'0.4584"E at the southeast, referencing the EPSG: 4326-WGS 84 coordinate system. The study site covers a comprehensive area of 5149,458 hectares (Table 1) and a total of 38 parcels were delineated *Figure* 3.8.

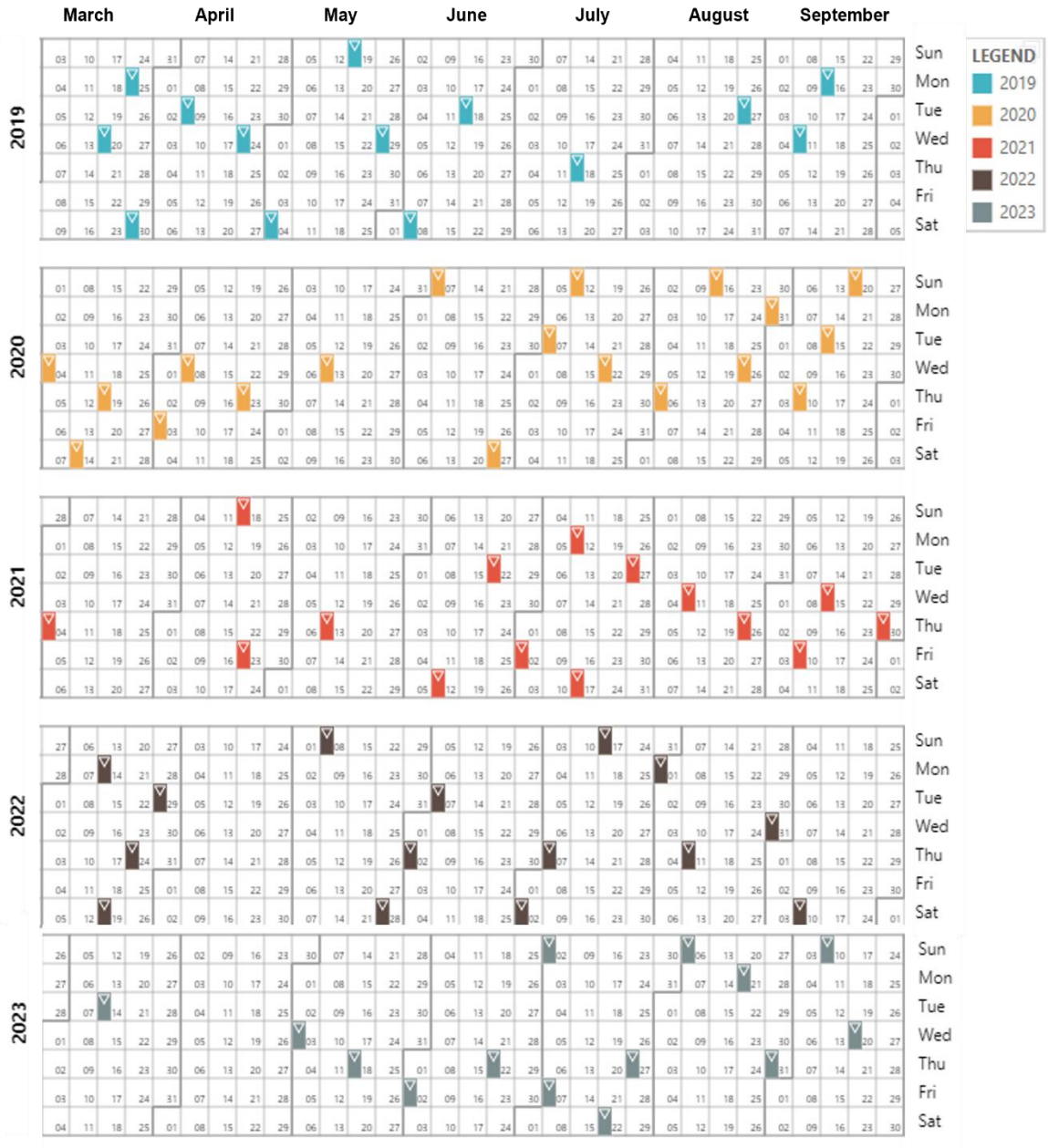

Figure 3.9 Acquisition dates of sentinel-2 images Zone B

The *Figure* 3.9 illustrates the Sentinel-2 satellite images used for this zone from March to September 2019-2023. All images were sourced from the European Space Agency (ESA) Copernicus Open Access Hub, ensuring minimal cloud coverage (<10%). The selected images, primarily utilizing visible bands 4 and near-infrared band (band 8), were carefully chosen. In 2019, there were 14 available images, 19 images in 2020, 15 images in 2021 each month featuring at least one image in this years, and 15 images in 2022,14 images in 2023, April lacked a cloud-free image in both years.

3.3.3. Zone C

Premise: This zone corresponds to a territory liberated by the Ukrainian government from Russian forces.

The study site is in the northwestern vicinity of Kherson city, a port city that serves as the administrative center of Kherson oblast. In 2019, 50.3% of its total land area was under cultivation. Kherson oblast is renowned for the cultivation of major crops such as sunflower, corn, wheat, sugar beet, soybean, rapeseed, barley, as well as potatoes, fruits, and vegetables. Notably, 13.6% of the country's total vegetable production is attributed to this oblast. Kherson has a humid continental climate, winters are mild and summers are typically warm to hot, with temperatures varying from 25 °C to 35 °C.

The study site is precisely located with geographical coordinates in Degrees, Minutes, and Seconds (DMS) as follows: 46°45'32.8392"N, 32°28'30.6948"E at the northwest and 46°40'52.5036"N, 32°30'20.8512"E at the southeast, referencing the EPSG: 4326-WGS 84 coordinate system. The study site covers a comprehensive area of 4058,273 hectares (Table 1), and a total of 53 parcels were delineated *Figure* 3.10

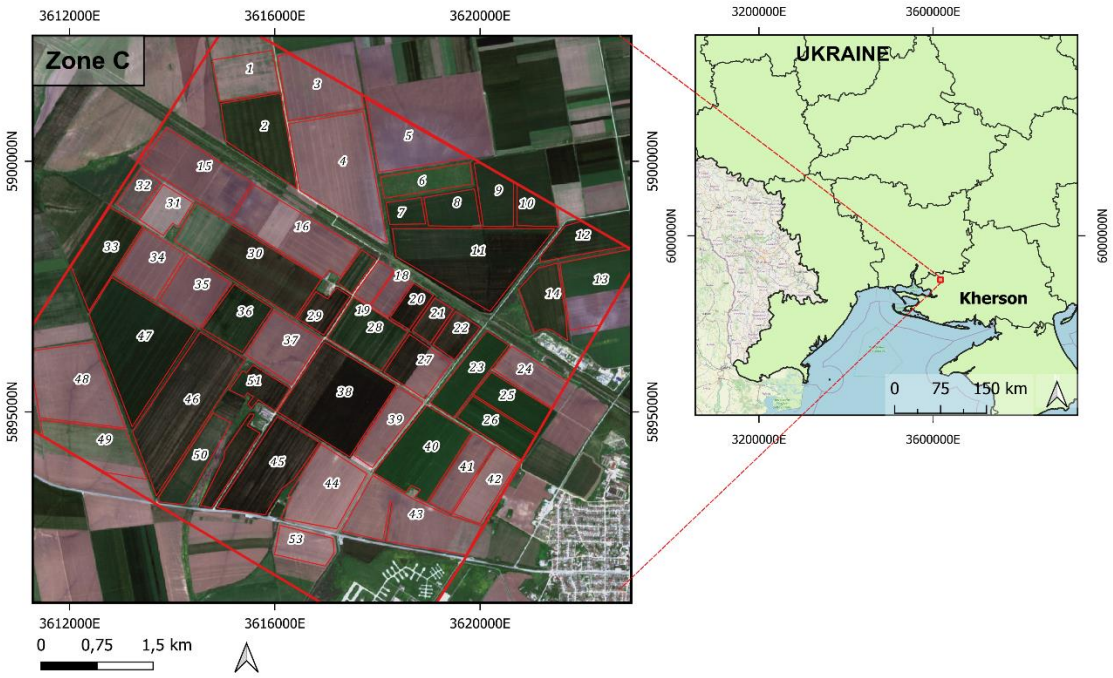

Figure 3.10 Zone C Kherson oblast, Ukraine

The Sentinel-2 satellite images utilized for this zone, spanning from March to September 2019-2023, are depicted in *Figure* 3.11. All images were sourced from the European Space Agency (ESA) Copernicus Open Access Hub. The chosen images exhibit minimal cloud coverage, with some months lacking scenes due to this criterion (less than 10% cloud coverage). Specifically, visible bands 4 and the near-infrared band (band 8) were employed. In 2019, a total of 19 images were available, with June lacking a cloud-free image. In 2020, 18 images were collected, ensuring at least one image for every month. For 2021, 12 images were collected, each month featuring at least one image. In 2022, 11 images were gathered, and September lacked a cloud-free image. Lastly, in 2023, a total of 14 images were obtained, with all months having at least one image.

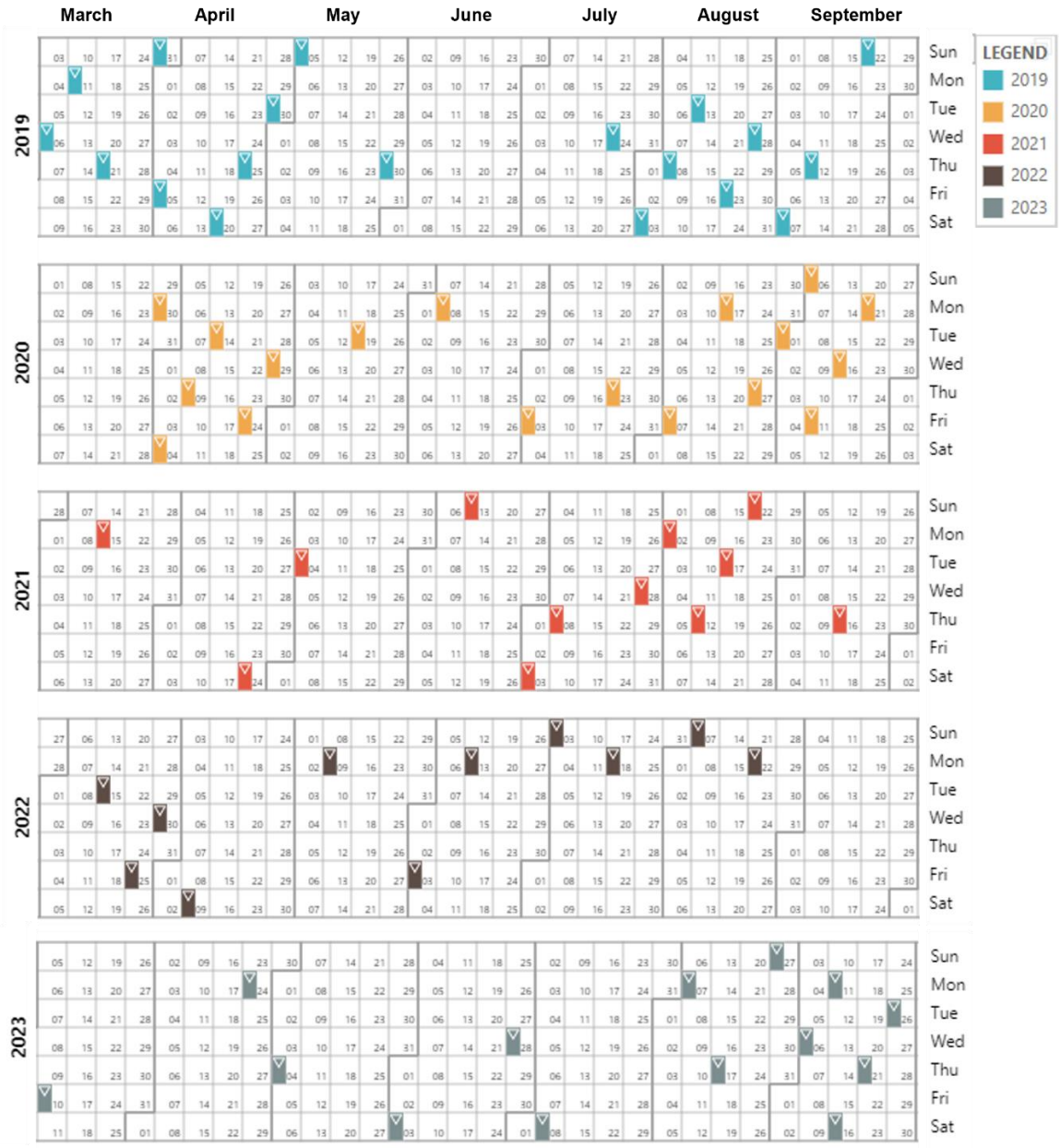

Figure 3.11 Acquisition dates of sentinel-2 images Zone C

4. Framework

The ability to observe the Earth's surface has brought a novel perspective of observation across various spatial scales (local, regional, global) and temporal scales (from real-time to decades). When applied to sectors like agriculture, this capability enables the monitoring of crop health, land use, prediction of harvest yields, optimization of production, and more, in a non-destructive and non-invasive manner. (Misra et al., 2020)

Research methodologies such as remote sensing provide the means to extract information from variables that are valuable for agricultural applications, including plant density, GAI/LAI (Green/Leaf Area Index), green cover, leaf biochemical content, leaf orientation, soil moisture, among others. By interweaving some of these variables within a specific temporal window, for instance, the crop growth cycle, one can derive features of interest such as crop productivity.(Weiss et al., 2020)

A brief theoretical overview of the foundations of remote sensing philosophy and the instruments used is provided below.

4.1. Spectral Signatures

The spectral signatures are the representation of reflectivity variation as a function of the wavelength of the reflected electromagnetic energy for homogeneous surfaces.

4.1.1. Water

The spectral signature of water surfaces is characterized by reflection values concentrated in the blue-green bands, with minimal reflection in the near-infrared (NIR) and subsequent bands, where non-reflection is observed (i.e., clear lake water and turbid river water lines in *Figure* 4.1). Visible reflection is also influenced by the presence of suspended elements such as organic matter, minerals, and chlorophyll.

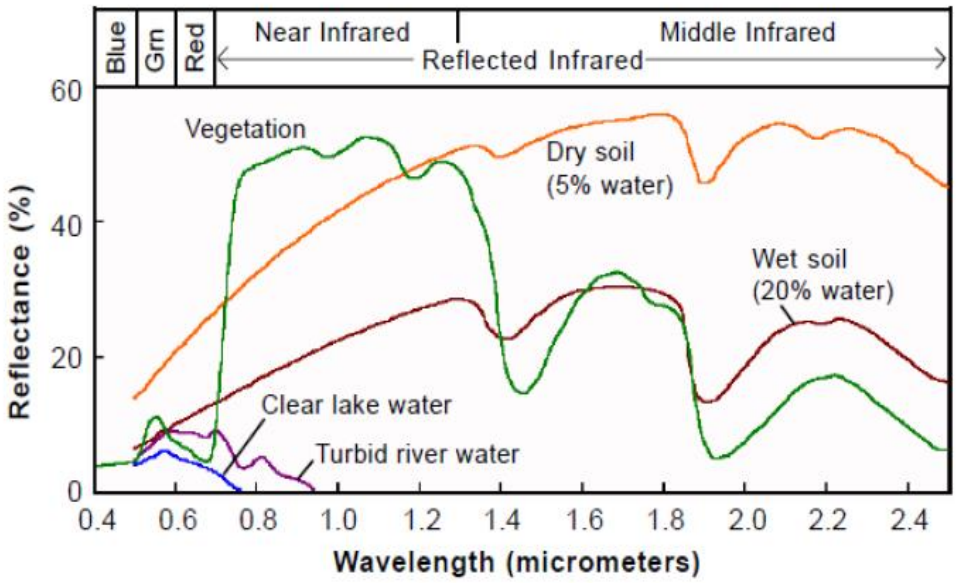

Figure 4.1 Representative spectral reflectance curves for several earth surface materials. (Boccardo, n.d.)

4.1.2. Soils

Reflectance increases from the visible to the infrared (IR) spectrum (i.e., Dry soil and Wet soil lines in *Figure* 4.1). Information derived from reflectivity curves includes details about the concentration of iron oxides, soil moisture content, and the presence of organic matter. Incident radiation can be affected by soil structure, texture, stony components, surface moisture, and soil color. Nevertheless, the spectral signature remains consistent regardless of soil type. The valleys within the profile are attributed to soil moisture content, with higher moisture content resulting in lower reflectance.

4.1.3. Vegetation

The characteristic curve of vegetation, shaped by leaf pigments, leaf structure, and water content, provides valuable insights of plant health and physiology. These three factors influence the energy reflected by the vegetation. In the visible bands, the curve's behavior is attributed to pigments like chlorophyll, xanthophyll, and carotene. Carotene becomes

prominent when chlorophyll is no longer part of the leaf, displaying orange and yellow tones. Chlorophyll, comprising 65% of total pigments, predominantly influences absorption in the blue and red bands.

Simultaneously, the structure of leaves, encompassing the spatial arrangement of cells, dictates the curve's characteristics in the near-infrared band, this region reveals a high reflectance as seen in *Figure* 4.2.

In the shortwave infrared bands, the curve's behavior is shaped by diverse compounds and chemical substances, with water content emerging as a key component.

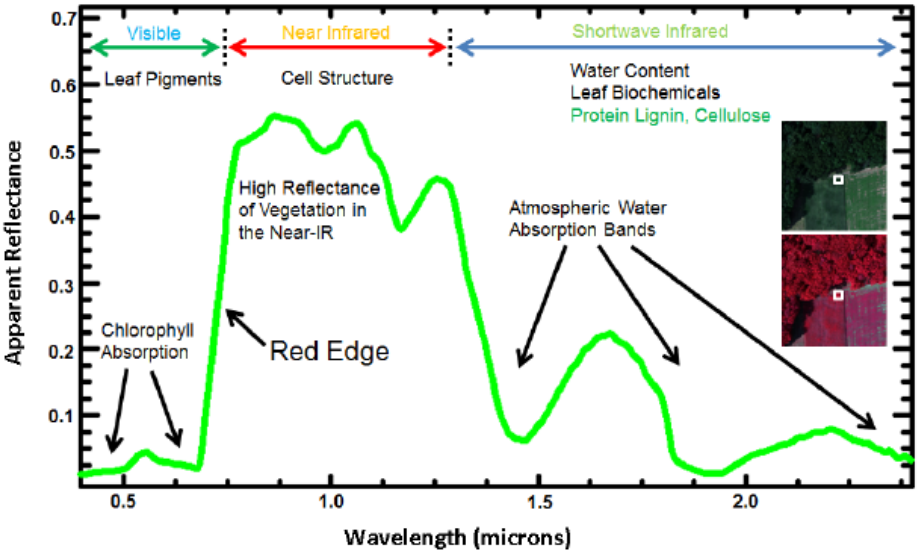

Figure 4.2 Spectral reflectance response of vegetation at different wavelengths(Chatterjee, 2018)

4.1.3.1. Vegetation index

Vegetation indices involve algebraic operations on the various spectral bands of plant reflective properties, and their interpretation provides insights into vegetation changes. The most widely utilized vegetation index is the NDVI (Normalized Difference Vegetation Index)

4.1.3.1.1. NDVI

The Normalized Difference Vegetation Index (NDVI) capitalizes on the pronounced contrast in light absorption within the narrow wavelength range of 620-800 nm. It is calculated as the ratio between the Near-Infrared (NIR) band and the Red band, normalized to obtain values between -1 and 1(Equation 1) (Helman, 2018). The curve is easily interpretable, rising at the beginning of the season and declining towards the end. This index is directly associated with vegetation health, indicating the amount of chlorophyll present.

$$NDVI = \frac{NIR - R}{NIR + R} \qquad \textit{Equation 1}$$

In *Figure* 4.3, the correlation of NDVI with other indices is depicted. It is evident that the correlation is close to 1 in most cases, substantiating the assertion that NDVI is a sufficiently robust index for vegetation studies.

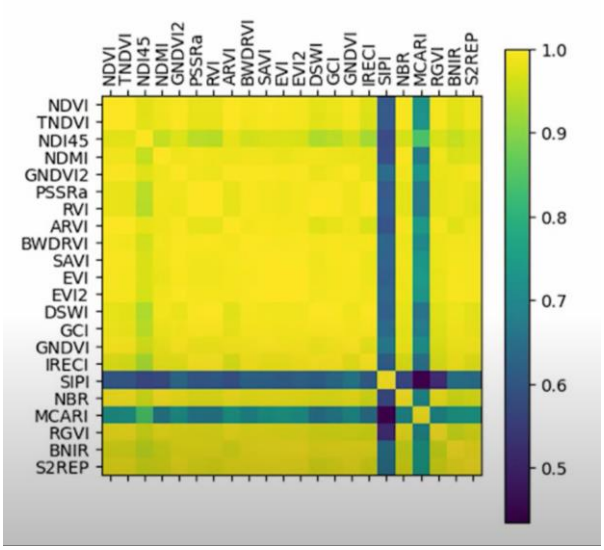

Figure 4.3 Correlation between different vegetation indices (ARSET, 2023)

NDVI is thus a classic method that is still frequently employed to assess vegetation health and to post-process high-resolution images for precision agriculture purposes. *Figure* 4.4 illustrates typical NDVI values for various surfaces. (Koroleva et al., 2017)

Table 1. NDVI scale

Object type	Reflection in the red band	Reflection in the infrared band	NDVI value
Dense vegetation	0.1	0.5	0.7
Sparse vegetation	0.1	0.3	0.5
Bare soil	0.25	0.3	0.025
Clouds	0.25	0.25	0
Snow and ice	0.375	0.35	−0.05
Water	0.02	0.01	−0.25
Artificial materials (concrete, asphalt)	0.3	0.1	−0.5

Figure 4.4 NDVI values for different surfaces(Koroleva et al., 2017)

4.2. Agricultural phenology

Phenology is the study of recurring stages in crop development and the dates on which they occur. These stages are dependent on the environment, as well as biotic and abiotic factors influencing crops. Historically, such studies have been conducted through field observations (ground-based sensors) in small areas and for short observation periods(Younes et al., 2021). The introduction of remote sensors in recent years has enabled monitoring seasonal changes in vegetation on larger scales and over longer periods using satellite imagery and derived vegetation indices, such as NDVI. Combining traditional methodology with remote sensing allows for a deeper understanding of crop responses to changes in environmental conditions.

Because each type of crop has a unique spectral and temporal signature, classifications based on this uniqueness can be carried out. Phenological monitoring can be conducted through the analysis of temporal series, examining a sequence of images within the year or the growth cycle *Figure* 4.5 A, or by extracting specific temporal metrics from crops, such as maximum red,

maximum positive slope, maximum NDVI, maximum negative slope, and minimum NDVI *Figure* 4.5 B.

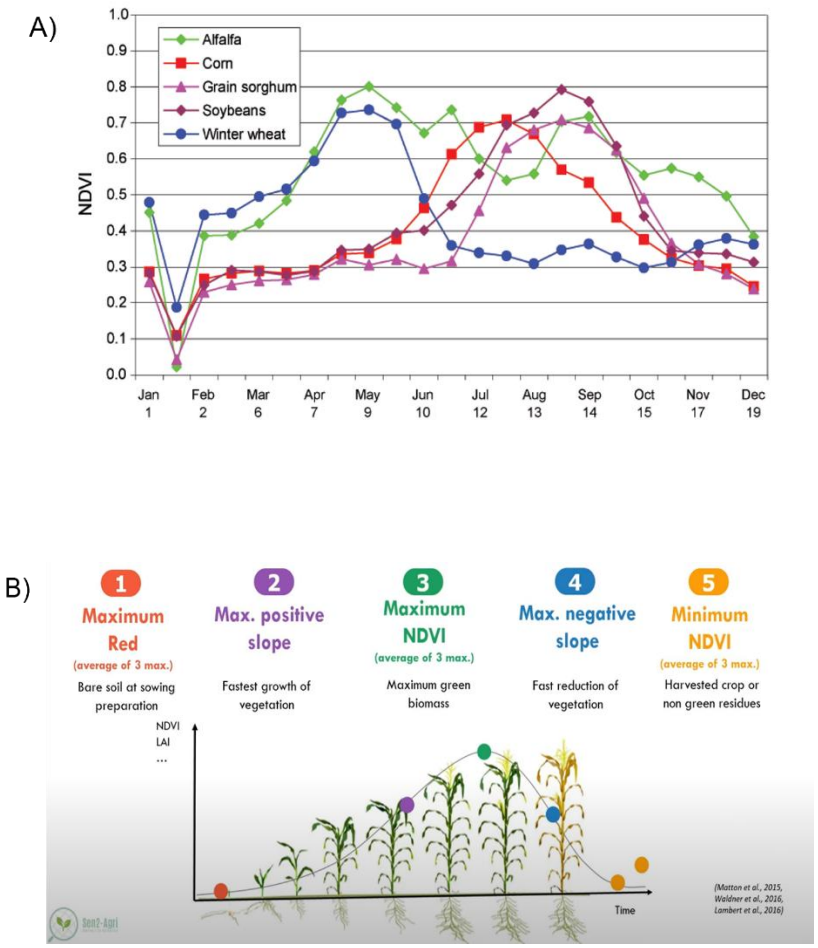

Figure 4.5 A. Full time series analysis.(Masialeti et al., 2010) *B. Crop-specific temporal metrics related to the crop phenology* (McNairn, 2021)

4.3. Sensors

The satellite images utilized for the study areas were procured through the Sentinel-2 mission satellites, a project managed by the European Space Agency (ESA) under the Copernicus program. These data play a pivotal role in supplying geographical information on land cover, facilitating disaster relief operations, contributing to climate change studies and for security programs (SENTINEL-2

User Handbook, 2013). The Sentinel-2 images stand out due to their optimal combination of spatial resolution, time resolution, and cost-effectiveness. All data were sourced from the Copernicus Open Access Hub. The selected Sentinel – 2 scenes for the three areas of interest are illustrated in *Figure*s *Figure* 3.7, *Figure* 3.9, *Figure* 3.11. Now, a brief presentation of the mentioned satellites' characteristics will follow.

4.3.1. Sentinel – 2

The Sentinel-2 constellation consists of two satellites, Sentinel-2A and Sentinel-2B, strategically positioned 180 degrees apart on the same orbit (*Figure* 4.7). These satellites are equipped with advanced sensors capable of capturing high-resolution multi-spectral images in 13 spectral bands, covering the spectrum from visible to shortwave. The spatial resolutions of these bands vary, ranging from 10m to 60m on the ground. *Figure* 4.6 provides a visual representation of the spatial resolution of these spectral bands.

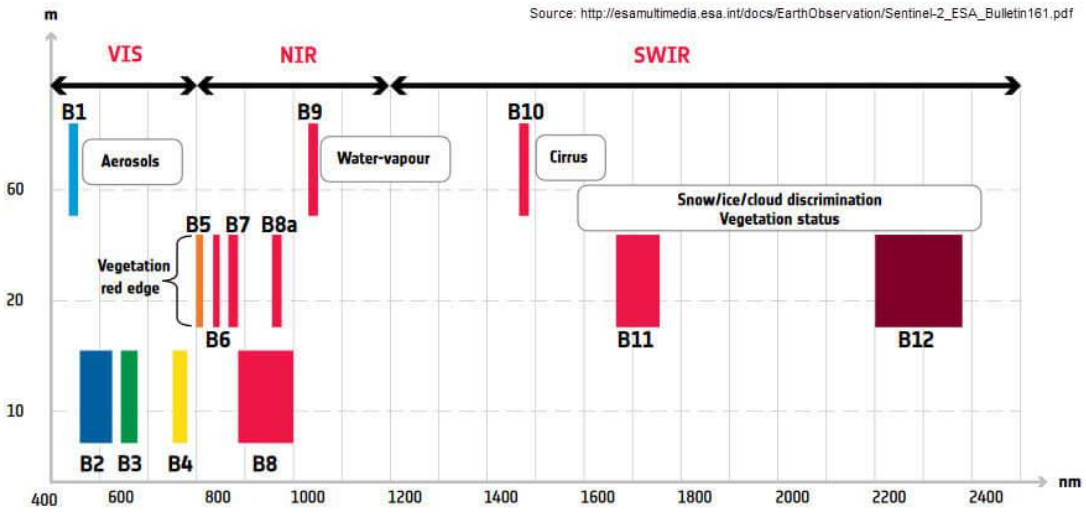

Figure 4.6 Spatial resolution vs wavelength of Sentinel-2 spectral bands (Martin et al., 2018)

At the 10 m blue, green, and red bands of the visible, and one on the near infrared (B2, B3, B4 and B8). At 20 m four bands at the red-edge and two in

the shortwave infrared (B5, B6, B7, B8a, B11 and B12). At 60 m the three atmospheric correction bands (B1, B9 and B10).

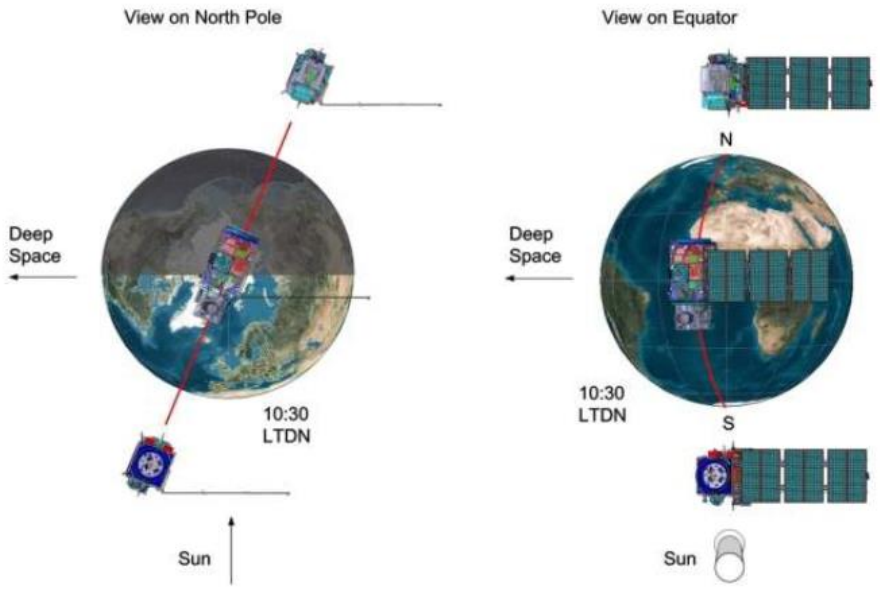

Figure 4.7 The Twin-Satellite SENTINEL-2 Orbital Configuration(SENTINEL-2 User Handbook, 2013)

These satellites are placed in a polar sun- synchronous orbit, allowing them to systematically observe the entire surface of the Earth. The revisit time of each single satellite is 10 days at the equator. The entire constellation revisit is 5 days. Additionally, they have a swath width of 290 km (SENTINEL-2 User Handbook, 2013).

4.4. Software's

The operations to identify areas of interest and the parcels within them, as well as image cropping, NDVI index calculation, and derivation of statistical values for each parcel, were performed using the open-source software QGIS, version 3.28.9. For visualizing NDVI time series and creating corresponding graphs, the Microsoft Excel and Power BI tools were employed.

5. Methodology

5.1. Image Processing

Sentinel-2 Level 2A satellite images fall under the category of Analysis Ready Data (ARD), denoting preprocessed and organized imagery for seamless and immediate analysis. This ensures interoperability over time and with other datasets. However, additional operations were performed to extract relevant information within the designated areas of interest. The flowchart in *Figure* 5.1 delineates the sequential stages involved in this process.

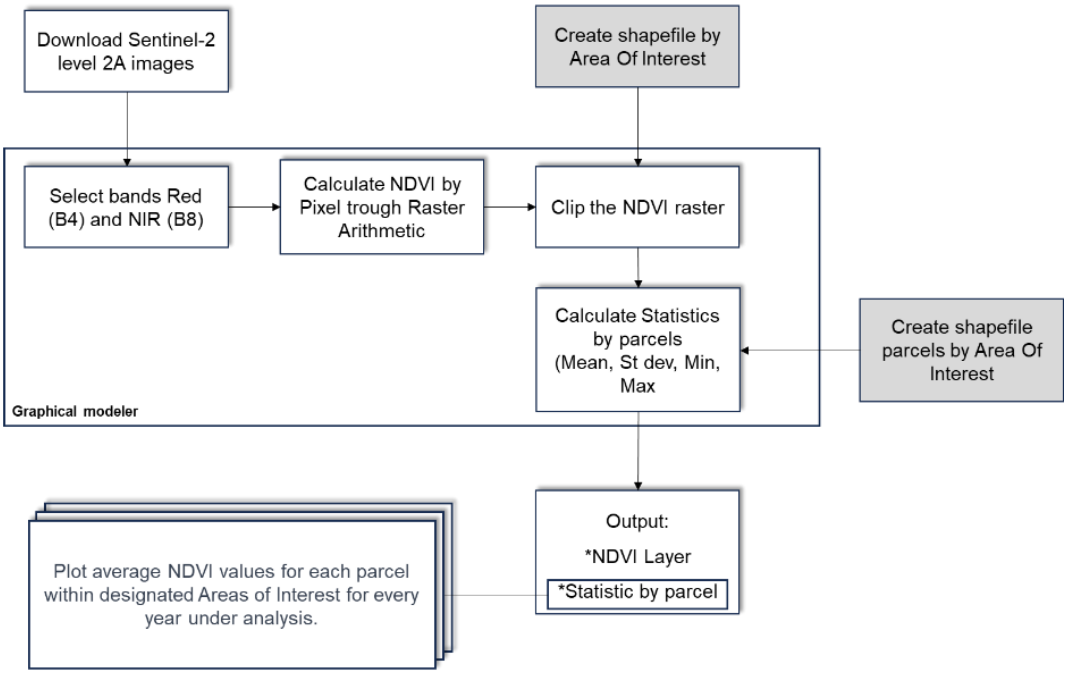

Figure 5.1 Flowchart for Generating Temporal NDVI Series

After downloading the images for each zone during the assessed temporal period, a model was developed using the graphical modeler tool in QGIS. This model aimed to automate various operations, including the calculation of the NDVI index, image cropping to retain only the regions of interest, and the computation of statistical values (*Figure* 5.2).

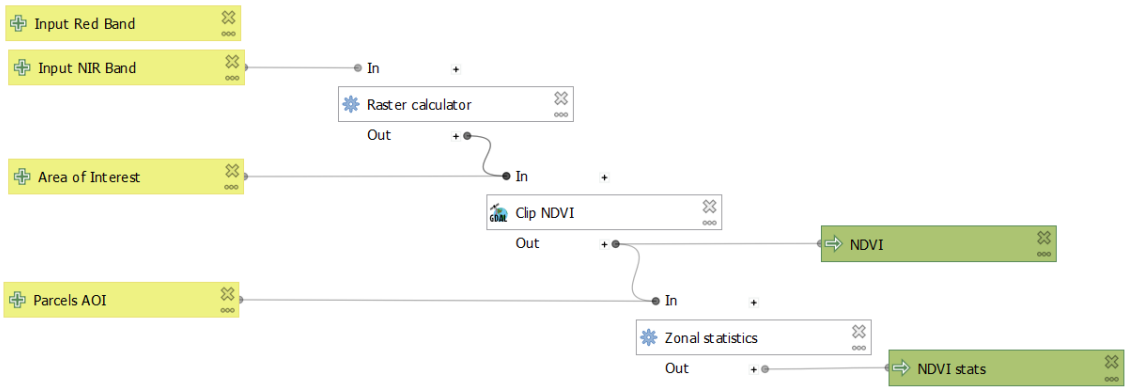

Figure 5.2 Automation Model for Operational Processes

In the initial stage of the model, the required inputs were defined: the red and near-infrared bands for NDVI calculation, the shapefile of the area of interest to clip the NDVI layer according to each study zone, and finally, the shapefile outlining the cultivated parcels within each zone to calculate the relevant statistical values for each.

5.1.1. Raster calculator (Raster Arithmetic)

The widely used vegetation index in phenology studies is the Normalized Difference Vegetation Index (NDVI). It is calculated as the ratio between the near-infrared (NIR) and red bands. The index is normalized to obtain values between -1 and 1. Values between -1 and 0 are associated with the presence of water bodies, bare soil, or urbanized areas. Values between 0 and 0.2 indicate sparse or unhealthy vegetation. Moderate to good vegetation cover corresponds to mean values between 0.2 and 0.5. Finally, high values between 0.5 and 1 represent healthy and dense vegetation with high photosynthetic capacity.

Utilizing the "Raster calculator" algorithm from the Geospatial Data Abstraction Library (GDAL), it is possible to apply the Equation 1 for the calculation of NDVI values pixel by pixel.

The input data consists of the B8 (NIR) and B4 (Red) bands. The model then proceeds to apply the established mathematical operation, as shown in the

"Expression" box in *Figure* 5.3. The outcome of this operation is a layer containing NDVI values for each pixel in the image, ranging from -1 to 1.

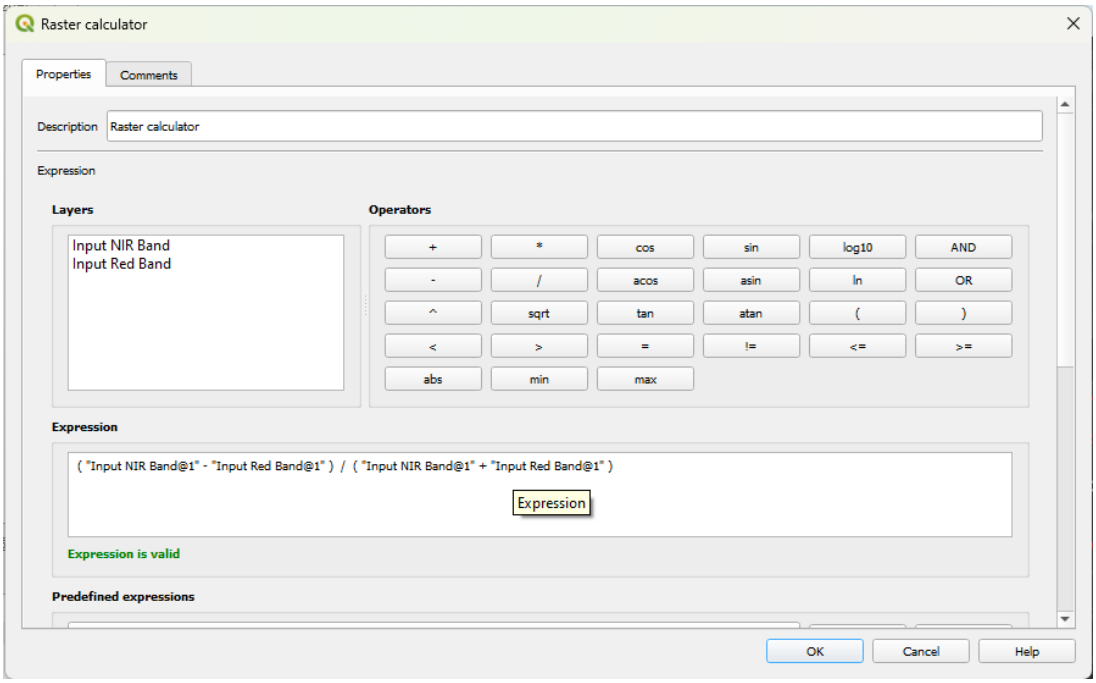

Figure 5.3 Raster Calculator configure

5.1.2. Clip Raster

The images obtained through The Copernicus Data Space Ecosystem platform extend beyond the boundaries of our specific interest. Therefore, it is imperative to perform clipping operations to focus attention on the areas of greater relevance. To carry out this procedure, the "Clip raster by mask layer" algorithm from the Geospatial Data Abstraction Library (GDAL) was employed *Figure* 5.4. The resulting image from this clipping process corresponds to the stratum containing the values of the Normalized Difference Vegetation Index (NDVI), previously calculated in the earlier phase of the analysis. This operation significantly reduces the computational processing times required in subsequent stages.

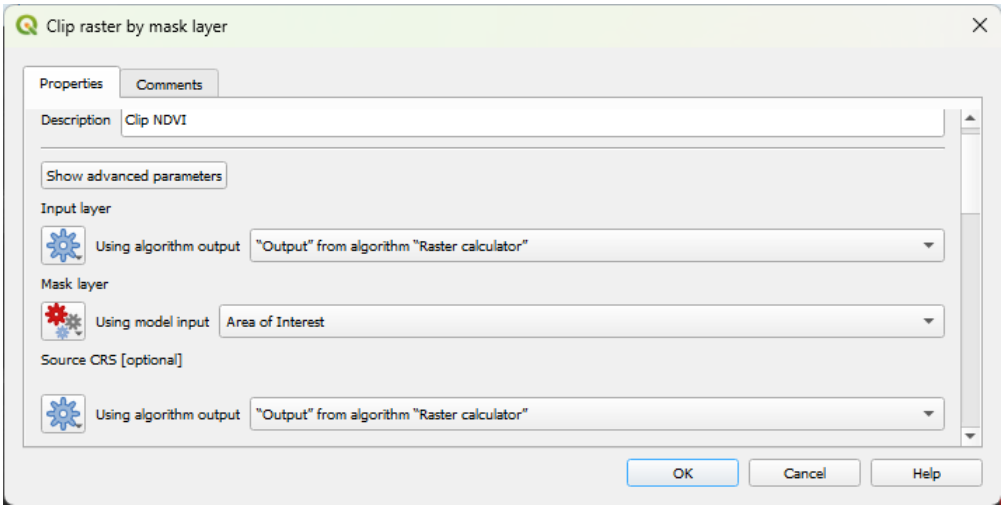

Figure 5.4 Clip raster by mask layer configure

5.1.3. Statistics by parcels

To compute the statistical indicators of interest within each parcel, the "Zonal statistics" algorithm integrated into QGIS was utilized. This tool allows the selection of which statistics to calculate within an assigned zone. In this context, the average, standard deviation, minimum, and maximum values of the Normalized Difference Vegetation Index (NDVI) were chosen *Figure* 5.5.

Before applying the algorithm, a shapefile was created to delimit the parcels for the temporal analysis. These parcels, selected from fields with diverse geometry and different background soils, met the criterion of having a minimum area of 8 hectares. This requirement was established to ensure sufficiently extensive areas for analysis, thereby avoiding discrepancies in NDVI values among pixels.

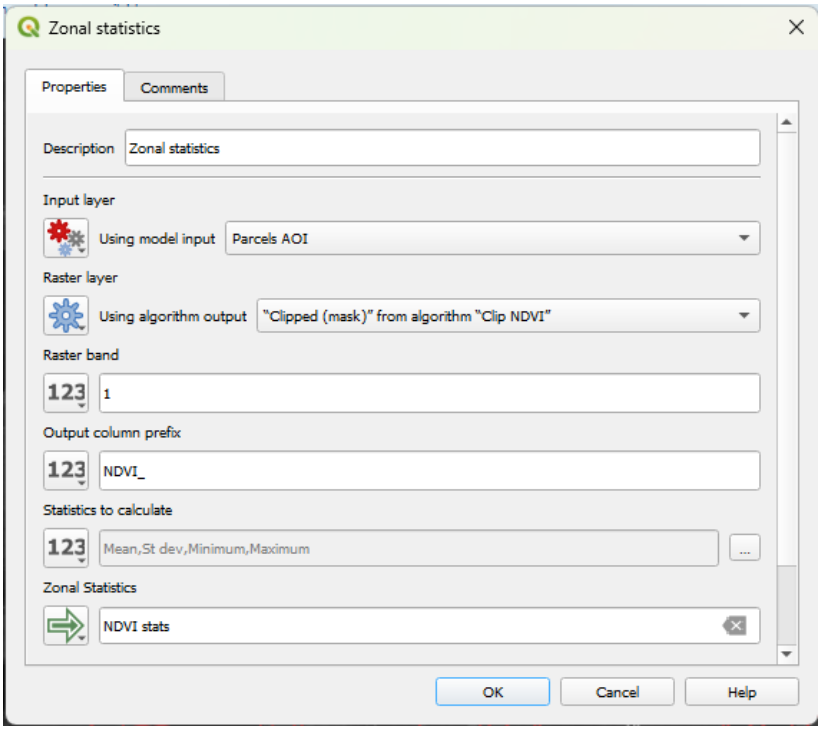

Figure 5.5 Zonal statistics configure

The execution of this operation generates a multipolygon-type file containing predefined statistical values for each parcel on the evaluated date. Subsequently, these values are exported to an Excel spreadsheet with the purpose of constructing the time series of the Normalized Difference Vegetation Index (NDVI).

5.2. Excel operations

By importing the NDVI values calculated for each pixel on various dates from the acquired images into Excel, an initial graph of NDVI against time is created for each year of study and for each parcel in the three zones of interest.

In this section, the assessment of the behavioral patterns of different crops in the study years was conducted through visual comparison. Subsequently, a clustering process based on phenological behavior was applied to facilitate the identification of crops.

6. Results and Discussions

The multitemporal NDVI profiles for the three study sites during the period from 2019 to 2023 are depicted below. The analysis is presented for each evaluated year in each of the three zones of interest. For each study area, NDVI values were graphed per year and per parcel to distinguish trends among plots with similar timing of green-up, peak greenness, and senescence. This approach aims to enhance the identification of crop types within each parcel.

6.1. Zone A

6.1.1. 2019

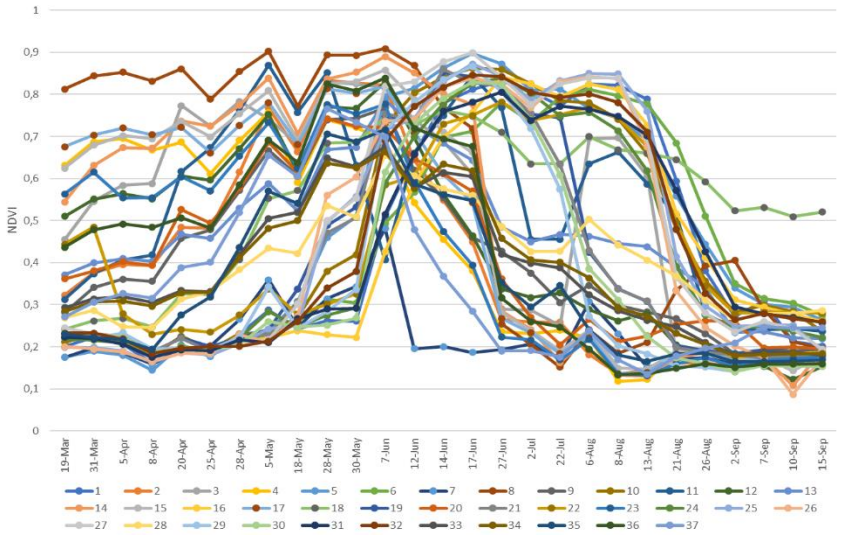

Figure 6.1. Zone A 2019 NDVI time series of all parcels

Pattern #1 (*Figure* 6.2) displays a later growth period which endure until late-May, after that reaches the peak NDVI values at mid-June. At early-July a slight decline in NDVI values is observed, after that the values increased persisting until late August, at which point values begin to decrease once again.

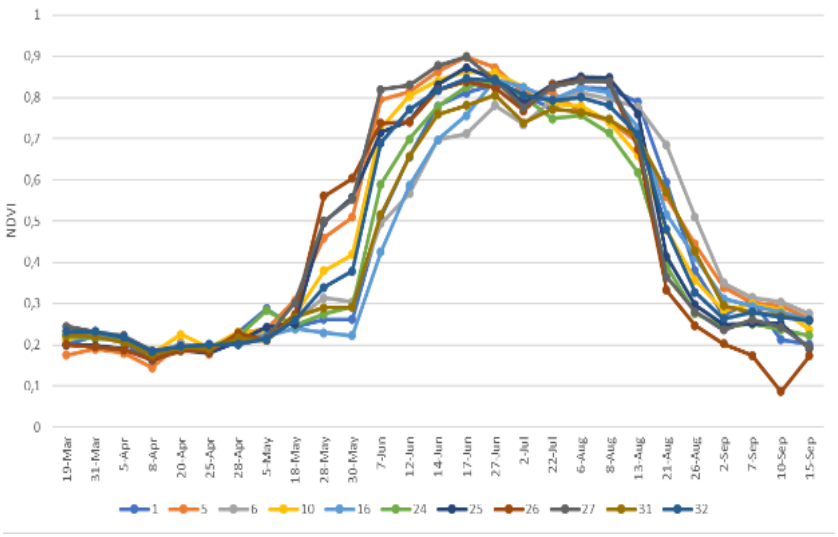

Figure 6.2 Zone A 2019 NDVI time series pattern #1

In the designated Pattern #2 (*Figure* 6.3) it is observed that, crops have similar temporal patterns, but NDVI values exhibit greater variability, particularly in the greening period, starting in March and peaking in late April. The crops in this pattern display two peaks in NDVI, the first in early May, and the second in early June. Followed by reduced greenness for the rest of the year.

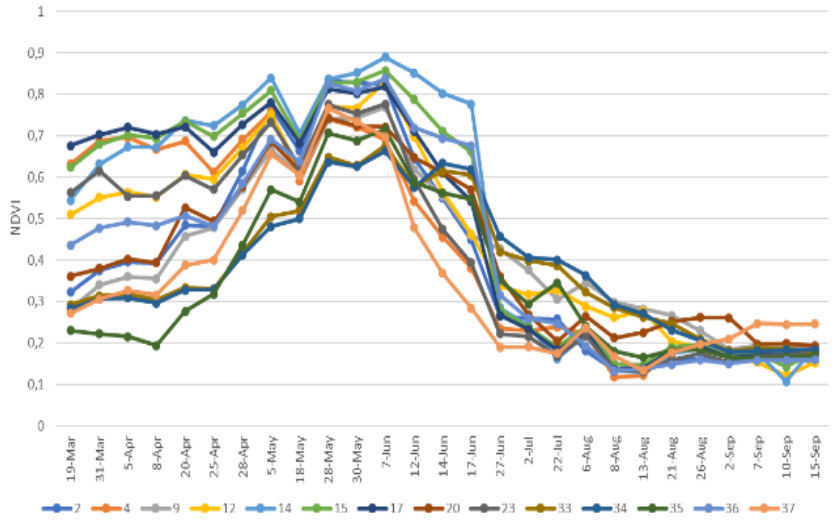

Figure 6.3 Zone A 2019 NDVI time series pattern #2

By comparing the two discernible patterns exhibited by crops in this region of interest during the evaluation year with the patterns found in the literature for

major grain crops, we can infer potential cultivation of Maize for parcels following Pattern #1 and Winter Wheat for parcels following Pattern #2.

6.1.2. 2020

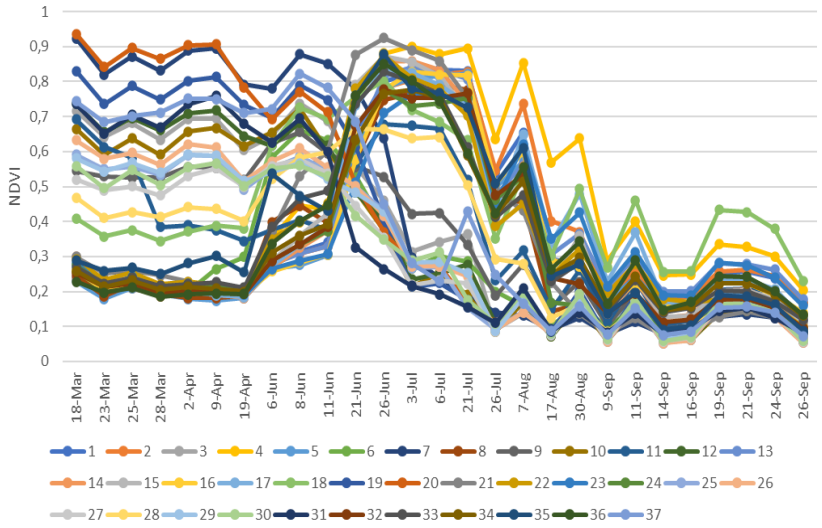

Figure 6.4 Zone A 2020 NDVI time series of all parcels

For the year 2020, two primary behavior patterns were identified among the crops. It is noteworthy that, for this year, cloud-free images for the month of May could not be obtained. In Pattern #1, the crop's greening stage occurs in early June and reaches its peak at the end of the same month (*Figure* 6.5). After these crops reach the maximum values, there is cyclicality as NDVI values decrease, with intermediate peaks. This behavior may be associated with growth and harvest cycles.

In *Figure* 6.6, Pattern #2 is presented. In the temporal evaluation period, the crop profile starts with maximum NDVI values in March. There is a brief decline at the end of April, followed by a second peak in June. It is important to note that data for the month of May are not available. After this second peak, the curve descends to reach minimum values.

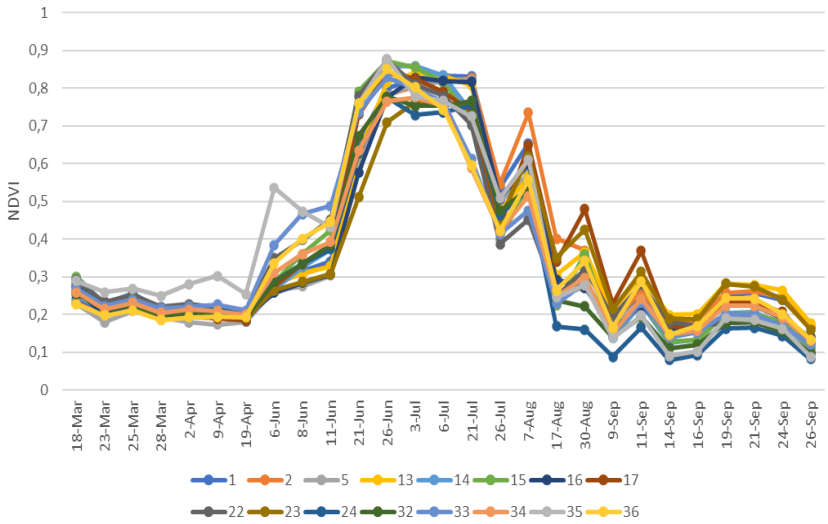

Figure 6.5 Zone A 2020 NDVI time series pattern #1

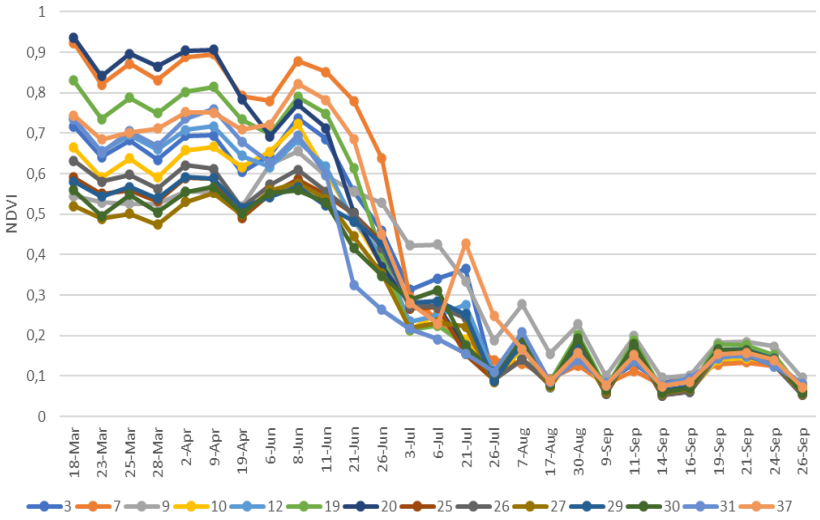

Figure 6.6 Zone A 2020 NDVI time series pattern #2

For this year, it was possible to determine the type of crop harvested in some study parcels, thanks to the crop map developed by the private company Onesoil for the year 2020(OneSoil, 2023). Parcels 2, 5, 13, 16, and 23 had maize crops, and these parcels aligned with Pattern #1. Meanwhile, parcels 3, 19, 25, 26, and 30 were cultivated with wheat, aligning with Pattern #2.

6.1.3. 2021

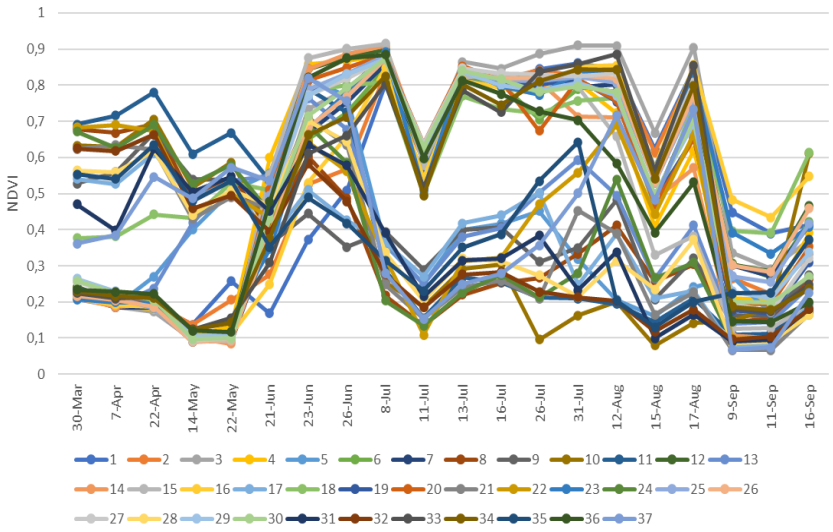

Figure 6.7 Zone A 2021 NDVI time series of all parcels

The data availability for the current year was comparatively lower than in preceding periods, resulting in less homogeneous curve patterns. Analogous to previous years, two predominant patterns have been discerned. The initial pattern, denoted as Pattern #1 (*Figure* 6.8), starts with low NDVI values until late May, followed by a progressive increase peaking in early July. Subsequently, a decline in NDVI values is observed, potentially attributable to an initial harvesting phase. Later, there is an upturn in values until mid-August, indicating another potential harvesting stage. Finally, a concluding cycle of growth and harvest is discernible between mid-August and mid-September. The entirety of satellite-captured images during July was processed, facilitated by minimal cloud content, ensuring continuity in the corresponding information for that month.

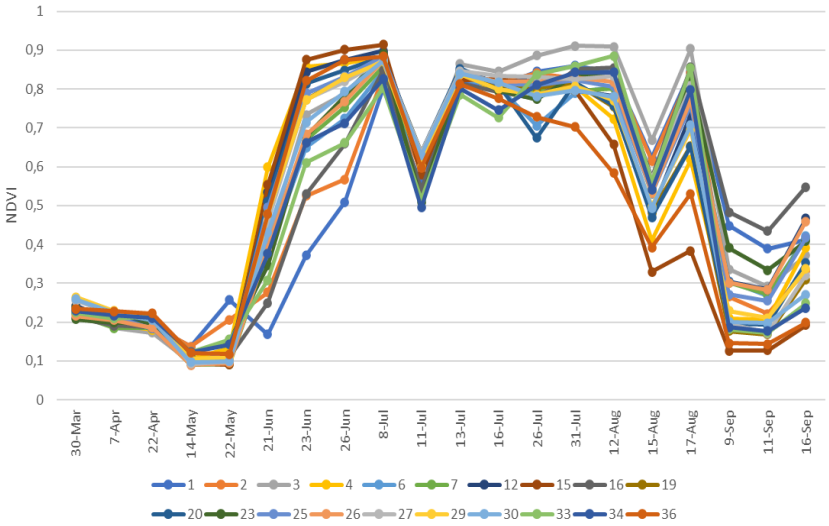

Figure 6.8 Zone A 2021 NDVI time series pattern # 1

The profile designated as Pattern #2 (*Figure* 6.9) initiates with high NDVI values, exhibiting cyclicity characterized by alternations between peaks and troughs, but with a tendency towards decreasing NDVI values. Between late July and mid-August, notable variability in the data pattern is observed, adding complexity to the phenological interpretation of spectral behavior during that period.

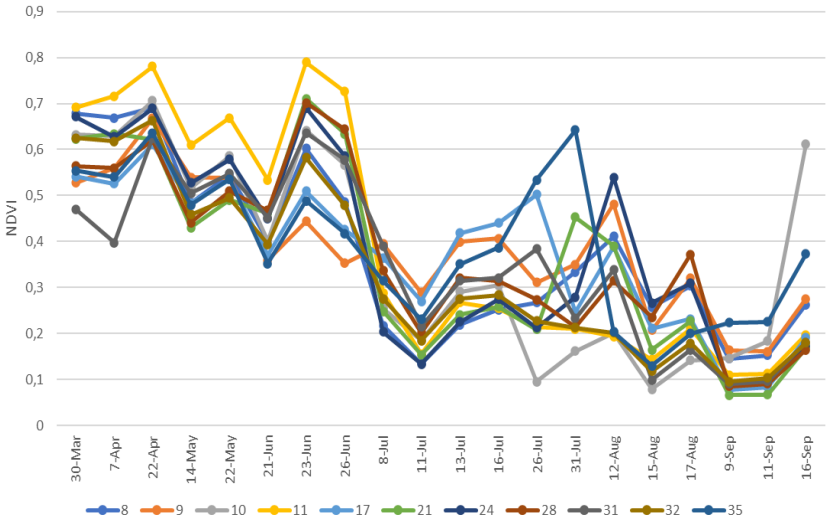

Figure 6.9 Zone A 2021 NDVI time series pattern #2

Based on information gathered from the World Cereal web portal, an initiative of the European Space Agency (ESA)(ESA, 2023), it is verified that parcels identified as 16 and 23 were allocated for maize cultivation during the harvesting period of the year 2021-2022, showing correlation with the previously outlined Pattern #1. Additionally, it is confirmed from the same source that parcels designated as 17, 24, 28, and 32 were dedicated to winter cereal cultivation, demonstrating alignment with the previously characterized Pattern #2.

6.1.4. 2022

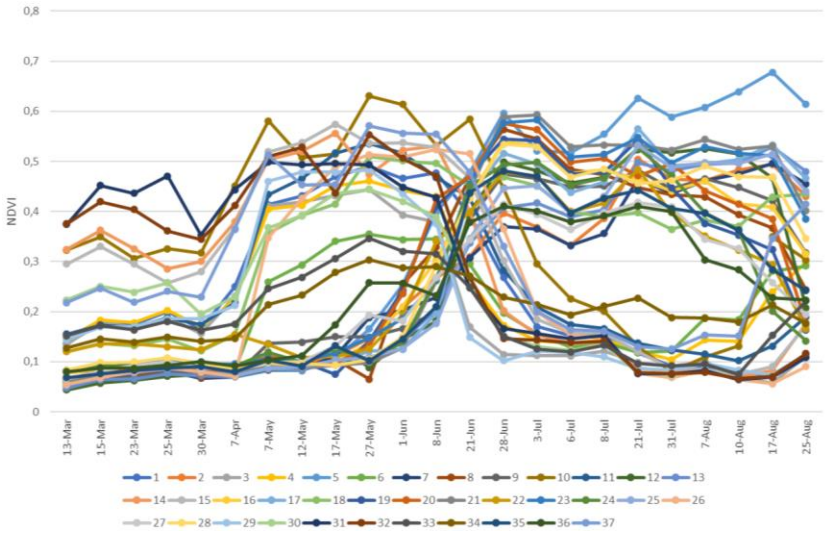

Figure 6.10 Zone A 2022 NDVI time series of all parcels

This year, the distribution of the obtained data exhibited greater uniformity throughout the months, except for April, where only one cloud-free image was possible to obtain, and September, in which it was not feasible to acquire a cloud-free scene, and therefore, the spectral behavior of the crops could not be observed. For the other months, between 4 and 5 monthly images free of clouds were obtained.

As in previous years, two main NDVI profiles are visually identified in this region. Crops adhering to Pattern #1 (*Figure* 6.11) had their greening phase between early April and early May, with their maximum NDVI values ranging

from mid-May to early June. Then, there is a decrease in greening that persists until mid-August.

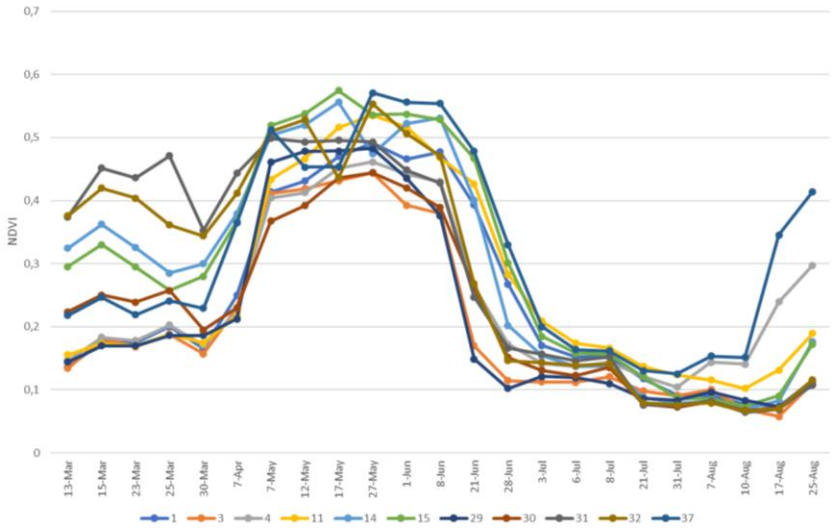

Figure 6.11 Zone A 2022 NDVI time series pattern #1

Pattern #2 starts with low NDVI values and has its peak growth phase in June. In July, there is a second greening peak with values lower than the previous one. The harvest stage begins at the end of August (*Figure* 6.12).

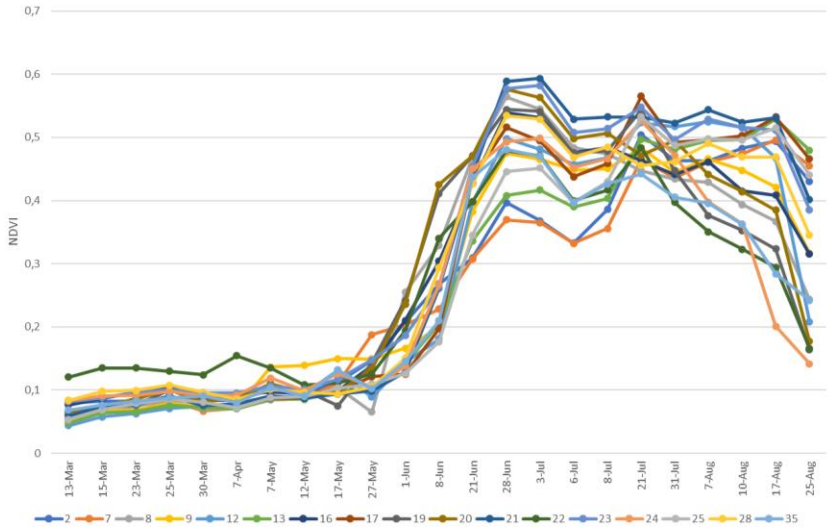

Figure 6.12 Zone A 2022 NDVI time series pattern #2

6.1.5. 2023

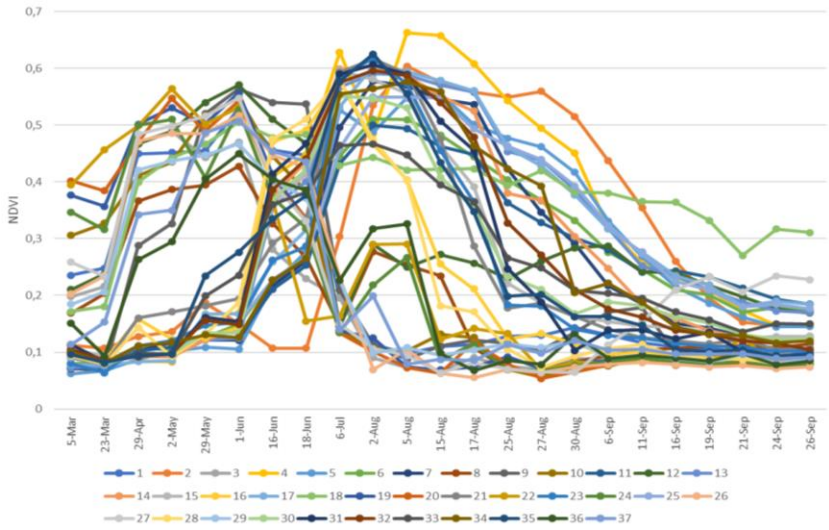

Figure 6.13 Zone A 2023 NDVI time series of all parcels

This year, a greater amount of data for the months of August and September was successfully collected, contributing to a smoother distribution of the curves towards the end of the analyzed period. Consistent with the trend of previous years, two main patterns were identified, to which the majority of the parcels were associated. However, the presence of a third pattern, designated as Pattern #3, was observed for parcels 16 and 28.

Pattern #1 (*Figure* 6.14) exhibits an increase in NDVI values from late March to mid-June. It is noteworthy that, for this year, only one scene for the month of July was available, corresponding to day 6, resulting in the maximum NDVI values on that day. Subsequently, a decrease in values is recorded, persisting from early August to late September.

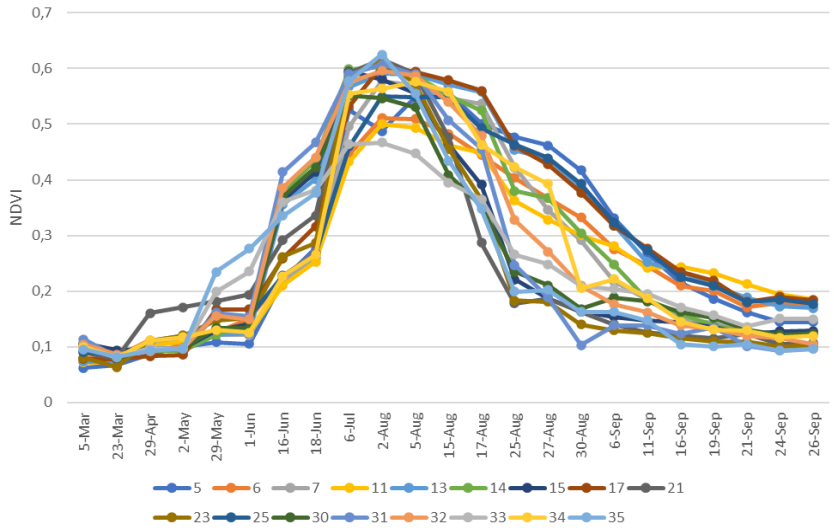

Figure 6.14 Zone A 2023 NDVI time series pattern #1

Pattern #2 (*Figure* 6.15) begins with a curve of values that experiences an increase from late March to late April. It reaches its maximum values in the months of May to mid-June, followed by a continuous decrease from July 6 to late September, a pattern observed in the majority of the parcels.

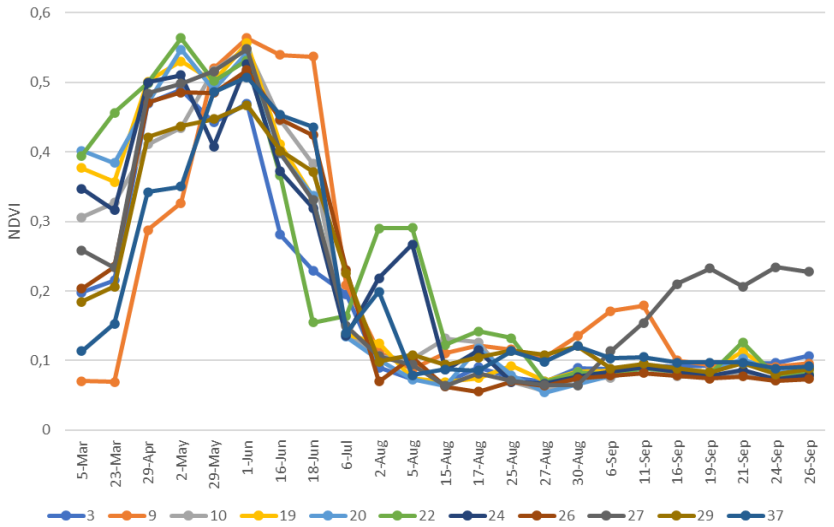

Figure 6.15 Zone A 2023 NDVI time series pattern #2

The pattern #3 (*Figure* 6.16), although presenting a profile similar to that of pattern #1, showed differences regarding the greening phase which begins in June, reaches its maximum value on July 6, and experiences a

pronounced decrease until mid-August. Subsequently, it shows a low persistence in NDVI values until late September.

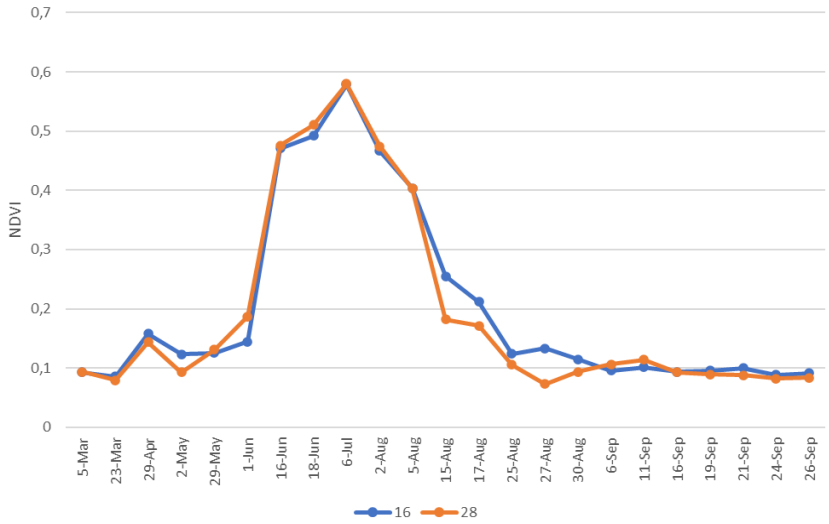

Figure 6.16 Zone A 2023 NDVI time series pattern #3

Finally, it is noteworthy that, in the last two years of the study, 2022-2023, a widespread decrease in NDVI values was observed for all evaluated parcels. The maximum values obtained during this period ranged between 0.7 and 0.6, in contrast to the three previous evaluation years (2019, 2020, 2021), where maximum values were recorded in the range of 0.9 to 0.8.

6.2. Zone B

6.2.1. 2019

The distribution of NDVI values for the parcels in the year 2019, present a uniform pattern. The crops exhibit a greening phase from late March to late May, reaching the maximum NDVI value during this period. Subsequently, a decrease in values is recorded from early June to mid-September *Figure* 6.17.

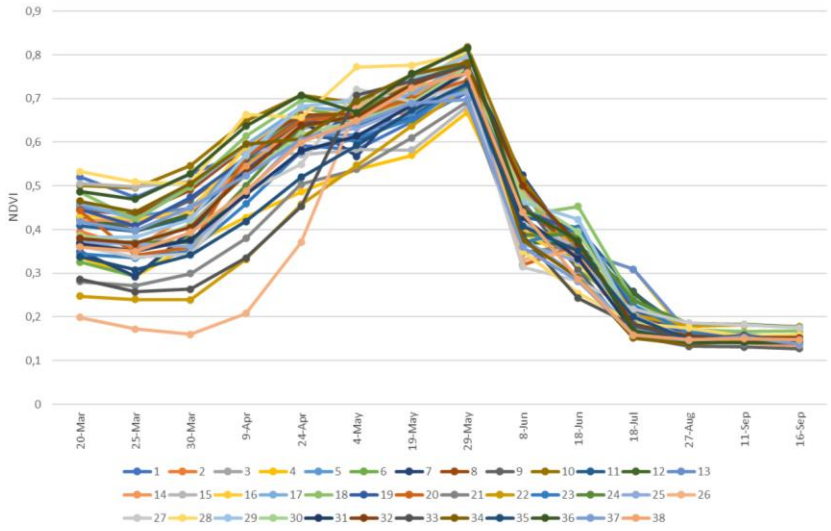

Figure 6.17 Zone B 2019 NDVI time series of all parcels

6.2.2. 2020

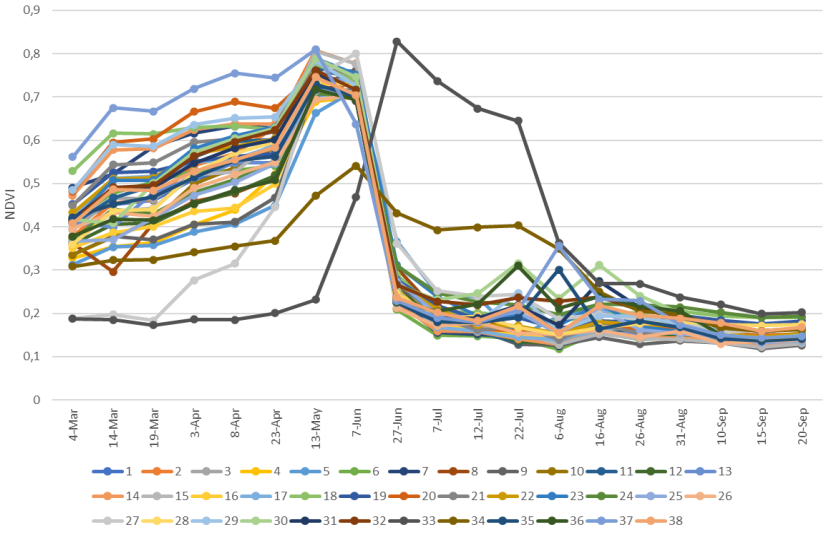

Figure 6.18 Zone B 2020 NDVI time series of all parcels

For the year 2020, a predominant trend was evident, aligning with the majority of the parcels and designated as Pattern #1 (*Figure* 6.19). This trend shares similarities with that observed in 2019, where an increase in values is recorded from March to April, reaching its peak in May. Subsequently, a decline in values is observed by the end of June, maintaining this trend until late September. It is essential to note that only

one image could be obtained for the month of May in the dataset compiled for this year.

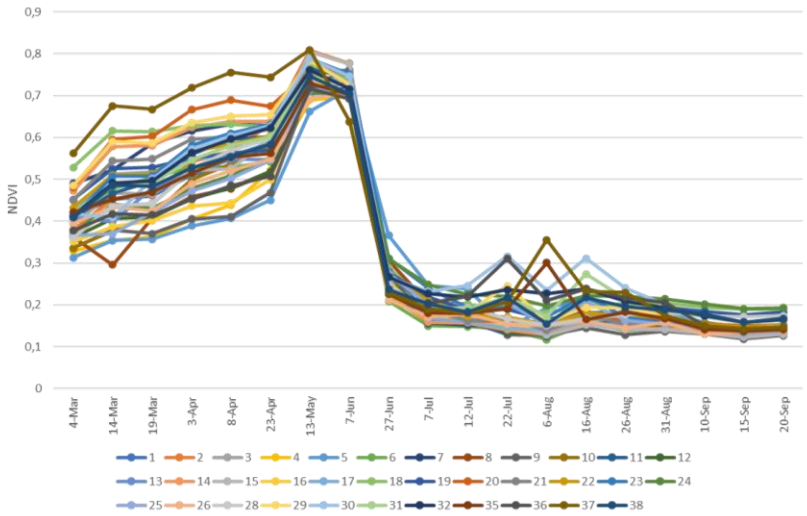

Figure 6.19 Zone B 2020 NDVI time series pattern #1

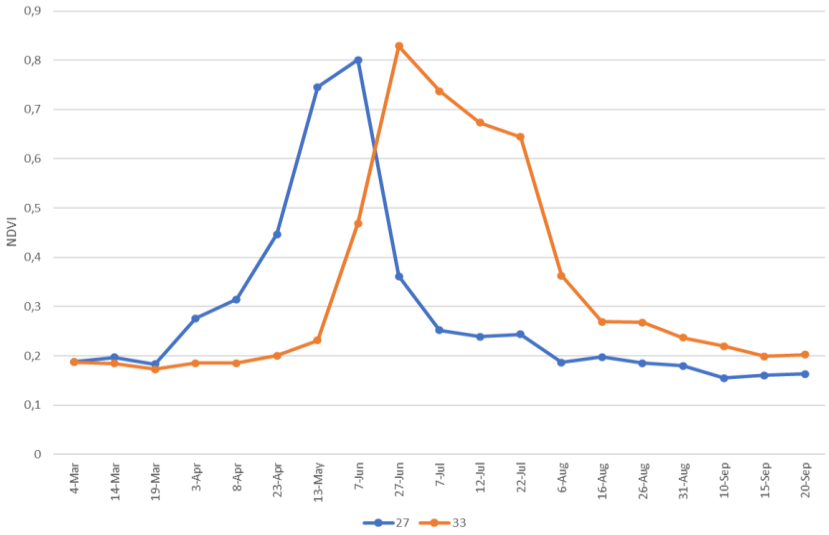

Figure 6.20 Zone B 2020 NDVI time series pattern #2

Figure 6.20 presents the value curves for two parcels that did not adhere to Pattern #1, specifically parcels number 27 and 33. The curve of parcel number 27, although exhibiting a profile similar to Pattern #1, starts with significantly lower NDVI values, and its greening phase begins in early April. On the other hand, the curve of parcel number 33 shows its greening phase

between mid-May and late June, reaching its maximum value in the latter month, followed by a decrease in values by late July.

It is worth mentioning that parcel number 34 was not included in the analysis, as it was cultivated with two types of crops with different temporal developments this year. This resulted in a flattened curve with lower values when averaging both crops.

Similar to other regions, for this year was possible determine the type of crop harvested in some of the study parcels, thanks to the crop map developed by the private company OneSoil for the year 2020(OneSoil, 2023). It was identified that parcel #27 was dedicated to barley cultivation; parcel #33 was cultivated with sunflower; while parcels 20, 21, 22, 29, 30, 31, 32, and 38 were cultivated with wheat.

6.2.3. 2021

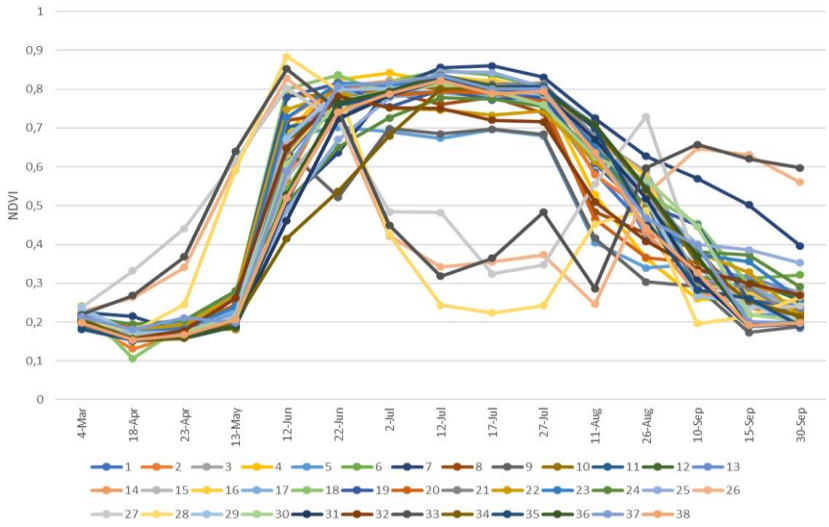

Figure 6.21 Zone B 2021 NDVI time series of all parcels

This year, a predominant trend was also identified in a large portion of the evaluated parcels; however, the pattern differs from the two previous years. The so-called Pattern #1 (*Figure* 6.22), in this case, is characterized by starting with low NDVI values, ranging between 0.2 and 0.1. Subsequently, it seems to initiate its greening period in mid-May and June. It is important to note that, in this case, only one image was available for analysis in May.

During the months of June to July, the crops reach their maximum NDVI values, afterwards, the values start to decrease until the end of September.

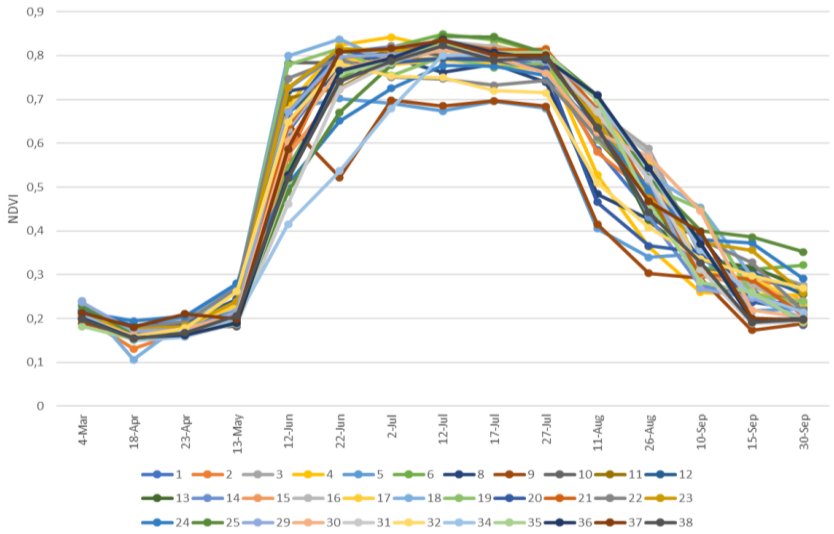

Figure 6.22 Zone B 2021 NDVI time series pattern #1

The second identified pattern (*Figure* 6.23) corresponds to parcels 26, 27, 28, and 33. Although there is greater variability in the behavior of the curves from mid-August to late September, the initial greening phases, the maximum NDVI, and the decline exhibit a similar pattern. Focusing on this part of the curve, an increase in values is observed from early March until reaching the peak in mid-June, followed by a decline until early July.

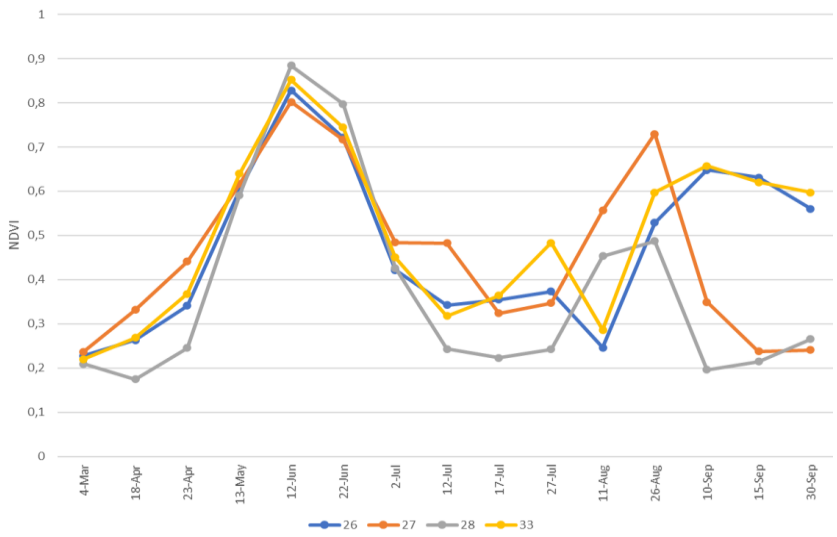

Figure 6.23 Zone B 2021 NDVI time series pattern #2

Out of the 38 selected parcels in this area for analysis, only 1 was excluded. Upon verifying the data provided by the World Cereal program for the year 2021 in the study region, it is confirmed that parcels 26 and 27 were dedicated to winter cereal cultivation, while no additional information was available for the rest of the parcels.

6.2.4. 2022

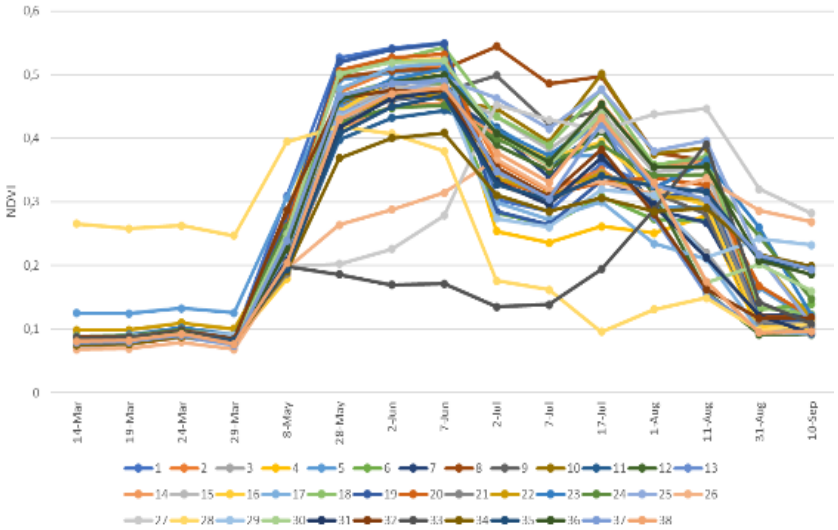

Figure 6.24 Zone B 2022 NDVI time series of all parcels

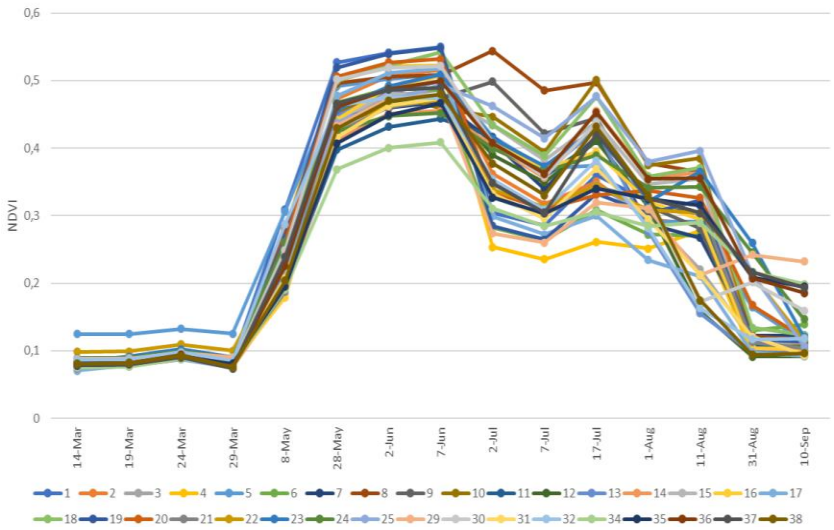

Figure 6.25 Zone B 2022 NDVI time series pattern #1

In accordance with the years previously analyzed, most of the harvested crops in the parcels adhered to a primary trend, specifically Pattern #1 (*Figure* 6.25). In this pattern, the greening process of the harvest begins in May, reaching its peak in June, and then undergoes a decline in NDVI values until mid-August. During this period, intermediate peaks are observed with values lower than the recorded maxima. It is noteworthy that in April, it was not possible to obtain images with cloud coverage low enough for processing. Among the 38 evaluated parcels, only 4 exhibited indistinguishable patterns.

6.2.5. 2023

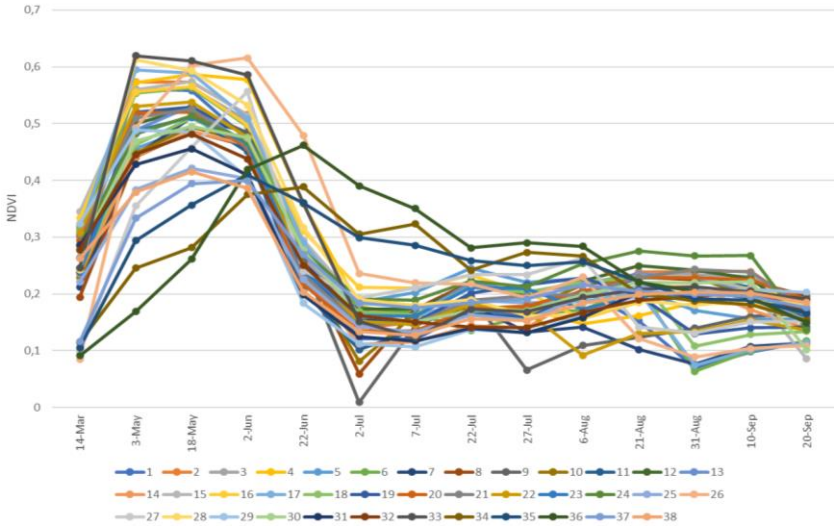

Figure 6.26 Zone B 2023 NDVI time series of all parcels

In the last analyzed year, a consistent behavior with the preceding years was observed, where most crops followed a common trend. The profile for this year displays an earlier greening stage, occurring between March and early May (*Figure* 6.27). It is pertinent to note that, for this dataset, no images were available for the month of April. The maximum NDVI values were recorded in May until early June, followed by a persistent decline in the subsequent months, lasting until the end of September.

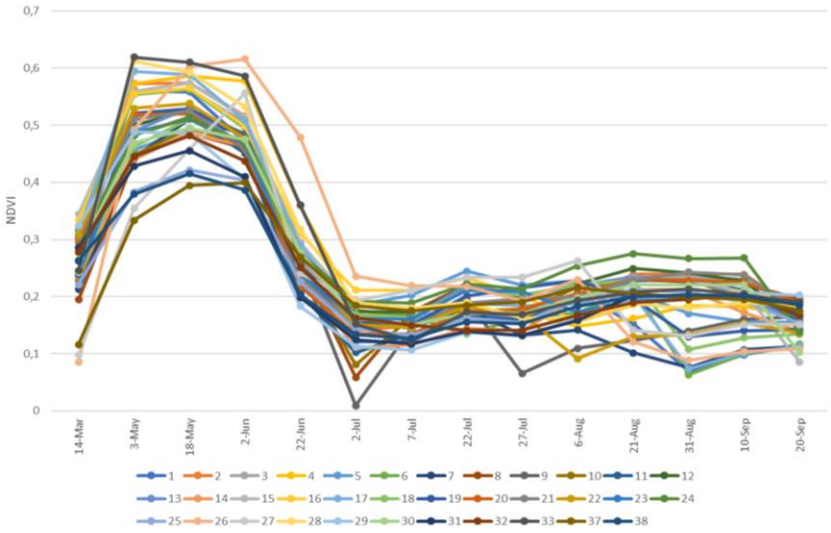

Figure 6.27 Zone B 2023 NDVI time series pattern #1

The profile exhibited by parcels 34, 35, and 36, designated as Pattern #2 (*Figure* 6.28), showcased its greening phase from mid-March to early June. It reaches its peak values in mid-June and exhibits a more gradual decline in values. Notably, the maximum values for this pattern are lower compared to those of Pattern #1. While for Pattern #1, the values ranged between 0.4 and 0.7, for Pattern #2, they vary in the range of 0.35 to 0.5.

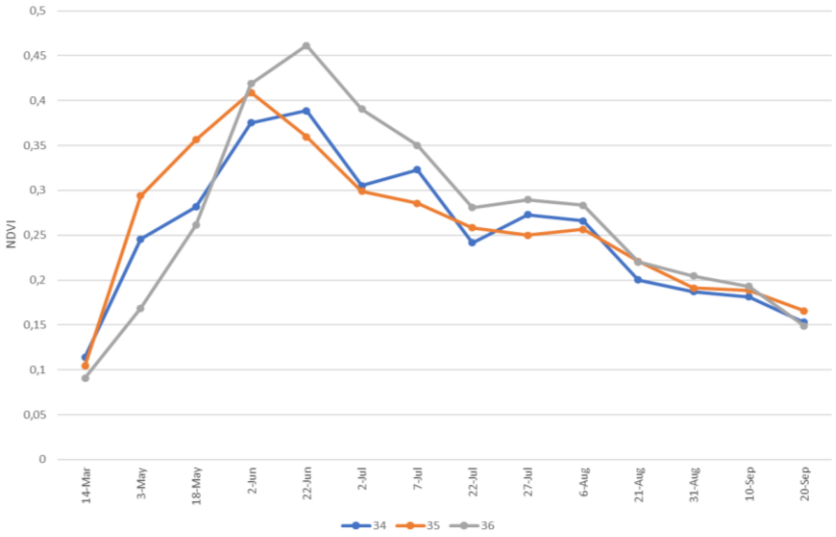

Figure 6.28 Zone B 2023 NDVI time series pattern #2

Consistent with the observations in Zone A, the last two years under analysis showed a decrease in the maximum NDVI values. While during the period from 2019 to 2021, the values reached maxima of up to 0.9, in the last two years of the study, these values were slightly above 0.6.

6.3. Zone C

6.3.1. 2019

Examining the phenological dynamics of the 53 delineated parcels within the third study area for the year 2019, five predominant patterns were discerned. This year, image processing for June was not feasible, and only one image was obtained for July due to a high percentage of cloud cover.

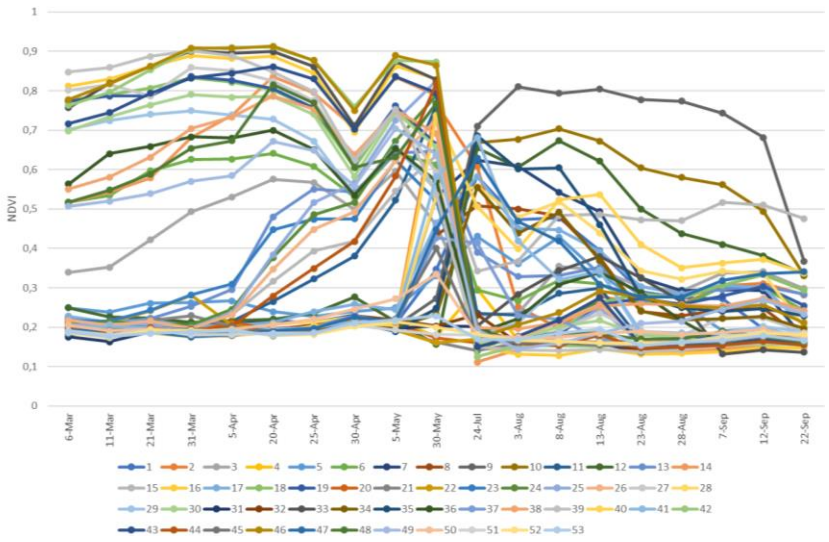

Figure 6.29 Zone C 2019 NDVI time series of all parcels

The predominant trend observed among the parcels was adherence to Pattern #1 (*Figure 6.30*). This pattern initiates with a growth phase extending from early March to late April, marked by a subtle decline. Subsequently, NDVI values experience an increase in May. In late July, a sudden decline in values is observed, attributed to limited image availability in the preceding months, followed by sustained diminished greenness for the rest of the year.

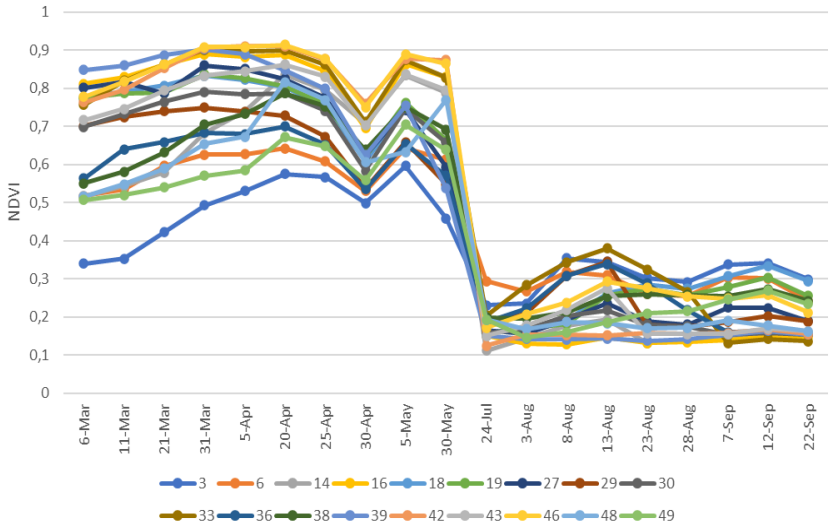

Figure 6.30 Zone C 2019 NDVI time series pattern #1

Pattern #2 (*Figure 6.31*) is characterized by initial low NDVI values persisting until May, where the phase of maximal growth initiates. In terms of the decline in values, there's an early trend for parcels 7 and 8, while it maintains higher levels until late September for parcels 9 and 10.

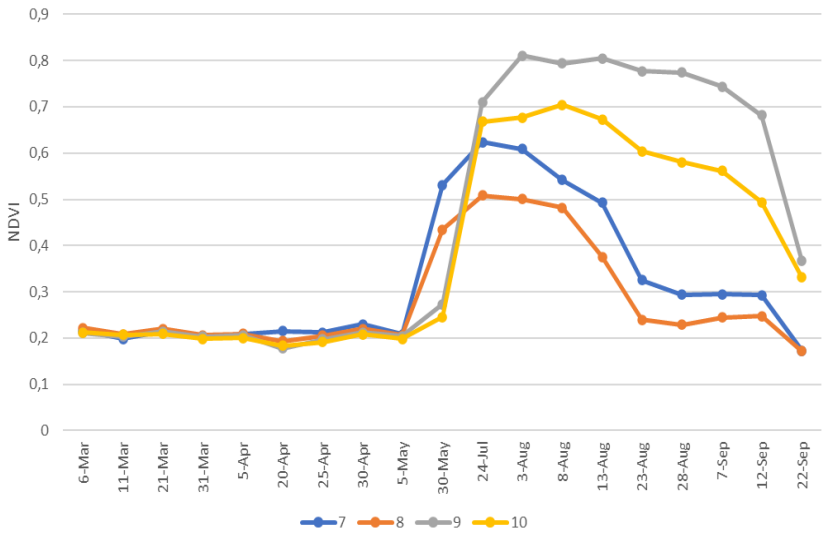

Figure 6.31 Zone C 2019 NDVI time series pattern #2

In Pattern #3 *(Figure 6.32*), the peak growth period occurs from April to late May. Due to the lack of data for the following months, a rapid decline in values is experienced towards the end of July, persisting until late September.

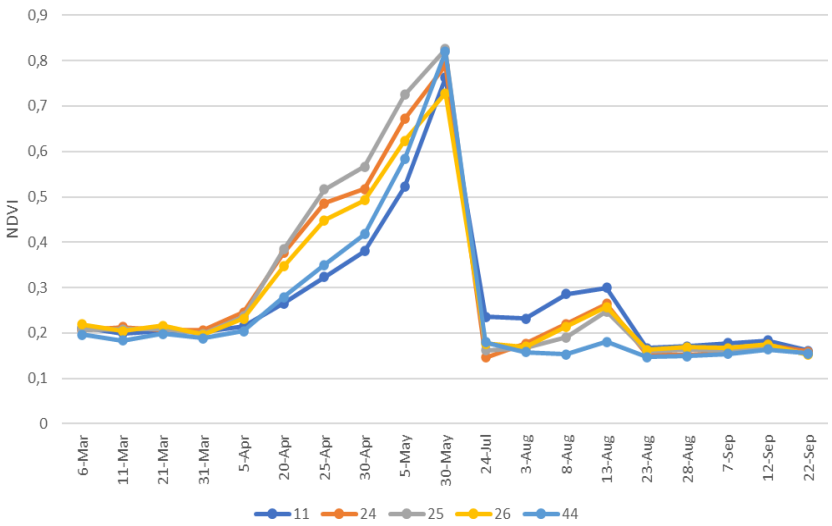

Figure 6.32 Zone C 2019 NDVI time series pattern #3

The time series of NDVI in pattern #4 (*Figure 6.33*) could be associated to bare soils NDVI profiles. The curves, except for some peaks, present values below 0.25 throughout the entire year.

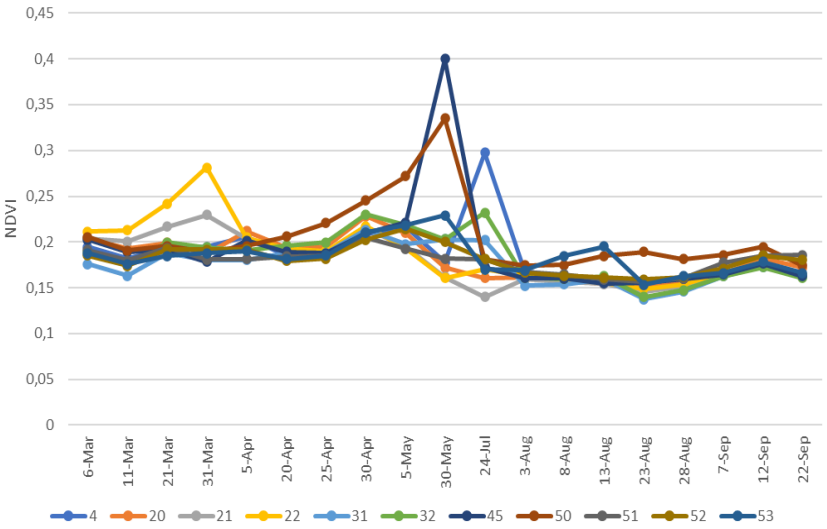

Figure 6.33 Zone C 2019 NDVI time series pattern #4

Pattern #5 (*Figure 6.34*) exhibits low NDVI values until early May, followed by an increase in values, reaching the maximum peak on the only available day for July. Subsequently, a decline ensues until late September. It is noteworthy that the maximum values in this pattern are lower than those observed in the previous patterns, excluding pattern #4.

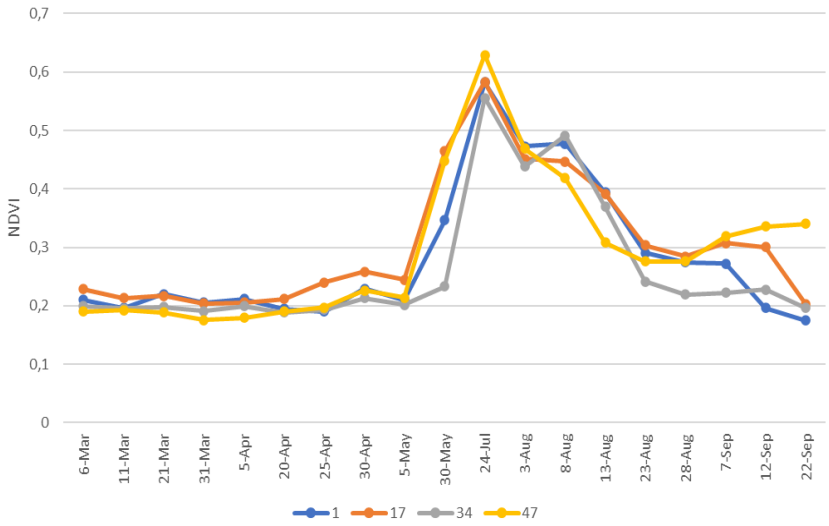

Figure 6.34 Zone C 2019 NDVI time series pattern #5

6.3.2. 2020

In the year of analysis, two distinct patterns have been identified. Among these, 32 out of the total 53 parcels conformed to these patterns, while the remaining parcels were not considered for analysis due to exhibiting complex temporal patterns.

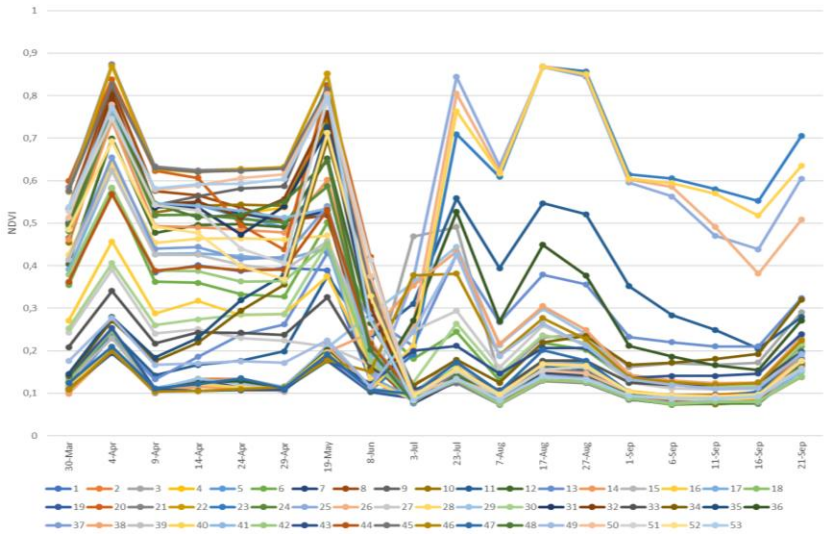

Figure 6.35 Zone C 2020 NDVI time series of all parcels

The primary pattern, designated as Pattern #1 (*Figure 6.36*), encompassed most of the parcels. This pattern has two greenness peaks, the first one from late march to early April, and the second one from late April to early June, followed by reduced greenness for the rest of the year.

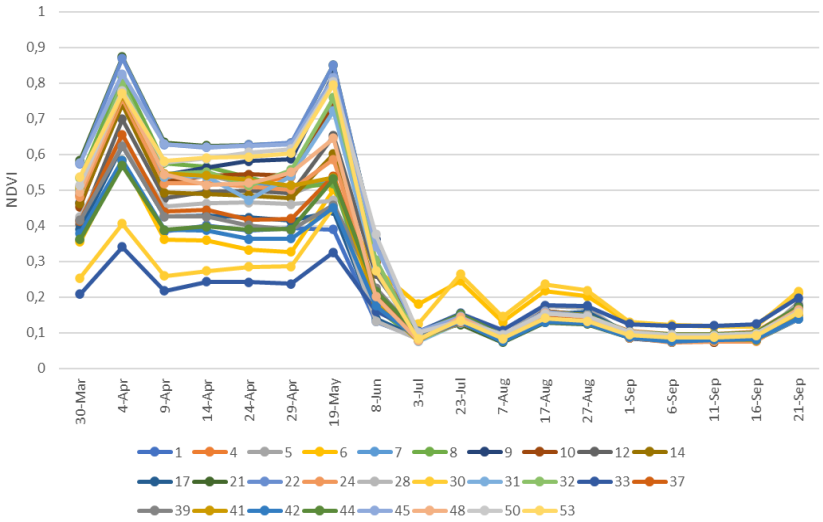

Figure 6.36 Zone C 2020 NDVI time series pattern #1

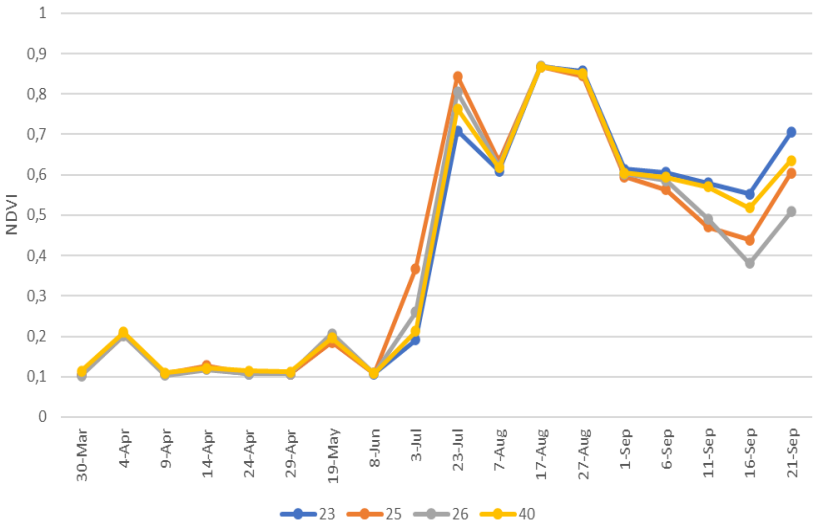

Figure 6.37 Zone C 2020 NDVI time series pattern #2

Pattern #2 (*Figure 6.37*) displays a later growth period which endure until mid-June, after that reaches the peak NDVI values at late July.

Similarly, to other regions, this year it was possible to ascertain the type of crop harvested in some of the study parcels, thanks to the crop map developed by the private company Onesoil for the year 2020(OneSoil, 2023). Parcel 40 was cultivated with sugar beet, assigned to Pattern #2. Parcels 4, 24, 42, 44, 45, 48, and 50 were cultivated with wheat, aligning with Pattern #1.

6.3.3. 2021

The phenological dynamics of crops during the year 2021 shows three distinct patterns in which the NDVI time series exhibited similarity among the crops.

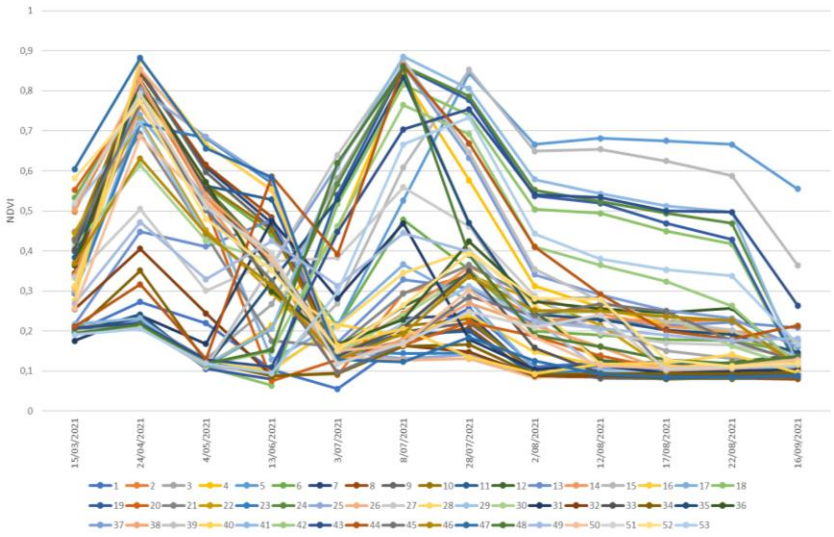

Figure 6.38 Zone C 2021 NDVI time series of all parcels

Crops assigned to Pattern #1 (*Figure 6.39*) emerge in March and reach the peak of their vegetative phase by late April. Subsequently, they undergo an initial harvesting period spanning from early May to late June. Towards the end of July, a second greening peak is observed, although with lower NDVI values compared to the first peak. Following this, NDVI values remain low for the rest of the year.

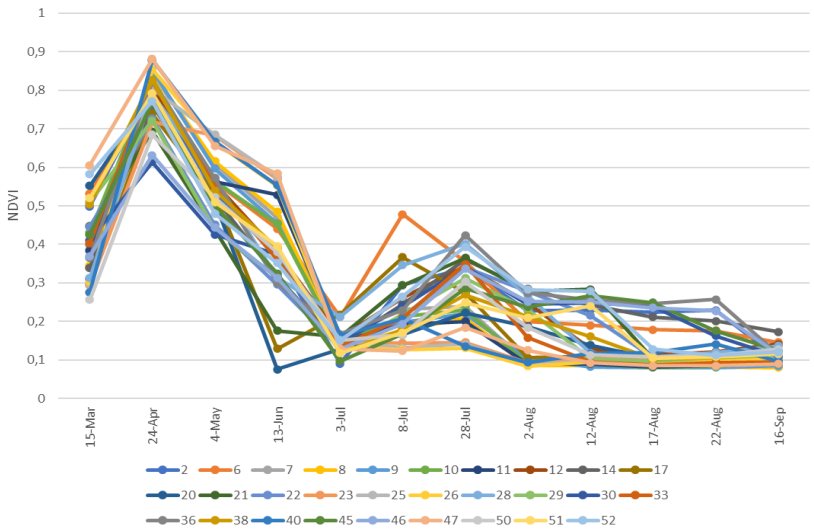

Figure 6.39 Zone C 2021 NDVI time series pattern #1

In Pattern #2 (*Figure 6.40*), the peak growth period occurs from mid-June to late July. Followed by a slight decline in NDVI values, persisting until late August, at which point values begin to decrease once again.

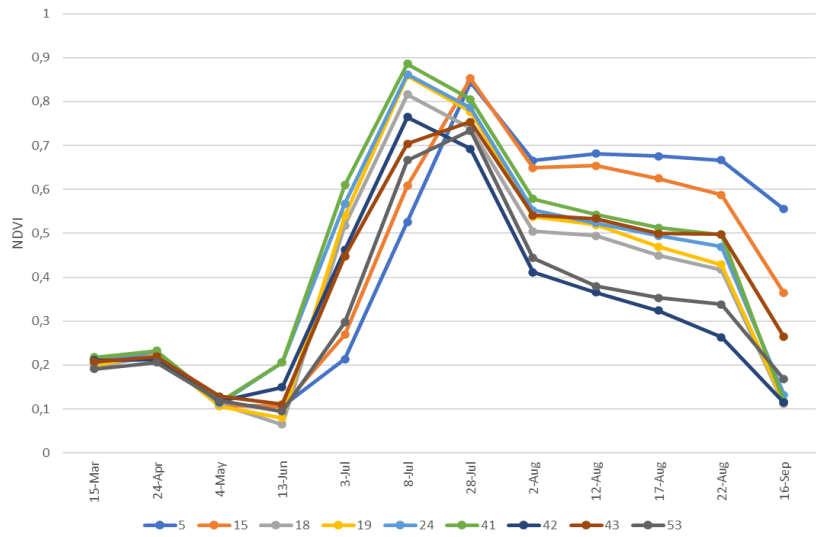

Figure 6.40 Zone C 2021 NDVI time series pattern #2

Pattern #3 (*Figure 6.41*), on the other hand, exhibits the peak of its vegetative phase in the month of June. Following this period, the crop is harvested, and NDVI values experience a decline that persists until late September.

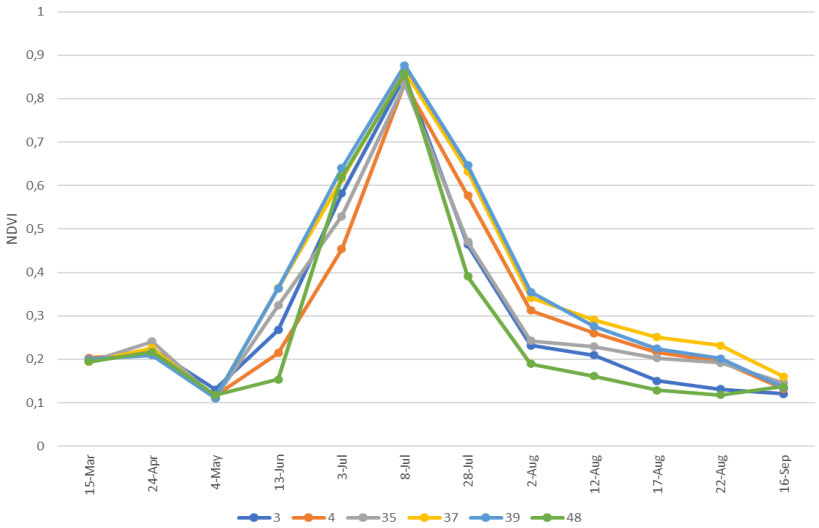

Figure 6.41 Zone C 2021 NDVI time series pattern #3

Upon verifying the data provided by the World Cereal program for the year 2021 in the study region (ESA, 2023), it is confirmed that parcels 2, 20, 21, 22, 23, 25, 26, 28, 29, 30, 33, 38, 40, 45, 46, 47, 50, 51, and 52 were dedicated to the cultivation of winter cereals.

6.3.4. 2022

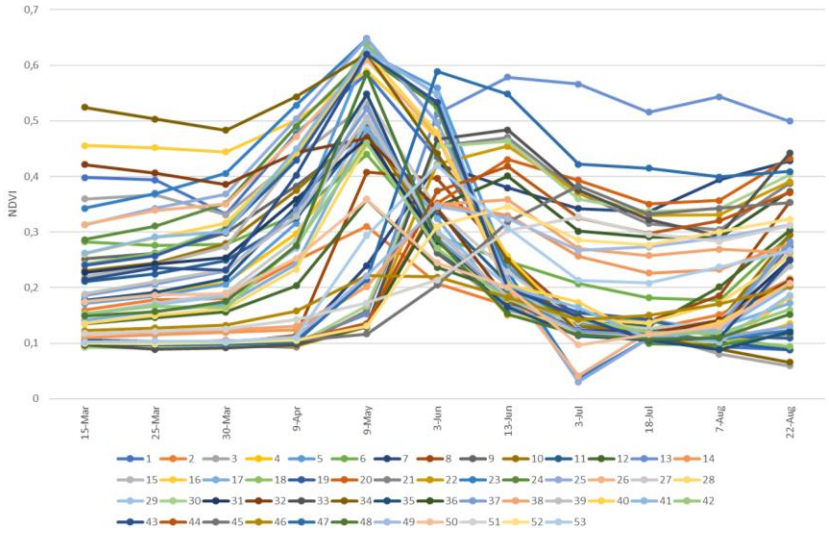

Figure 6.42 Zone C 2022 NDVI time series of all parcels

In the NDVI time series of the year 2022, four distinct behavior patterns were discerned among the crops. It is important to emphasize that, for the months

of April and May, access to a cloud-free image was limited to one per month. In September, cloud-free images were unattainable, rendering the spectral behavior of crops for that month unobservable.

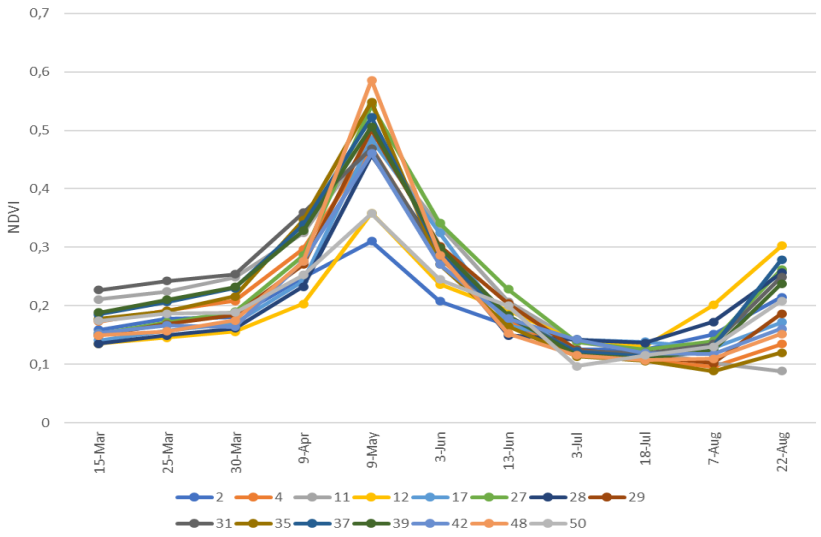

Figure 6.43 Zone C 2022 NDVI time series pattern #1

The first pattern (*Figure 6.43*) exhibits a singular cycle of greening and harvesting, with peak NDVI values in early May. In August, the behavior suggests a potential second emergence period.

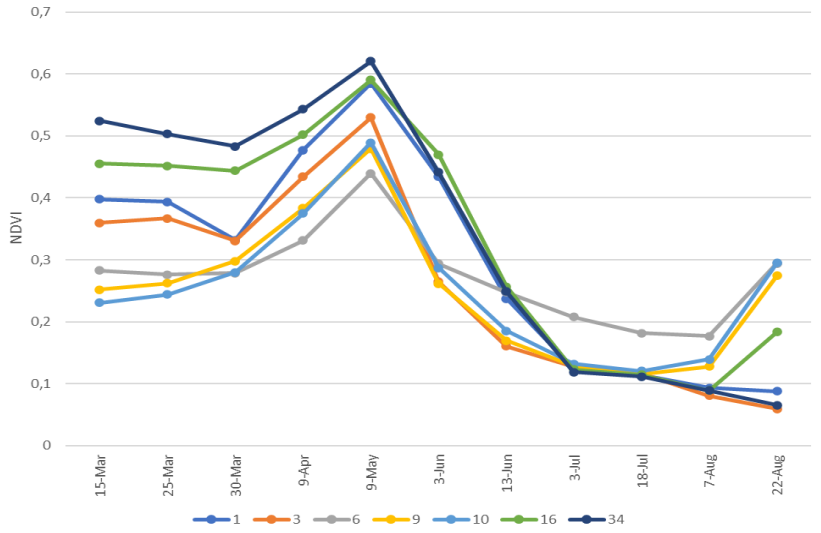

Figure 6.44 Zone C 2022 NDVI time series pattern #2

Pattern #2 (*Figure 6.44*) experiences its peak growth phase from March to May, followed by a reduction in greenness extending until late August, where a new greening phase appears to begin.

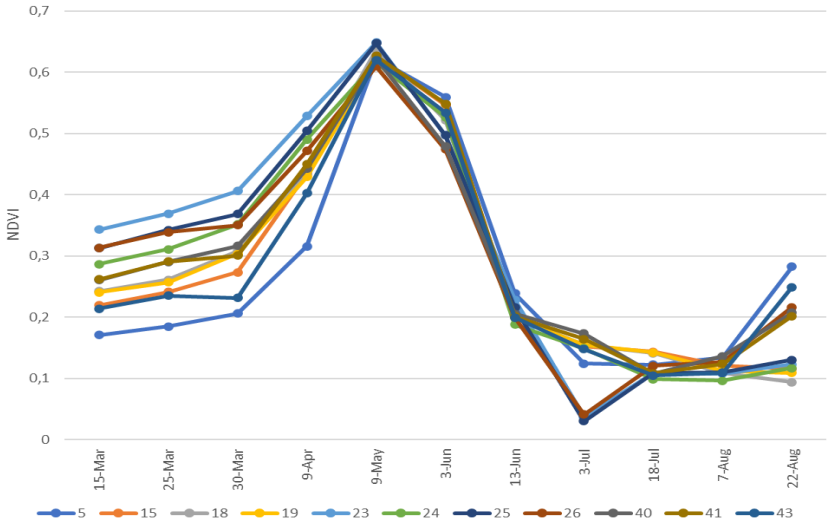

Figure 6.45 Zone C 2022 NDVI time series pattern #3

Pattern #3 (*Figure 6.45*) reaches its peak NDVI values in early May, followed by a decline persisting until early August. As in the previous patterns, at the end of August the crop seems to present a second stage of greening.

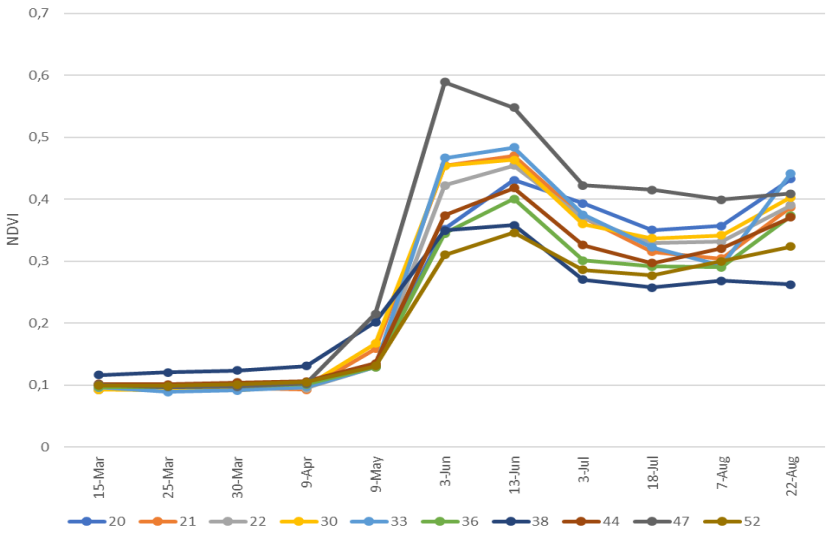

Figure 6.46 Zone C 2022 NDVI time series pattern #4

The fourth pattern displays a later growth period. The crop exhibits its lowest NDVI values in the first half of the year, with the peak growth phase occurring between mid-May and mid-June. Subsequently, a slight decline in values occurs until late August.

6.3.5. 2023

In the concluding year of the analysis, the response of NDVI time series from different parcels exhibited greater heterogeneity, challenging the identification of common patterns among them. However, two patterns encompassed a significant number of parcels. It is noteworthy that, for the months of March, April, May, and July, only one cloud-free image could be obtained per month.

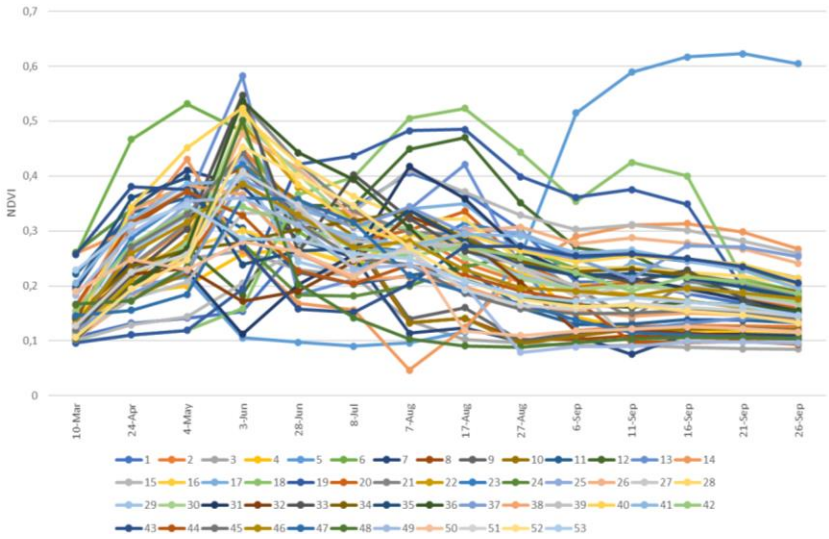

Figure 6.47 Zone C 2023 NDVI time series of all parcels

Pattern #1 (*Figure 6.48*) begins its vegetative phase in mid-March and reaches peak NDVI values in early June, followed by reduced greenness for the rest of the year. Pattern #2 (*Figure 6.49*) has the peak of its growth period between the months of March and April. After reaching this peak, it reduces its NDVI values below 0,3 for the rest of the year.

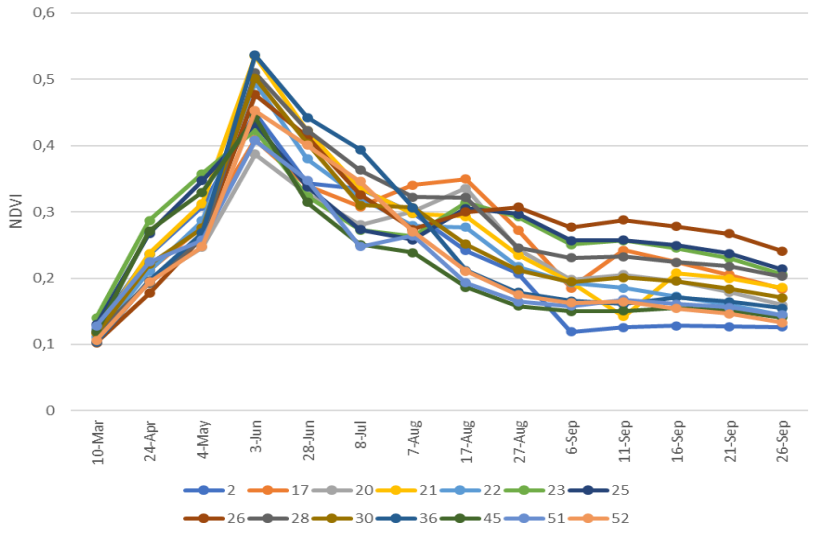

Figure 6.48 Zone C 2023 NDVI time series pattern #1

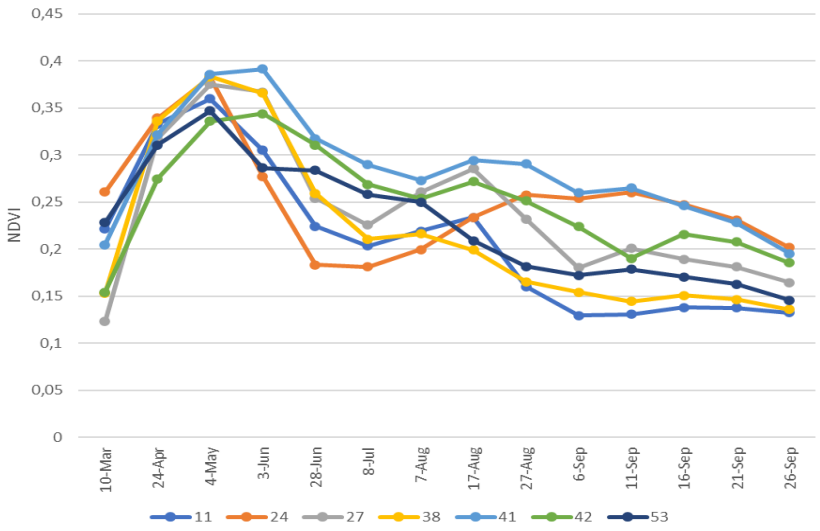

Figure 6.49 Zone C 2023 NDVI time series pattern #2

In this region, a general decrease in NDVI values is observed during the years 2022 and 2023, a behavior analogous to that recorded in zones A and B. In contrast to the first three years of analysis, where maximum values reached 0,9, in 2022 and 2023, the highest values stayed around 0.6.

6.4. Discussion

This study examined phenological changes in three study areas in Ukraine through the analysis of time series of the Normalized Difference Vegetation Index (NDVI) derived from Sentinel-2 images. Additionally, it investigated the potential association of these changes with the current conflict between Russia and Ukraine.

In this phase of the analysis, efforts were made to identify crops that exhibited similar behavior in their profiles over the five years of study in each area of interest. Curves were generated using the monthly average values of vegetation indices for each year. To explore any potential relationship with the ongoing conflict, dates of relevant events at both national and local levels were highlighted on the graphs, referencing those occurring in the major cities near the study areas (Zone A: Kropyvnytskyi city; Zone B: Mariupol city; and Zone C: Kherson city). These events ranged from the onset of the war, city occupations, illegal annexation of territories, displacement of civilians, bombings, to international condemnations related to these events.

Figure 6.50 illustrates the temporal average NDVI profiles for summer crops over the 5 years under analysis. These crops initiate their emergence in spring, reaching their peak during the summer months, typically in July. Upon comparing the curves, two notable aspects become apparent: the lower NDVI maximum values observed in the years 2022 and 2023, and the delayed emergence of crops during these same years (highlighted in red markers for the 2022 and 2023 periods in *Figure 6.50*).

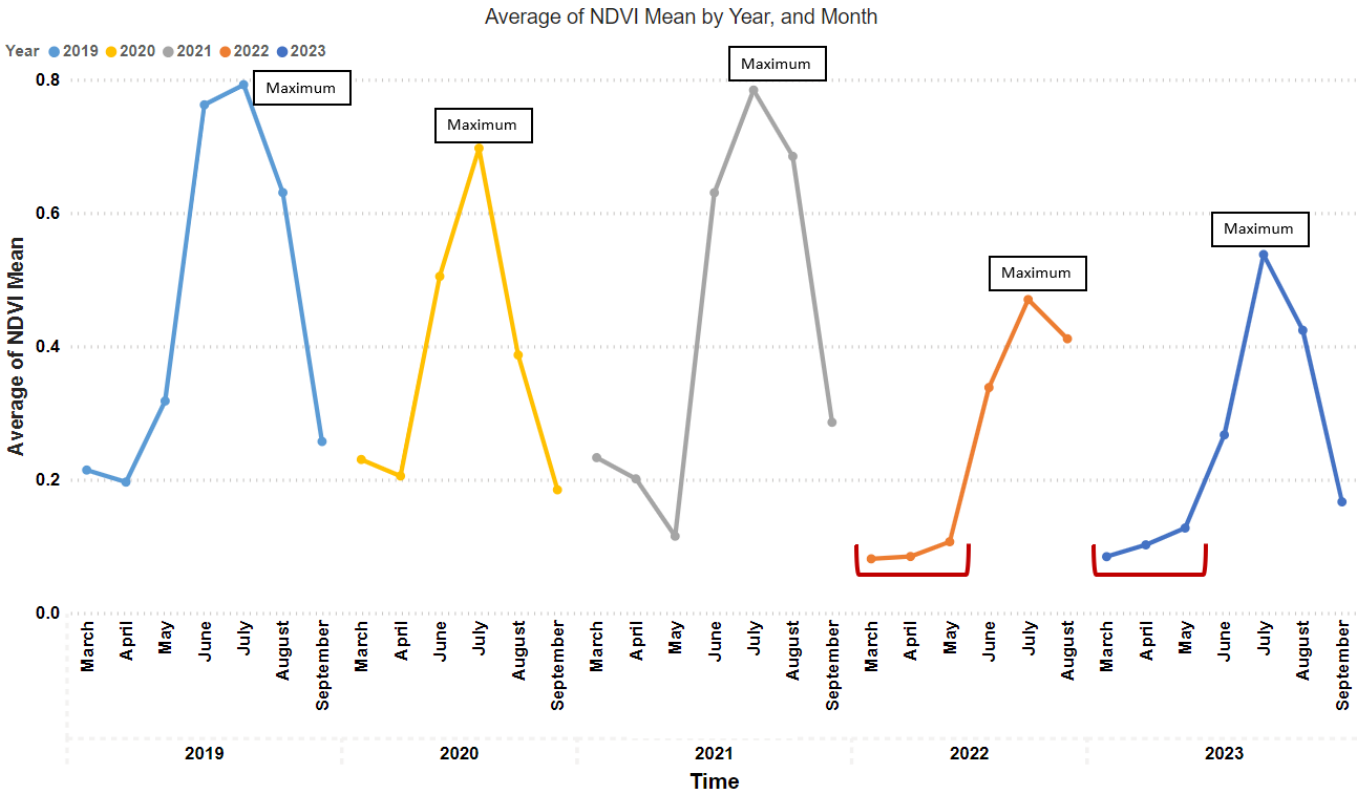

Figure 6.50 Average NDVI profiles of summer crops by month, Zone A

In *Figure 6.51* the temporal average NDVI profiles for winter crops are depicted. These profiles delineate a greening phase, typically spanning from March to April, with their peak NDVI values occurring in May. In alignment with the observations related to summer crops, the highest NDVI values for the years 2022 and 2023 exhibit the lowest magnitudes within the assessed temporal series. Concerning the patterns' for the same years, there are no significant changes.

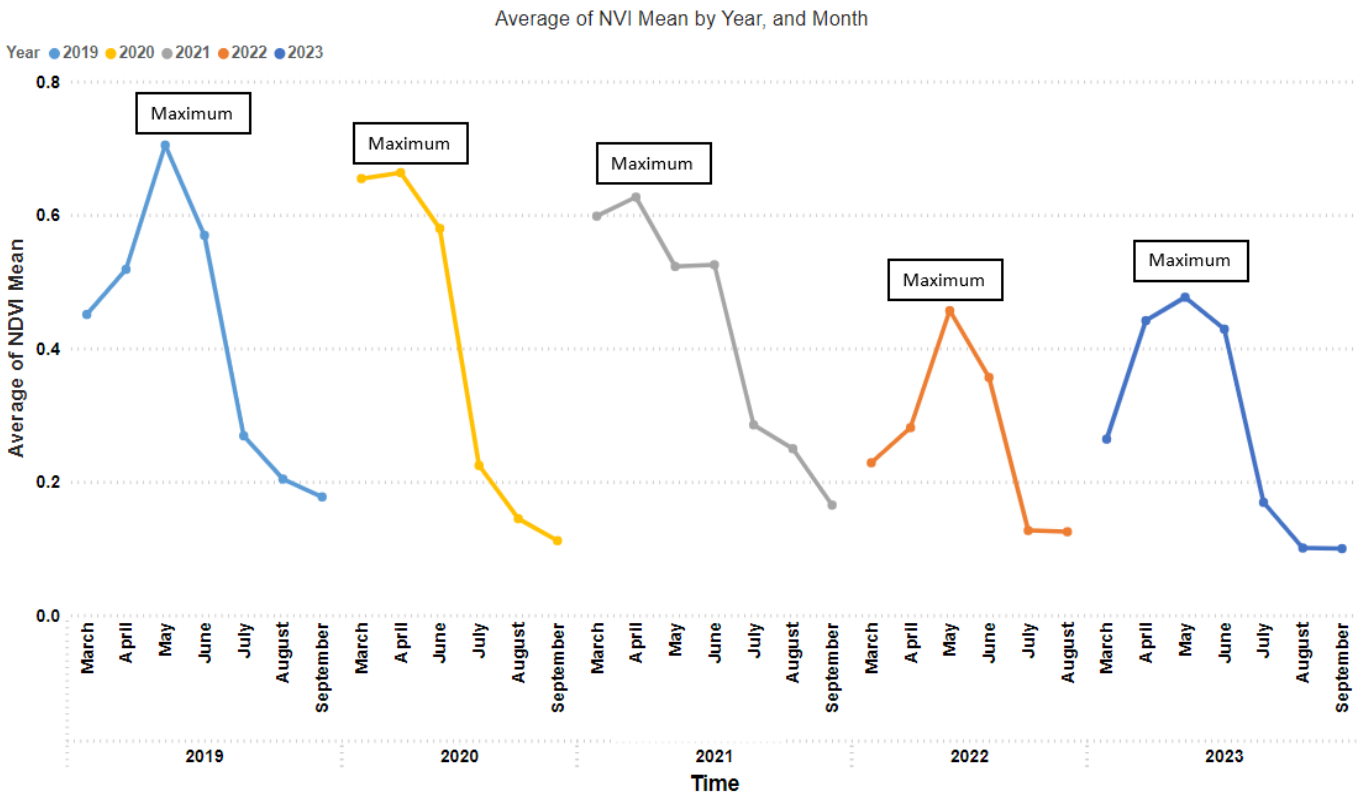

Figure 6.51 Average NDVI profiles of winter crops by month, Zone A

Even though the nearest major city to this study area, Kropyvnytskyi, has experienced only on June 4, 2023, was there a report of the impact of two missiles on an aerodrome near the city, red dotted line in *Figure 6.52*, is therefore considered the least affected zone, lower NDVI values are observed compared to previous years, especially in 2022, the year the invasion began.

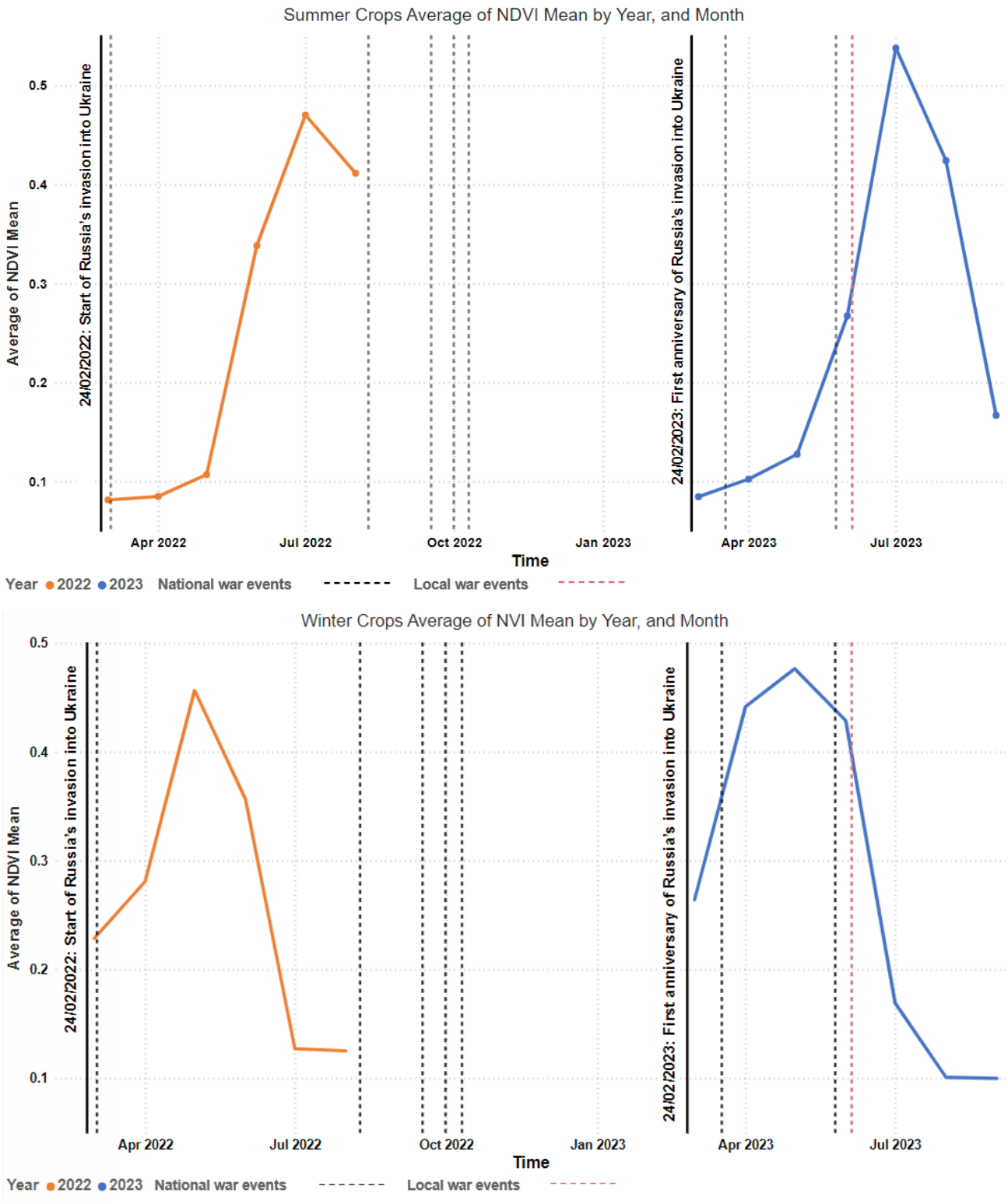

Figure 6.52 Key war events dates in Zone A

In Zone B, due to the consistent and prevailing trends observed across most parcels during the analyzed years, the temporal analysis is not divided between winter and summer crops. Instead, the average of the predominant time series for each year was graphed. In the majority of the years, the temporal pattern displayed characteristics consistent with a winter crop profile, with the exception of 2021, which exhibited attributes typical of a summer crop, as the extended period of emergence, highlighted by the red bracket in *Figure 6.53*.

Like Zone A, the NDVI profiles for the years 2022 and 2023 exhibited lower temporal patterns compared to previous years, *Figure 6.53*. In this case, both profiles showed similarity in their patterns, initiating with a period of maximum growth (green-up) until reaching the highest vegetative phase in the months of May to June.

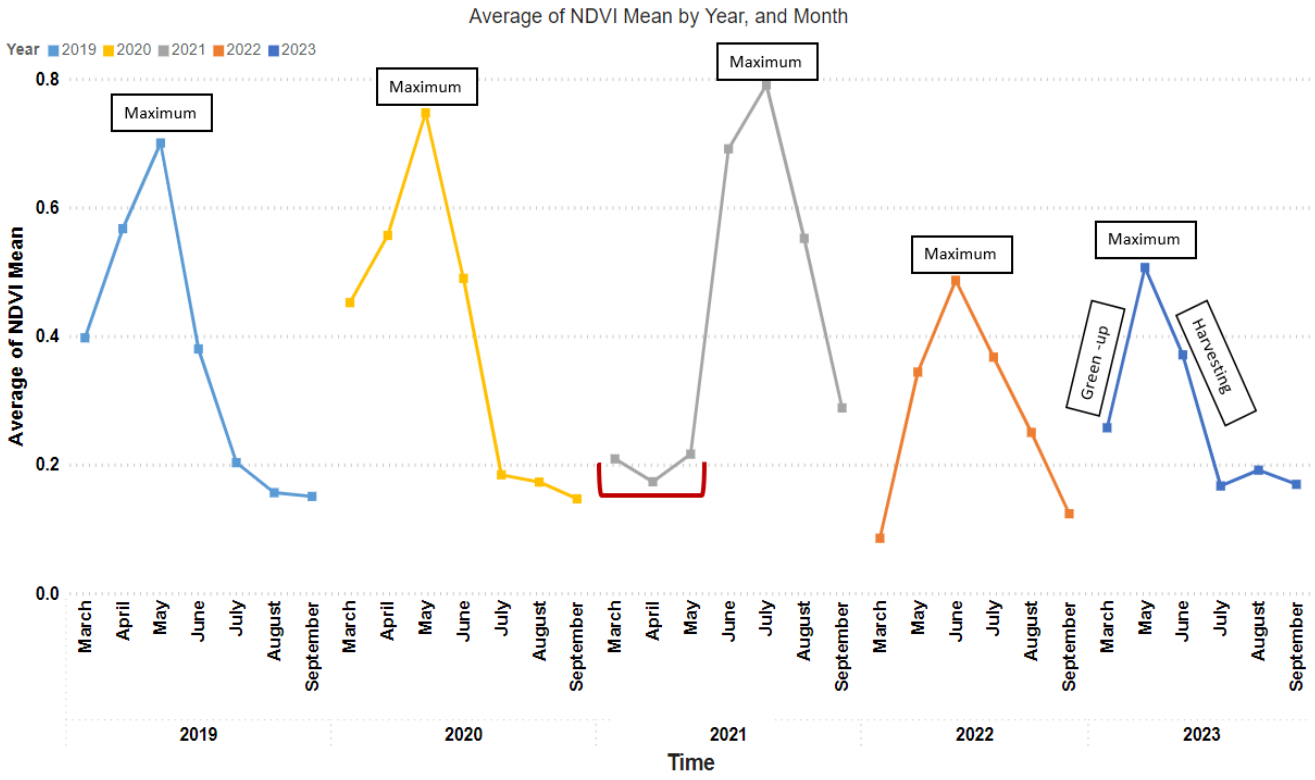

Figure 6.53 Average NDVI profiles by year, and month Zone B

Figure 6.54 show the local attacks experienced in the main city in this zone, Mariupol. The siege of Mariupol began on the same day as the invasion and lasted until May 20, concluding with a victory for Russia (dotted blue line in *Figure 6.54*). All Ukrainian forces surrendered on May 20, 2022, resulting in the city remaining under Russian control to date.

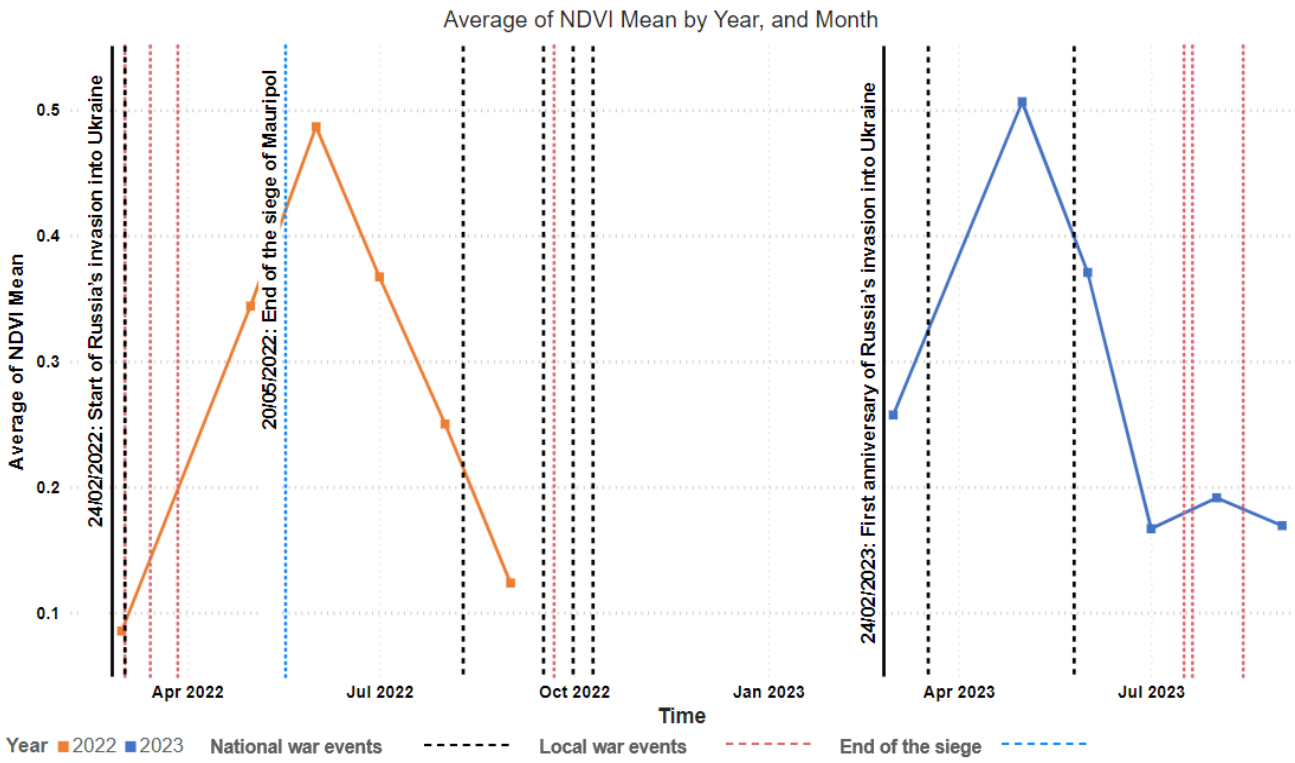

Figure 6.54 Key war events dates in Zone B

In the calculation of the average time series for the parcels in Zone C, only patterns with a higher number of contained parcels were considered. This approach aimed to capture the dominant patterns that encompassed a larger number of curves, reflecting the greater phenological diversity observed in Zone C compared to Zones A and B. The NDVI profiles shown in *Figure 6.55* corresponded to winter crops, characterized by greening in the spring months and harvesting in the summer, as shown in curve of year 2022.

In *Figure 6.55* a substantial decrease in NDVI values is observed for the year 2023 in Zone C, unlike the previous zones where a similar decline was also noted in 2022. The curve consistently exhibits values below 0.4 throughout the temporal period, with its peak occurring in the month of June, opposed to previous years when the peak occurred between April and May.

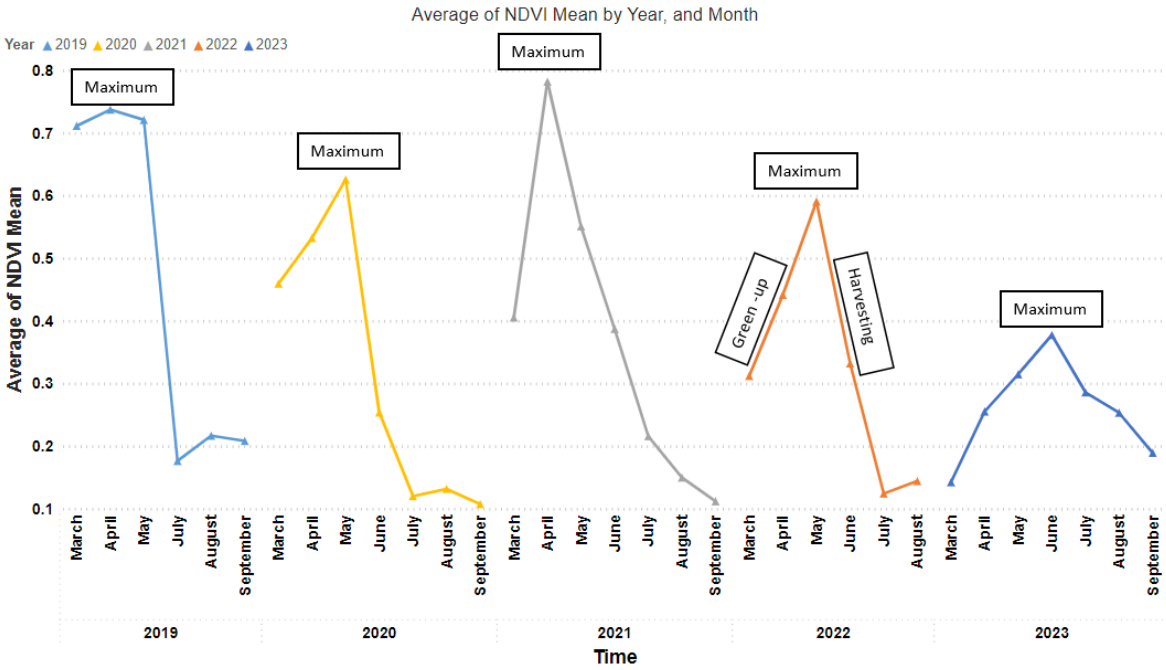

Figure 6.55 Average NDVI profiles by month, by year, Zone C

The military occupation by Russian forces in the city of Kherson commenced on March 15, 2022, and concluded on November 12, 2022 (dotted blue lines in *Figure 6.56*). After 8 months, the city was liberated by Ukrainian troops. Kherson, in particular, experienced a significant number of attacks on civil and energy infrastructure during the occupation. Most local attacks (dotted red lines in *Figure 6.56*) occurred in the early months after the invasion began and towards the end of the occupation, coinciding with the reestablishment of Ukrainian government control.

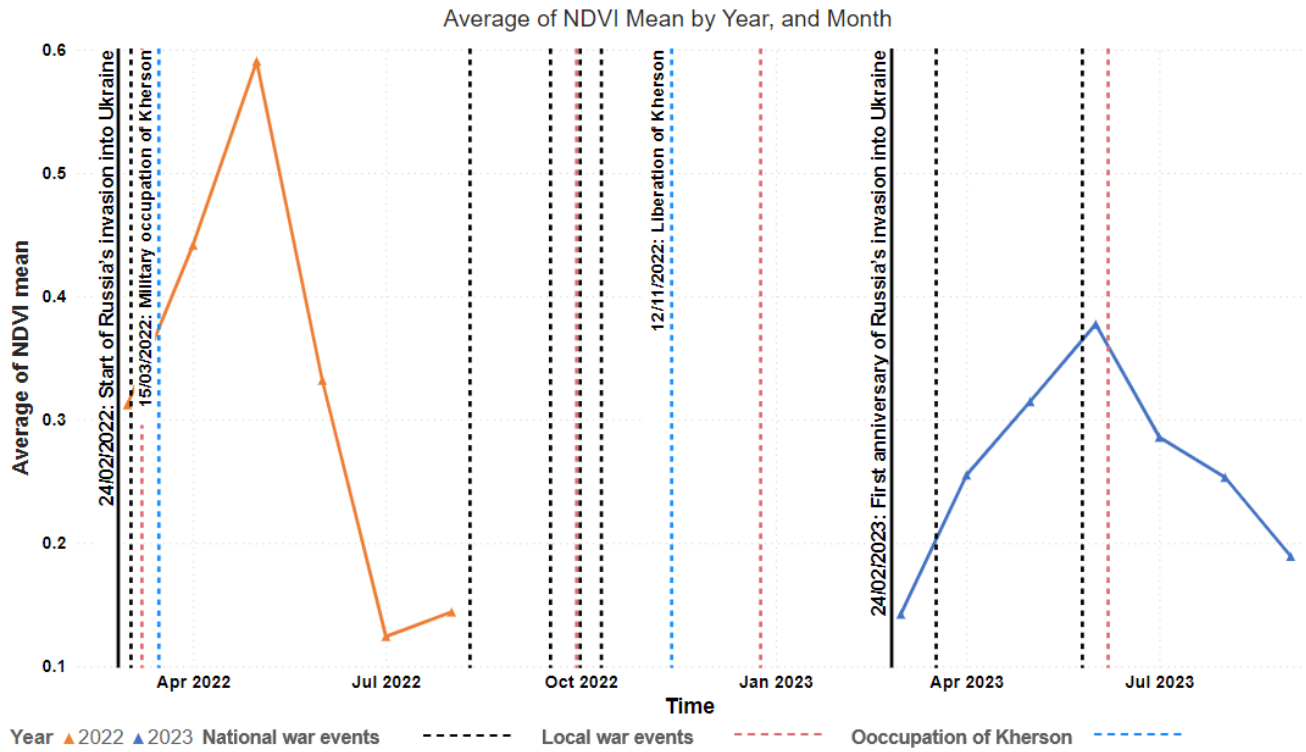

Figure 6.56 Key war events dates in Zone C

7. Conclusions

The objective of this study was to undertake an initial investigation into the implications of the ongoing conflict between Ukraine and Russia on phenological alterations in the territory and, therefore, the direct impacts on agriculture and food security inside Ukraine and globally.

The results reveal that, for all three zones, it is evident that the NDVI temporal profiles have decreased in the last two years of the analyzed time series, coinciding with the onset of Russia's invasion in Ukraine. Among the three study zones, Zone C exhibited a greater variability in crop phenology, making it more challenging to identify the specific type of crop or grain cultivated each year. In contrast, Zone B displayed the highest uniformity in phenology, facilitating the identification of the cultivated grain type based on the phenological profile. In Zone A, apart from the decrease in values observed in the years 2022 and 2023, it is important also to highlight the delayed emergence of crops on mentioned years. Regarding the changes induced by the war, while a significant decrease in maximum NDVI values was observed in each zone from the year 2022 onward, coinciding with the invasion, Zone C experienced a more pronounced reduction in 2023. The lower NDVI values observed in the last two years may be indicative of disruptions in the normal vegetation development cycle. The delayed greening period aligns with the regional context, illustrating potential impacts of the conflict on agricultural practices and vegetation health. We can conclude, therefore, that while the zones had different classifications regarding the direct impacts resulting from the war, a general decrease in NDVI values was observed after the onset of the conflict.

Although this study has provided insights on the impacts that the ongoing conflict has had on agriculture, specifically concerning phenological changes in three zones of Ukraine that were affected to varying extents by the war, there are still challenges to be addressed. One notable challenge is the need to broaden the scope of the study to quantify the impacts at a national level. This could be

achieved by utilizing datasets from satellites with higher resolution, and revisit time enabling a more precise classification of crop types. Additionally, conducting field verifications, whenever feasible, would significantly enhance the robustness and comprehensiveness of the study.

8. References

Agricultural sector of Ukraine Securing the global food supply. (2018).

ARSET. (2023). *Crop Mapping using Synthetic Aperture Radar (SAR) and Optical Remote Sensing. NASA Applied Remote Sensing Training Program (ARSET)*. Http://Appliedsciences.Nasa.Gov/Get-Involved/Training/English/Arset-Crop-Mapping-Using-Synthetic-Aperture-Radar-Sar-and-Optical.

At Least 10 Killed in Kherson Shelling, Fueling Anger Over Christmas Strikes. (2022, December 24). Https://Www.Nytimes.Com/2022/12/24/World/Europe/Russia-Kherson-Ukraine-Shelling.Html.

Boccardo, P. (n.d.). *REMOTE SENSING BASICS*.

Central Intelligence Agency. (2023). *The World Factbook, Ukraine*. https://www.cia.gov/the-world-factbook/countries/ukraine/#geography

Chatterjee, S. (2018). *Time Series Crop Monitoring of an Agricultural Scheme on a Plot Basis Using Complementary Remote Sensing*.

Chen, Y., Cao, R., Chen, J., Liu, L., & Matsushita, B. (2021). A practical approach to reconstruct high-quality Landsat NDVI time-series data by gap filling and the Savitzky–Golay filter. *ISPRS Journal of Photogrammetry and Remote Sensing*, *180*, 174–190. https://doi.org/10.1016/j.isprsjprs.2021.08.015

Dryancour, G. (2023). *CEMA aisbl-European Agricultural Machinery*. www.cema-agri.org

ESA. (2023). *World Cereal Global cropland monitoring based on Sentinels*. Https://Vdm.Esa-Worldcereal.Org/.

Fao. (2014). *Ukraine: Soil fertility to strengthen climate resilience Preliminary assessment of the potential benefits of conservation agriculture*. www.fao.org/investment/en

FAO. (2022). Ukraine: Impact of the war on agriculture and rural livelihoods in Ukraine. In *Ukraine: Impact of the war on agriculture and rural livelihoods in Ukraine*. FAO. https://doi.org/10.4060/cc3311en

Fao, Ó., & Stepanov, A. (2022). *INFORMATION NOTE THE IMPORTANCE OF UKRAINE AND THE RUSSIAN FEDERATION FOR GLOBAL AGRICULTURAL MARKETS AND THE RISKS ASSOCIATED WITH THE WAR IN UKRAINE EXECUTIVE SUMMARY*.

Fao, Ó., & Stepanov, A. (2022). *INFORMATION NOTE THE IMPORTANCE OF UKRAINE AND THE RUSSIAN FEDERATION FOR GLOBAL AGRICULTURAL*

MARKETS AND THE RISKS ASSOCIATED WITH THE WAR IN UKRAINE EXECUTIVE SUMMARY.

Helman, D. (2018). Land surface phenology: What do we really 'see' from space? In *Science of the Total Environment* (Vol. 618, pp. 665–673). Elsevier B.V. https://doi.org/10.1016/j.scitotenv.2017.07.237

ICC judges issue arrest warrant for Vladimir Putin over alleged war crimes. (2023, March 17). Https://Www.Theguardian.Com/World/2023/Mar/17/Vladimir-Putin-Arrest-Warrant-Ukraine-War-Crimes.

"It's 2 p.m. in Kyiv. Here's what you need to know." (2022, March 27). Https://En.Wikipedia.Org/Wiki/Timeline_of_the_Russian_invasion_of_Ukraine_(24_February_%E2%80%93_7_April_2022)#cite_note-3.

JRC MARS Bulletin-Global outlook Crop monitoring European neighbourhood Ukraine. (2022).

Kherson ours': Ukraine celebrates after Russian retreat. (2022, November 12). Https://Www.Aljazeera.Com/News/2022/11/12/Ukrainians-Celebrate-as-Russia-Withdraws-from-Kherson.

Koroleva, P. V., Rukhovich, D. I., Rukhovich, A. D., Rukhovich, D. D., Kulyanitsa, A. L., Trubnikov, A. V., Kalinina, N. V., & Simakova, M. S. (2017). Location of Bare Soil Surface and Soil Line on the RED–NIR Spectral Plane. *Eurasian Soil Science*, *50*(12), 1375–1385. https://doi.org/10.1134/S1064229317100040

Land Degradation Neutrality Target Setting Programme (LDN TSP). (2018). *NATIONAL TARGET SETTING TO ACHIEVE LAND DEGRADATION NEUTRALITY IN UKRAINE FINAL COUNTRY REPORT*.

Li, J., Li, C., Xu, W., Feng, H., Zhao, F., Long, H., Meng, Y., Chen, W., Yang, H., & Yang, G. (2022). Fusion of optical and SAR images based on deep learning to reconstruct vegetation NDVI time series in cloud-prone regions. *International Journal of Applied Earth Observation and Geoinformation*, *112*. https://doi.org/10.1016/j.jag.2022.102818

Longest battle ends as Ukrainian troops evacuated from Mariupol steel mill. (2022, May 17). Https://Www.Smh.Com.Au/World/Europe/Last-Fighters-Evacuated-from-Besieged-Azovstal-Mill-in-Mariupol-20220517-P5aly5.Html.

Loud explosions heard in occupied Luhansk, Berdiansk, Mariupol. (2023, July 16). Https://Kyivindependent.Com/Loud-Explosions-Strike-Occupied-Luhansk-Berdiansk-Mariupol/.

Ma, Y., Lyu, D., Sun, K., Li, S., Zhu, B., Zhao, R., Zheng, M., & Song, K. (2022). Spatiotemporal Analysis and War Impact Assessment of Agricultural Land in

Ukraine Using RS and GIS Technology. *Land*, *11*(10). https://doi.org/10.3390/land11101810

Martin, A., Badger, M., & Hansen, L. B. (2018). *COPERNICUS EVOLUTION AND APPLICATIONS WITH SENTINEL ENHANCEMENTS AND LAND EFFLUENTS FOR SHORES AND SEAS*.

Masialeti, I., Egbert, S., & Wardlow, B. (2010). A comparative analysis of phenological curves for major crops in Kansas. *GIScience and Remote Sensing*, *47*(2), 241–259. https://doi.org/10.2747/1548-1603.47.2.241

Matuszak, S. (2021). *THE BREADBASKET OF THE WORLD? AGRICULTURAL DEVELOPMENT IN UKRAINE THE BREADBASKET OF THE WORLD?* www.osw.waw.pl

McNairn, H. ; D.-R. L. ; F. M. ; R. F. ; K. G. ; R. T. ; B. S. ; D. P. (2021). *Agricultural Crop Classification with Synthetic Aperture Radar and Optical Remote Sensing. NASA Applied Remote Sensing Training Program (ARSET)*. Https://Appliedsciences.Nasa.Gov/Join-Mission/Training/English/Arset-Agricultural-Crop-Classification-Synthetic-Aperture-Radar-And.

Meijl, H. van, Bartelings, H., Berkum, S. van, Cui, D., Smeets-Kristkova, Z., & Zeist, W. J. van. (2022). *Impacts of the conflict in Ukraine on global food security*.

Military: Russian forces shell bordering Chernihiv, Sumy oblasts. (2023, June 25). Https://Kyivindependent.Com/Military-Russian-Forces-Shell-Bordering-Chernihiv-Sumy-Oblasts/.

Misra, G., Cawkwell, F., & Wingler, A. (2020). Status of phenological research using sentinel-2 data: A review. *Remote Sensing*, *12*(17). https://doi.org/10.3390/RS12172760

Morton, R., Sharp, K., Chomiak, B., Stepanets, N., Muliar, O., & Oleshko, N. (2005a). *FARM REFERENCE HANDBOOK FOR UKRAINE*.

Morton, R., Sharp, K., Chomiak, B., Stepanets, N., Muliar, O., & Oleshko, N. (2005b). *FARM REFERENCE HANDBOOK FOR UKRAINE*.

Movchan, V. (2022). *Ukraine's Role in Global Food Supply: Individual Countries' Vulnerability*. https://doi.org/DOI: 10.11586/2022069

Mousseau, F., & Devillers, E. (2023). *War and Theft: The Takeover of Ukraine's Agricultural Land*. www.oaklandinstitute.org

Official: Partisans set Russian base on fire in Mariupol. (2023, August 13). Https://Kyivindependent.Com/Official-Partisans-Set-Russian-Base-on-Fire-in-Mariupol/.

On day two of massive air strikes, Russia targeted Ukraine's power infrastructure Ukrainian regions report how much damage they took today. (2022, October 11). Https://Meduza.Io/En/Feature/2022/10/11/on-Day-Two-of-Massive-Air-Strikes-Russia-Targeted-Ukraine-s-Power-Infrastructure.

OneSoil. (2023). *Agricultural OneSoil Map with AI detected fields and crops*. Https://Map.Onesoil.Ai/2020/Ukr/Kirovohrad_oblast#8.91/48.4709/32.2915.

Perry, E., Sheffield, K., Crawford, D., Akpa, S., Clancy, A., & Clark, R. (2022). Spatial and Temporal Biomass and Growth for Grain Crops Using NDVI Time Series. *Remote Sensing*, *14*(13). https://doi.org/10.3390/rs14133071

Putin signs decrees recognizing so-called independence of Kherson, Zaporizhzhia regions. (2022, September 30). Https://Www.Aa.Com.Tr/En/World/Putin-Signs-Decrees-Recognizing-so-Called-Independence-of-Kherson-Zaporizhzhia-Regions/2698636.

Russian air strikes repelled over Kyiv, but hit regional airfield. (2023, June 4). Https://Www.Reuters.Com/World/Europe/Air-Defence-Systems-Engaged-Repelling-Air-Attacks-Kyiv-Ukrainian-Officials-2023-06-04/.

Russian troops enter Ukraine's Kherson Oblast: Defense Ministry. (2022, February 5). Https://Www.Aa.Com.Tr/En/Europe/Russian-Troops-Enter-Ukraines-Kherson-Oblast-Defense-Ministry/2513722.

Russia-Ukraine updates: Russia opens probe into Kremlin attack. (2023, May 3). Https://Www.Aljazeera.Com/News/Liveblog/2023/5/3/Russia-Ukraine-Live-Moscow-Intensifies-Night-Attacks-on-Kyiv.

Russia-Ukraine War Explosion on 12-Mile Crimea Bridge Kills 3. (2022, October 8). Https://Www.Nytimes.Com/Live/2022/10/08/World/Russia-Ukraine-War-News.

SENTINEL-2 User Handbook. (2013).

Skakun, S., Justice, C. O., Kussul, N., Shelestov, A., & Lavreniuk, M. (2019). Satellite Data Reveal Cropland Losses in South-Eastern Ukraine Under Military Conflict. *Frontiers in Earth Science*, *7*. https://doi.org/10.3389/feart.2019.00305

Ukraine accuses Russia of bombing Mariupol school sheltering 400. (2022, March 20). Https://Www.Aljazeera.Com/News/2022/3/20/Ukraine-Accuses-Russia-of-Bombing-Mariupol-School-Sheltering-400.

Ukraine Announces Exchange Of 215 Prisoners Of War. (2022, September 21). Https://Www.Barrons.Com/News/Ukraine-Announces-Exchange-of-215-Prisoners-of-War-01663799406?Tesla=y.

Ukraine conflict: Russia bombs Kharkiv's Freedom Square and opera house. (2022, March 1). Https://Www.Bbc.Com/News/World-Europe-60567162.

Ukraine conflict: Russian forces attack from three sides. (2022, February 24). Https://Www.Bbc.Com/News/World-Europe-60503037.

Ukraine hit by second wave of missile strikes – official. (2022, February 24). Https://Nationalpost.Com/Pmn/News-Pmn/Ukraine-Hit-by-Second-Wave-of-Missile-Strikes-Official.

Ukraine launches 'most massive strike' on occupied Donetsk region since 2014, Russia-installed mayor says. (2022, December 15). Https://Edition.Cnn.Com/2022/12/15/Europe/Russia-Ukraine-Donetsk-Kherson-Strikes-Intl/Index.Html.

Ukraine live updates: Russia attacks key Ukraine cities as invasion intensifies. (2022, March 2). Https://Www.Bbc.Com/News/Live/World-Europe-60582327.

Ukrainian forces destroy last remaining bridge used by Russian military in Kherson region. (2022, August 13). Https://Euroweeklynews.Com/2022/08/13/Ukrainian-Forces-Destroy-Last-Remaining-Bridge-Used-by-Russian-Military-in-Kherson-Region/.

Ukrainian officials accuse Russia of shelling civilians fleeing Mariupol. (2022, March 16). Https://Www.Theguardian.Com/World/2022/Mar/16/Mariupol-Ukraine-Russia-Seized-Hospital.

Walker, N. (2023). *Conflict in Ukraine: A timeline (current conflict, 2022-present)*.

Weiss, M., Jacob, F., & Duveiller, G. (2020). Remote sensing for agricultural applications: A meta-review. *Remote Sensing of Environment*, *236*. https://doi.org/10.1016/j.rse.2019.111402

What Happened on Day 7 of Russia's Invasion of Ukraine. (2022, March 2). Https://Www.Nytimes.Com/Live/2022/03/02/World/Ukraine-Russia-War.

World data Ukraine. (n.d.). Retrieved December 17, 2023, from https://www.worlddata.info/europe/ukraine/climate.php

Younes, N., Joyce, K. E., & Maier, S. W. (2021). All models of satellite-derived phenology are wrong, but some are useful: A case study from northern Australia. *International Journal of Applied Earth Observation and Geoinformation*, *97*. https://doi.org/10.1016/j.jag.2020.102285

Zelenskyy says new air raids launched in Russian-held Kherson. (2022, June 11). Https://Www.Aljazeera.Com/News/2022/6/10/Ukrainians-Evacuated-from-Eastern-City-amid-Battles-in-Donbas-Liveblog.